

Aus der Medizinischen Klinik und Poliklinik IV
Klinik der Ludwig-Maximilians-Universität München
Direktor: Prof. Dr. med. Martin Reincke

Mdm2 Prevents Spontaneous Tubular Epithelial Cell Death and Acute Kidney Injury

Dissertation
zum Erwerb des Doktorgrades der Medizin
an der Medizinischen Fakultät der
Ludwig-Maximilians-Universität zu München

vorgelegt von

Moying Li

aus Wuhan, China

2019

**Mit Genehmigung der Medizinischen Fakultät
der Universität München**

Berichterstatter: Prof. Dr. med. Hans-Joachim Anders

Mitberichterstatter: Prof. Dr. Gunnar Schotta

Prof. Dr. Wolfgang Neuhofer

Mitbetreuung durch die
promovierte Mitarbeiterin: PD. Dr. med. Dana Thomasova, PhD

Dekan: Prof. Dr. med. dent. Reinhard HICKEL

Tag der mündlichen Prüfung: 02.05.2019

Eidesstattliche Versicherung

von Moying Li

Ich erkläre hiermit an Eides statt, dass ich die vorliegende Dissertation mit dem Thema

Mdm2 Prevents Spontaneous Tubular Epithelial Cell Death and Acute Kidney Injury

selbständig verfasst, mich außer der angegebenen keiner weiteren Hilfsmittel bedient und alle Erkenntnisse, die aus dem Schrifttum ganz oder annähernd übernommen sind, als solche kenntlich gemacht und nach ihrer Herkunft unter Bezeichnung der Fundstelle einzeln nachgewiesen habe.

Ich erkläre des Weiteren, dass die hier vorgelegte Dissertation nicht in gleicher oder in ähnlicher Form bei einer anderen Stelle zur Erlangung eines akademischen Grades eingereicht wurde.

Folgende Personen haben an der Durchführung dieser Arbeit mitgewirkt:

- PD. Dr. Dana Thomasova, Ph.D., LMU München
Sie fertigte Aufnahmen der immunhistologischen Schnitte an.
- Prof. Dr. Helen Liapis, Washington University, USA. Sie führte die elektronenmikroskopischen Aufnahmen durch.
- Janina Mandelbaum und Dan Draganovici, LMU München
Sie fertigten die histologischen Schnitte an und führten die Genotypisierung der Versuchstiere durch.

München, 04.06.2018

Moying Li

Die vorliegende Arbeit wurde im Zeitraum zwischen August 2014 und Juli 2015 am Nephrologischen Zentrum der Medizinischen Klinik und Poliklinik IV an der Ludwig-Maximilians-Universität München durchgeführt. Die Arbeit wurde von Herrn Prof. Dr. med. Hans Joachim Anders betreut.

Förderung des Projekts:

Munich-International Nephrology and Internal Medicine (MINI) Research School

Aus dem Projekt hervorgegangene Veröffentlichungen:

Publikation:

Thomasova, D., Ebrahim, M., Fleckinger, K., **Li, M.**, Molnar, J., Popper, B., Liapis, H., Kotb, A. M., Siegerist, F., Endlich, N., Anders, H.-J.: MDM2 prevents spontaneous tubular epithelial cell death and acute kidney injury. Cell Death Dis, 2016. 7(11): p. e2482. (Impact factor: 5,965)

Poster:

Doktamed (Studentenkongress an der Ludwig-Maximilians-University Munich) 2015, Munich. **Li, M.**, Thomasova, D, Ebrahim, M, Anders, HJ: Murine Double Minute-2 (MDM2) maintains homeostasis in renal tubular cells by preventing p53-overactivation-regulated cell death.

“Let us try to teach generosity and altruism, because we are born selfish. Let us understand what our own selfish genes are up to, because we may then at least have the chance to upset their designs, something that no other species has ever aspired to do.”

— Richard Dawkins, *The Selfish Gene*

TABLE OF CONTENTS

	Page
Zusammenfassung.....	1
Summary	3
1 Introduction	5
1.1 Acute kidney injury.....	5
1.1.1 Epidemiology and clinical aspects	5
1.1.2 Pathophysiology of ischemic acute kidney injury.....	9
1.1.3 Biomarkers for acute kidney injury.....	14
1.2 p53: guardian of genome	17
1.2.1 The protein p53.....	17
1.2.2 p53 and apoptosis	20
1.3 Mdm2: master inhibitor of p53	23
1.3.1 The protein Mdm2.....	23
1.3.2 p53-Mdm2 autoregulatory feedback loop	23
1.3.3 Biological functions of Mdm2	25
1.3.4 Mdm2 in the kidney.....	28
1.4 Targeting p53-MDM2 interaction: clinical potential	30
2 Research hypothesis	32
3 Materials and Methods	33
3.1 Materials.....	33
3.1.1 Instruments	33
3.1.2 Materials for animal experiments	34
3.1.3 Materials for molecular biology methods	34
3.1.4 Materials for histological methods	37
3.1.5 Softwares	38
3.2 Animal experiments	39
3.2.1 Animal housing	39
3.2.2 Generation of <i>Pax8rtTA-Cre;Mdm2^{flox/flox}</i> mouse line.....	39
3.2.3 Doxycycline treatment regime	41
3.2.4 Genotyping	42
3.2.5 Blood sample collection	43
3.3 Molecular biological methods.....	44
3.3.1 RNA isolation	44
3.3.2 RNA quantification and purity check.....	44
3.3.3 RNA integrity check	45
3.3.4 cDNA synthesis.....	46
3.3.5 Real-time quantitative polymerase chain reaction (RT-PCR)	47
3.3.6 Creatinine measurement	49
3.3.7 BUN measurement	50
3.4 Histological methods.....	51
3.4.1 Histological sections	51
3.4.2 Periodic acid-Schiff (PAS) staining	51

3.4.3	Immunohistochemistry	51
3.4.4	Immunofluorescence	53
3.4.5	Histopathological evaluations	54
3.4.6	Transmission Electron Microscopy	54
3.5	Statistical analysis.....	55
4	Results	56
4.1	<i>Mdm2</i> expression is reduced exclusively in renal tubular epithelial cells of <i>Pax8rtTA-Cre;Mdm2^{flox/flox}</i> mice treated with doxycycline (<i>Mdm2^{-/-tubulus}</i>).....	56
4.2	Continuous tubule-specific <i>Mdm2</i> depletion results in acute kidney injury ...	59
4.2.1	Oliguria, weight loss and shortened life span	59
4.2.2	Impaired renal function	60
4.2.3	Upregulation of <i>p53</i> , <i>p21</i> and <i>Puma</i> in the kidney.....	61
4.2.4	Upregulation of tubulus damage markers in the kidney.....	63
4.2.5	Acute tubular injury under light microscope	64
4.2.6	Cellular loss in proximal tubules, distal tubules and collecting ducts...	66
4.2.7	Ultrastructural pathology of tubular cells under electron microscope ..	68
4.2.8	Apoptosis and proliferation assays with immunostaining	70
4.3	Intermittent tubule-specific <i>Mdm2</i> depletion results in kidney fibrosis	73
4.4	Summary of results	78
5	Discussion	79
5.1	<i>Mdm2</i> is required for the homeostasis of renal tubular cells.....	81
5.2	Tubular cells cannot fully recover from <i>Mdm2</i> -deletion induced injury	85
5.3	MDM2 inhibitors might have detrimental effects on patients	88
5.4	How do tubular cells die in the absence of <i>Mdm2</i> ?	90
5.5	Limitations of study and future directions.....	91
6	Abbreviations	92
7	List of Figures	94
8	Liste of Tables	96
9	Bibliography	97
10	Acknowledgment	107

Zusammenfassung

Murine Double Minute 2 (Mdm2) Protein ist ein wichtiger negativer Regulator des Tumorsuppressors p53. Mdm2, eine E3-Ubiquitin-Ligase, unterdrückt p53-Aktivität vor allem durch Ubiquitinierung und führt zum proteasomalen Abbau von p53. Umgekehrt stimuliert p53 die Mdm2-Expression durch transkriptionale Aktivierung. Somit steuern Mdm2 und p53 ihre Konzentrationen gegenseitig in einer autoregulatorischen Rückkopplungsschleife. Mdm2 und p53 spielen bedeutende Rollen bei der Zellzykluskontrolle und beim Zelltod, während deren Dysregulation mit verschiedenen Pathologien wie z. B. Tumor assoziiert ist. Klinisch werden niedermolekulare MDM2-Antagonisten aufgrund ihrer Fähigkeit, die p53-Aktivität wiederherzustellen, als vielversprechende Tumormedikamente untersucht.

Bei akutem Nierenversagen hat Mdm2 ambivalente Eigenschaften: auf der einen Seite pro-inflammatorisch (schädlich) und auf der anderen Seite pro-proliferativ (vorteilhaft). Unter physiologischen Bedingungen wird Mdm2 in renalen Tubuluszellen stark exprimiert, aber der Grund dafür ist noch nicht bekannt. Wir stellten die Hypothese auf, dass Mdm2 die Homöostase von renalen Tubuluszellen und ihre physiologischen Funktionen aufrechterhält. Um diese Hypothese zu testen, wurden induzierbare Tubuluszellen-spezifische *Mdm2*-Knockout-Mäuse *Pax8rtTA-Cre;Mdm2^{flox/flox}* generiert. Unter Doxycylin-Induktion exprimieren diese Mäuse Cre Rekombinase, die *loxP*-Stellen erkennt und *Mdm2* Gendeletion ausschließlich in den renalen Tubuluszellen hervorruft (als *Mdm2^{-tubulus}* bezeichnet). Mit diesem transgenen Mausmodell können die Rollen von Mdm2 in renalen Tubuluszellen präzise untersucht werden.

Unter kontinuierlicher Doxycylin-Behandlung für 4, 8 oder 11 Tage zeigten erwachsene *Mdm2^{-tubulus}* Mäuse im Vergleich zu ihren Kontrollmäusen beeinträchtigte Nierenfunktion und histologische Tubulusschäden mit zunehmender Zeit. Dieser Phänotyp stimmt mit akutem Nierenversagen überein. Außerdem wurden *Mdm2^{-tubulus}* Mäuse oligurisch, moribund und starben wenige Tage nach der Doxycylin-Behandlung. Darüber hinaus war die intrarenale Genexpression von *p53* und seine Effektorgene *p21* und *Puma* in Knockoutmäusen signifikant erhöht, was zu Zelltod und einem fortschreitenden Zellverlust in den Nierentubuli führte. Ein erheblicher Anstieg der Biomarker für Tubulusschaden wurde ebenfalls festgestellt. Diese Daten legen nahe, dass Mdm2 und seine negative Regulation von p53 für das Überleben

der renalen Tubuluszellen unerlässlich ist. Ohne Mdm2 verlieren Tubuluszellen ihre physiologischen Funktionen und sterben aufgrund der p53-Überaktivierung.

Um die hohe Letalität der kontinuierlichen Doxycyclin-Behandlung bei *Mdm2*-Knockout-Mäusen zu vermeiden, wurde eine intermittierende Doxycyclin-Behandlung angewandt. *Mdm2*-Knockout-Mäuse überlebten während der gesamten Versuchsdauer von 4 Wochen und waren äußerlich unauffällig. Sie wiesen jedoch eine prominente Nierenfibrose und eine deutlich erhöhte intrarenale Expression von Fibrose-Markern auf. Dies ist vergleichbar mit einer unzureichenden Heilung („maladaptive repair“) nach dem akuten Nierenversagen, die das Fortschreiten zu chronischen Nierenerkrankungen begünstigt. Wir schließen daraus, dass renale Tubuluszellen den durch die *Mdm2*-Deletion verursachten Zellverlust nicht vollständig kompensieren können.

Zusammenfassend liefert unsere Studie den ersten Beweis dafür, dass Mdm2 die Homöostase der renalen Tubuluszellen aufrechterhält. *Mdm2*-Deletion führt zum spontanen Zelltod und akutem Nierenversagen. Diese Beobachtungen tragen zu einem besseren Verständnis der Nierenphysiologie bei, insbesondere in Bezug auf Zellzykluskontrolle und Zelltod. Nicht zuletzt ist bei der Tumorbehandlung mit MDM2-Antagonisten besondere Vorsicht hinsichtlich der Nierenfunktion erforderlich, da sowohl akutes Nierenversagen als auch chronische Nierenerkrankung auftreten können.

Summary

Murine double minute 2 (Mdm2) is the key negative regulator of tumor suppressor p53. Mdm2 downregulates p53 by ubiquitination, nuclear export and direct binding. In turn, p53 upregulates Mdm2 by transactivation. Thus, Mdm2 and p53 control their levels mutually in an autoregulatory feedback loop. Mdm2 and p53 together play important roles in cell cycle control and cell death, and an imbalance can lead to diseases, such as tumor. Clinically, small molecule MDM2 antagonists are studied as promising anticancer drugs due to its ability to restore p53 activity.

In acute kidney injury, Mdm2 exerts dual functions: pro-inflammatory (harmful) and pro-proliferative (beneficial). Under physiological conditions, Mdm2 is highly expressed in renal tubular cells, but what for is not known. We hypothesized that Mdm2 maintains the homeostasis of renal tubular cells and their physiological functions. To test our hypothesis, we generated inducible tubule-specific *Mdm2* knockout mice *Pax8rtTA-Cre;Mdm2^{flox/flox}* mice. Upon doxycycline induction, these mice express Cre recombinase, which recognizes *loxP* sites and causes *Mdm2* gene deletion exclusively in renal tubular cells (referred as *Mdm2^{-/-tubulus}*). The transgenic mouse model provides an exceptional way to precisely study roles of Mdm2 in renal tubular cells.

Subjected to continuous doxycycline treatment for 4, 8 and 11 days, adult *Mdm2^{-/-tubulus}* mice showed progressively impaired kidney function and tubular damage in the histology with increasing time, compared to their control littermates. This phenotype is consistent with acute kidney injury. Also, *Mdm2^{-/-tubulus}* mice became oliguric, moribund and died rapidly upon doxycycline treatment. Moreover, intrarenal gene expression of *p53* and its downstream genes *p21* and *Puma* was significantly upregulated, leading to progressive cell death in renal tubules. Substantial increase of tubulus damage markers were detected as well. These data suggest that Mdm2 and its negative regulation of the p53 are indispensable for the survival of the renal tubular cells. Without Mdm2, renal tubules loss their physiological functions and undergo cell death due to p53 overactivation.

To avoid the high lethality of the continuous doxycycline treatment in knockout mice, we exploited intermittent doxycycline administration regime on *Mdm2^{-/-tubulus}* mice. Knockout mice survived during the whole experimental period of 4 weeks and appeared normal. However, they developed profound kidney fibrosis as detected by

histopathology and markedly increased gene expression of fibrosis markers such as TGF-beta. This is reminiscent of maladaptive repair after acute kidney injury, which accelerates the progression into chronic kidney disease. We conclude that renal tubular cells cannot fully compensate for cellular loss caused by *Mdm2* deletion.

In summary, our study provides the first evidence that Mdm2 maintains homeostasis in renal tubular cells by preventing spontaneous cell death and acute kidney injury. Moreover, tubular cells can only partially recover from *Mdm2* deletion. These findings help shed additional light on understanding the physiology in homeostatic kidneys, especially concerning cell cycle control and cell death. On the other hand, extra caution regarding kidney function is required when treating cancer with MDM2 antagonist, as both acute kidney injury and chronic kidney disease can occur in the absence of MDM2.

1 Introduction

1.1 Acute kidney injury

Acute kidney injury is a global health concern that is associated with increasing incidence, high mortality and economic burden [1-4]. Yearly, AKI impacts about 13,3 million patients, contributes to about 1,7 million deaths in the world [5] and causes enormous costs [6-8]. Moreover, there is no pharmacological cure or therapeutic interventions for AKI other than dialysis, which can significantly improve survival or promote recovery [2]. It is also noteworthy that long-term complications of AKI represent a social burden. Progression of AKI into chronic kidney disease and end-stage renal disease requiring dialysis or transplantation can lead to poor life quality or disability of patients [5]. Thus, a better awareness and understanding of AKI is of paramount importance.

1.1.1 Epidemiology and clinical aspects

Acute kidney injury is characterized by rapid decline of kidney function, as measured by serum creatinine (SCr) and urine output. The 2012 guideline of Kidney Disease: Improving Global Outcomes (KDIGO) defines AKI as any of the following [9]:

- Increase in SCr by ≥ 0.3 mg/dl (≥ 26.5 μ mol/l) within 48 hours; or
- Increase in SCr to ≥ 1.5 times baseline, which is known or presumed to have occurred within the prior 7 days; or
- Urine volume < 0.5 ml/kg/h for 6 hours.

As illustrated in Table 1, AKI has a worldwide high incidence in hospitalized patients despite geographic differences [5]. Approximately one in five hospitalized patients is affected by AKI by KDIGO definition, predominately at KDIGO stage 1 [5]. Moreover, patients with critical illness and cardiovascular surgery are more susceptible to develop acute kidney injury [5, 10, 11]. In intensive care unit, more than 50% of patients suffer from AKI [12] and 4-5% of patients require renal replacement therapy, which contributes to prolonged hospital stay, worse outcomes and greater costs [1].

Table 1: Pooled incidence rate of acute kidney injury in hospitalized patients.

These data are derived from Mehta et al., 2015 [5].

	Region	Pooled incidence rate of AKI
Europe	Northern Europe	19.3%
	Eastern Europe	23.8%
	Southern Europe	25.2%
	Western Europe	20.8%
Asia	Central Asia	9.0%
	Eastern Asia	19.4%
	Southern Asia	7.5%
	Southeastern Asia	31.0%
Africa	Eastern Africa	13.4%
	Middle Africa	23.5%
America	North America	22.3 %
	South America	31.0%
Australia	Australia and New Zealand	16.9%

AKI is associated with high mortality —the overall pooled mortality of AKI in hospitalized patients is 20%-30% [5, 10]. Furthermore, patients with severe AKI at KIDGO stage 3 and those who need dialysis have a high mortality of 42% and 46% respectively [5].

AKI can be acquired in community, hospitals or critical care settings. According to its etiology, AKI can be divided into three following categories [6, 13, 14]:

- 1) Prerenal: caused by decreased renal blood flow, e.g. due to intravascular volume depletion (in cases of vomiting, diarrhea, hemorrhage and burns etc.), heart failure, hypotension or shock. Approximately 70 percent of community acquired AKI is attributable to prerenal causes [14, 15].
- 2) Intrinsic renal: caused by pathological processes within the kidney. It could be categorized by the primarily affected renal components: glomerular, tubular, interstitial or vascular [13, 14]. Overall, acute tubular necrosis is the most frequent cause of intrinsic renal AKI in hospitalized patients, which is commonly triggered by ischemic or toxic injury [6, 14]. Nephrotoxic compounds can be exogenous such as contrast agents or medications, and can also be endogenous such as myoglobin released from rhabdomyolysis [14].

- 3) Postrenal: caused by impeded drainage of urine distal to kidneys, e.g. due to intrarenal obstruction by stones or crystals, or extrarenal obstruction such as prostate hypertrophy that is the most common cause in older men [13, 14].

Notably, the causes of AKI vary from country to country. Whereas sepsis, cardiovascular surgery and polypharmacy are main insults to trigger AKI in high-income countries, the more frequent causes of AKI in low-income countries include diarrhea, tropical diseases such as malaria, animal venoms such as from snake bites and intake of traditional herbal preparations [5].

Risk factors for AKI have been increasingly recognized. There are patient-modifiable risk factors including dehydration, volume depletion and exposure to nephrotoxic drugs. On the other hand, patient-non-modifiable risk factors contribute to the patient's individual susceptibility, such as comorbidities (preexisting chronic kidney disease, diabetes, cancer, chronic heart disease and chronic lung disease) and demographic aspects (female gender, older age and black race) [5].

Clinical symptoms of patients suffering from AKI are unspecific, varying from asymptomatic over oliguria to confusion and lethargy, the latter due to accumulation of nitrogen-containing metabolic wastes such as urea in blood. Staging of AKI is performed based on serum creatinine and urine output, to evaluate disease severity (Table 2).

Diagnosis of AKI relies on the combination of a patient's history, physical examination, kidney function assessment, renal imaging studies and eventually renal biopsy [6]. Urine output and serum creatinine as two parameters for AKI definition should be promptly determined. Also, blood test covering blood urea nitrogen (BUN), GFR and electrolytes, as well as urine studies with urine osmolality and sediment analysis help estimate injury severity and localize injury site. Furthermore, renal ultrasound can reveal or exclude post-renal obstructions. Renal biopsy is helpful for diagnosis or exclusion of rapid progressive glomerulonephritis, vasculitis and interstitial nephritis.

Table 2: Staging of acute kidney injury (table from KDIGO 2012 [9])

Stage	Serum creatinine	Urine output
1	1.5–1.9 times baseline OR ≥ 0.3 mg/dl (≥ 26.5 μmol/l) increase	< 0.5 ml/kg/h for 6–12 hours
2	2.0–2.9 times baseline	< 0.5 ml/kg/h for ≥12 hours
3	3.0 times baseline OR Increase in serum creatinine to ≥ 4.0 mg/dl (≥ 353.6 μmol/l) OR Initiation of renal replacement therapy OR, in patients < 18 years, decrease in eGFR to < 35 ml/min per 1.73 m ²	< 0.3 ml/kg/h for ≥ 24 hours OR Anuria for ≥12 hours

Management of AKI is complex. First of all, identify the underlying cause as a timely causal treatment may help kidney recover completely. Second, stop any administration of nephrotoxic agents if possible. Third, closely monitor the patient's volume status and electrolyte levels, and subscribe medications for supportive treatment if indicated, such as diuretics. Finally, renal replacement therapy should be started immediately in cases of life-threatening changes in fluid, electrolyte, and acid-base balance.

AKI can lead to a multitude of complications. The short-term complications include electrolytes disorders, metabolic acidosis, fluid overload, uremia and coagulopathy [6]. Moreover, AKI can induce dysfunction of distant organs including heart, lung, liver and central nerve system [16-20], thereby increasing the risk of multi organ failure in critically ill patients [6]. The long-term complications of AKI include accelerated chronic kidney disease, end stage renal disease and death. Remarkably, even subtle increases of serum creatinine can lead to long-term complications.

Last but not least, prevention of AKI is of paramount importance. One key preventive strategy is identification of patients at risk and correction of modifiable risk factors such as volume depletion [13]. Avoidance of nephrotoxic drugs and drug dose adjustment in patients with impaired kidney function is of great importance. In incipient acute kidney injury, prompt diagnosis and appropriate treatment can prevent irreversible loss of nephrons and thus save the kidney [13].

1.1.2 Pathophysiology of ischemic acute kidney injury

Ischemia is one of the most common causes for acute kidney injury. The complex pathophysiology of ischemic AKI has been intensively studied in animal models. In simple words, the reduced renal blood flow disrupts the homeostasis in kidneys, which is maintained by coordinated communication and interactions of various cell types [21]. Inadequate oxygen and nutrient supply to the kidney results in tissue injury (especially in renal epithelium and endothelium) and sterile inflammation, followed by repair process [22].

Epithelial injury

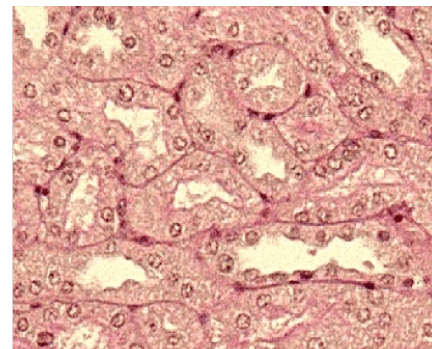
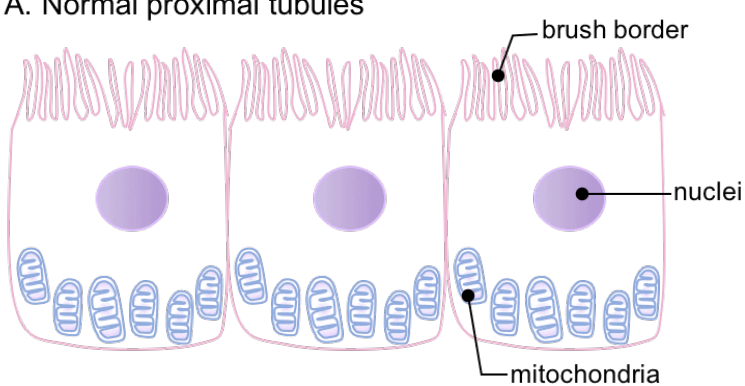
Proximal tubular cells are the most susceptible component of the nephron during ischemic injury [22]. Tubular epithelial cells are very sensitive to hypoxia, because their metabolic rate is high which is required for maintaining ion and molecule transport [22]. Additionally, there is markedly reduced perfusion in the outer medulla after injury, making tubules in this region particularly vulnerable [23]. Even after restoration of total renal blood flow, this regional hypoperfusion persists and mediates continued hypoxia. This phenomena is known as extension phase of AKI [24].

Proximal tubular cells display characteristic morphological changes during ischemia injury (Figure 1), which is caused by impaired cytoskeletal integrity and loss of cell polarity and tight junctions. The morphological hallmarks include loss of apical brush border caused by disrupted microvilli, tubular dilatation as a compensation to cell loss, and intraluminal cast formation containing exfoliated cells and microvilli remnants [25]. Cast formation can obstruct tubular lumen, thereby increasing the intraluminal pressure and further impairing the glomerular filtration rate [22]. Injured tubular cells fail to maintain ion and molecule transport, which causes direct decline of renal function.

Sustained hypoxia leads to cellular injury, and if severe enough, cell death by necrosis and apoptosis [22]. Apoptosis is a programmed, highly organized cell death without causing inflammation, whereas necrosis is induced by extreme injury and triggers inflammatory responses. Apoptosis is regulated by p53 and its effector genes such as *PUMA* and *BAX*, which is described in detailed in the capital 1.2.2. Several studies have reported that intrarenal p53 expression is increased during AKI and inhibition of p53 can protect kidneys from ischemic injury [26-28].

Tubular cells are not only passive victims, but also active contributors to acute kidney injury by mediating inflammation [23]. Injured tubular cells release cytokines and chemokines such as tumor necrosis factor (TNF)- α , interleukin (IL)-6, IL-1 β and IL-8 that attract inflammatory cells [23, 29]. Additionally, tubular cells express increased Toll-like receptors during AKI, which initiate a proinflammatory response [23]. Moreover, tubular cells undergo cell death if the injury is lethal, resulting in inevitable loss of function of affected cells [30]. Damage-associated molecular patterns (DAMPs) are frequently released during death of tubular cells, thereby amplifying the inflammation in tissue damage [30, 31].

A. Normal proximal tubules



B. Acute tubular injury

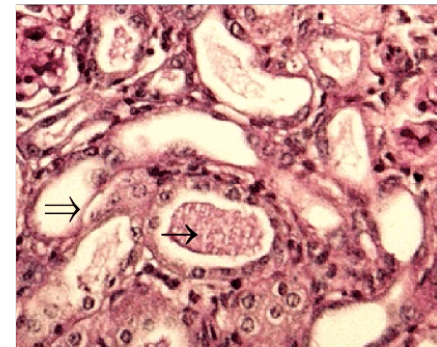
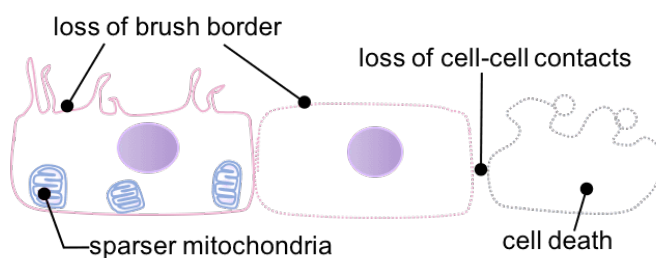


Figure 1: Morphological hallmarks of tubular epithelial cells during ischemic injury.

Illustrations are depicted left and PAS staining of kidney sections are shown right.

A. Normal proximal tubules are characterized with brush border composed of surface microvilli, and abundant mitochondria along the tubular basement membrane.

B. Tubular cells undergoing acute ischemic injury display morphological hallmarks. These include loss of brush border, sparser mitochondria in comparison with normal tubules and loss of epithelial cell-cell contacts. Also, tubular dilatation and cell death can be observed.

Further hallmarks are reduced number of nuclei (\Rightarrow) and intraluminal cast formation (\rightarrow), as shown in the PAS staining.

Endothelial injury

Ischemia has also profound effects on renal endothelium of microcirculation, causing increased vascular permeability, vasoconstriction and occlusion of microvasculature [22, 32, 33]. During ischemic injury, endothelial cells increase the expression of cell adhesion molecules such ICAM-1, which activate patrolling leukocytes in the blood stream [34]. Also, tight junctions and adherent junctions among endothelial cells are disrupted, leading to the loss of cell-cell contacts and breakdown of endothelial barrier function [22]. Moreover, sustained vasoconstriction impairs blood flow and further compromises microcirculation. Finally, platelet aggregation and decreased level of protein C contribute to a hypercoagulable environment. These together leads to microvascular dysregulation in the kidney. Consequently, leukocytes transmigrate through injured renal endothelium into tissues and produce pro-inflammatory cytokines, which aggravates AKI [22].

Inflammation

Ischemic acute kidney injury is accompanied by sterile inflammation, which occurs in the absence of infection by microorganisms [22, 23, 35, 36]. Similar to microbially induced inflammation, sterile inflammation is characterized by recruitment of neutrophils and macrophages, release of cytokines and activation of T and B lymphocytes [35]. Here, both innate and adaptive immune system are involved. The innate immune response is the first line of defense [36] and comprises neutrophils, monocytes, macrophages, dendritic cells and natural killer cells [23]. During AKI, the innate immune response is initiated by Toll-like-receptors (TLRs) [37]. TLRs are transmembrane proteins and located at cell surface or in endosomes [35, 38]. TLRs belong to pathogen recognition receptors (PRRs), and can recognize pathogen-derived as well as nonpathogen-derived immunogenic molecules [37]. Particularly TLR 2 and 4 play a key role to trigger inflammatory responses in AKI [39, 40]. They are stimulated by endogenous non-infectious materials released during tissue injury, referred as damage-associated molecular pattern (DAMP) [35]. This results in production of pro-inflammatory cytokines such as IL-1 β , type I interferon and NF- κ B-dependent cytokines and chemokines [37], which amplify immune responses and attract inflammatory cells [23, 36]. TLR-2 and -4 are expressed on immune cells and renal tubular cells, and their expression is significantly increased during AKI [41, 42].

Repair

Tubular epithelial cells play a key role in kidney repair after ischemic injury. During homeostasis, most renal tubular cells are quiescent and remain in the post-mitotic G0 phase of the cell cycle. They have a low turnover—less than 1% of renal tubular cells are proliferating [43-45]. After injury, however, studies suggest that surviving tubular cells dedifferentiate, spread across to denuded basement membrane, reenter into cell cycle and proliferate [46-48]. This is followed by differentiation of cells with reassembly of cytoskeleton and reestablishment of cell polarity, so that renal epithelium regenerate with restoration of cell number as well as cell function [49] (Figure 2). Due to the high proliferative capacity of renal tubular cells, the kidney can completely recover from an ischemic insult, namely “restitution at integrum” [23, 48]. This is described as adaptive repair. Nevertheless, the mechanisms of kidney repair are under ongoing debate, another opinion is that the tubular compartment is repaired by proliferation of tubular progenitor cells.

However, incomplete repair after kidney injury occurs frequently, especially when injury is severe or sustained, resulting in serious sequelae such as fibrosis. Different factors contribute to this maladaptive repair. First, incompletely repaired tubular cells are arrested in the G2/M phase of the cell cycle and fail to proliferate properly. Moreover, growth-arrested tubular cells secrete profibrotic growth factors such as TGF- β , leading to increased production of extracellular matrix [44]. Second, it is observed that the capillary density in kidneys can be reduced after AKI, known as the phenomena of vascular dropout [50, 51]. This results in chronic hypoxia in kidneys due to decreased blood supply and hypertension. Third, pathological immune responses participate in post-ischemic fibrosis, including chronic activation of macrophages and release of pro-fibrogenic cytokines such as IL-13 and TGF- β [23]. As a result, fibroblasts are activated, inducing interstitial fibrogenesis. Finally, kidney function is impaired due to loss of functional nephrons. Notably, maladaptive repair after AKI accelerates the progression into CKD with more rapid onset of ESRD, which are clinical important long-term complications of AKI.

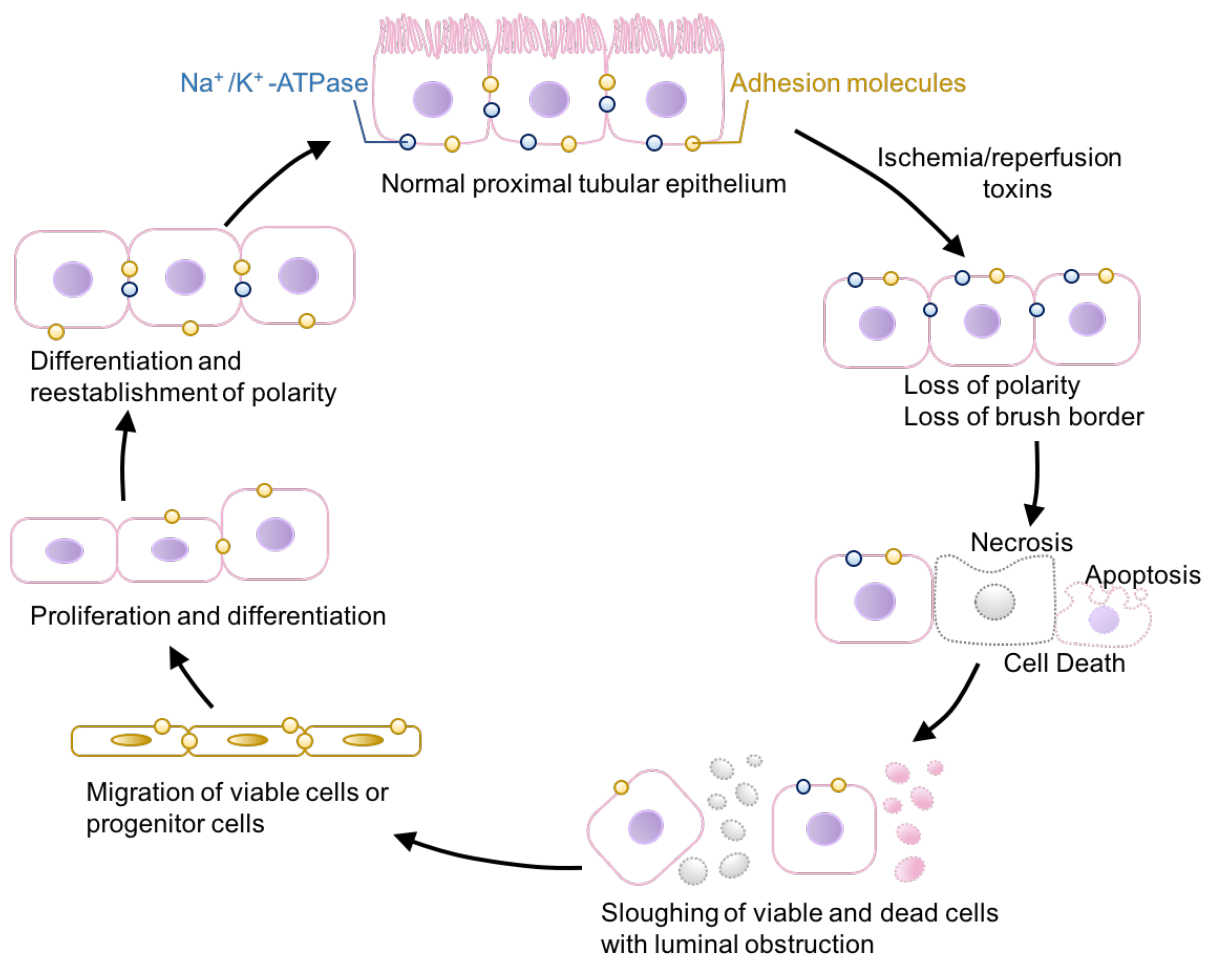


Figure 2: Ischemic injury and adaptive repair in renal epithelium.

With ischemic injury, proximal epithelial cells lose their brush border due to disrupted cytoskeletal integrity. Moreover, $\text{Na}^+/\text{K}^+-\text{ATPase}$ pumps and adhesion molecules, which are located at the basolateral membrane under physiological conditions, redistribute to the apical membrane of proximal tubular cells, leading to loss of cell polarity. With increasing time or severity of ischemia, cells undergo either necrosis or apoptosis, whereas the dead and detached viable cells can obstruct the tubular lumen. After injury, surviving epithelial cells or progenitor cells migrate to denuded basement membrane, differentiate and replace the lost cells. Integrity of functional nephrons is restored. This picture is adapted from Bonventre et al., 2011 [23].

1.1.3 Biomarkers for acute kidney injury

Biomarkers are objectively measured indicators for various biological processes, including disease [52, 53]. For instance, serum creatinine is an endogenous produced substance and is mainly excreted by kidneys, thus it is used for diagnosis and staging of acute kidney injury. However, serum creatinine as a biomarker of AKI has its limitations. First, level of serum creatinine depends on its generation and secretion, whereas the former is influenced by liver synthesis function and muscle mass [3]. Second, serum creatinine is determined as a concentration and varies by volume status. For example, the value decreases in patients with volume overload, such as in case of congestive heart failure [3]. Finally, serum creatinine rises delayed, namely after the actual occurrence of renal parenchymal damage or functional deterioration, thus hindering early detection of AKI [3, 54-56]. This has led to great enthusiasm in discovery and validation of more sensitive and specific biomarkers for AKI. The aim is to detect AKI faster, before there is an irreversible loss of organ function [2].

Biomarkers for AKI can be categorized in inflammatory, tubular injury and cell cycle arrest markers [54, 57] (Table 3). Neutrophil gelatinase-associated lipocalin (NGAL) and interleukin 18 (IL-18) mediate inflammation and are elevated already in the early stage of AKI [58-60]. Tubular injury markers include kidney injury molecule-1 (KIM-1) and liver-type fatty acid-binding protein (L-FABP) that are released during tubular damage [57, 61].

Table 3: Novel biomarkers for acute kidney injury (modified from [57, 62])

Biomarker types	Biomarkers	Samples	Production
Inflammatory	NGAL	Urine	25 kDa glycoprotein produced by epithelial tissues
	IL-18	Urine, serum	18 kDa cytokine released from proximal tubules, macrophages and intestines
Tubular injury	KIM-1	Urine	Transmembrane glycoprotein produced by proximal tubules
	L-FABP	Urine	14 kDa intracellular lipid chaperone produced in proximal tubules, liver, intestines and lung
Cell cycle arrest	TIMP-2	Urine	Produced by all epithelial cells
	IGFBP-7		

Recently, two mediators for cell cycle arrest have been identified as novel biomarkers for AKI, namely urinary tissue inhibitor of metalloproteinase-2 (TIMP-2) and insulin-like growth factor-binding protein-7 (IGFBP7). They were discovered and validated in independent, multicenter prospective clinical studies in over 1,000 critically ill patients [54, 63]. TIMP2 and IGFBP7 are expressed in tubular cells in response to DNA damage and initiate cell cycle arrest at G1/S checkpoint [64, 65]. This is a protective effect, because division and proliferation of damaged cell can be avoided [57, 66]. Interestingly, the product of these two markers, i.e. [TIMP-2] x [IGFBP7] were found to have a significantly superior performance in risk stratification for AKI, compared to all previously known biomarkers. These findings also underscore the importance of cycle arrest implicated in AKI, providing new insights into the pathophysiology of AKI.

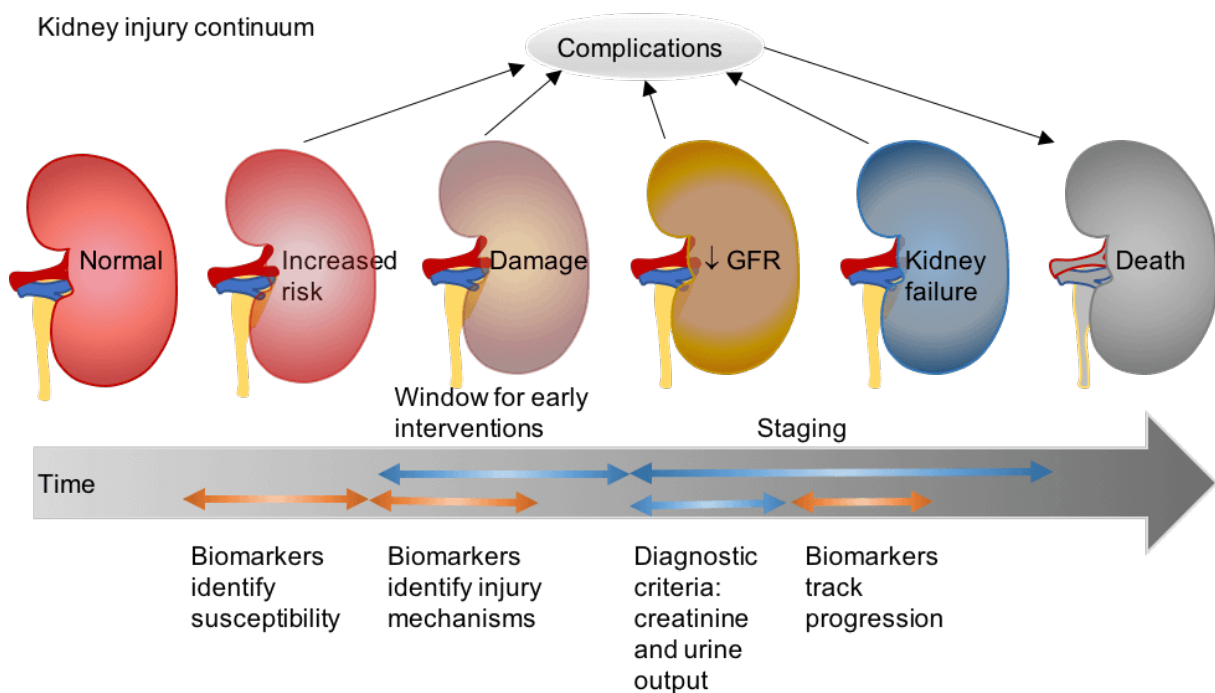


Figure 3: Potential use of new biomarkers for acute kidney injury.

Conventional markers for AKI such as creatinine is insensitive and non-specific, which can lead to delayed recognition and treatment of disease. A series of new biomarkers is discovered as more sensitive and specific in kidney injury and can be utilized in all stages of disease development. Biomarkers tested in urine or plasma may facilitate identification of susceptibility of individual patients, early detection of kidney damage, differentiation of injury mechanism and track disease progression at advanced stage. Thus, new biomarkers can promote timelier diagnosis and therapy, thereby reducing complications and improving the overall outcomes. This picture is modified from Lameire et al., 2008 [67].

Kidney-specific biomarkers may provide valuable aid in the assessment and management of AKI (Figure 3). First, they can detect renal structural damage even before kidney functional alterations occurs or serum creatinine rises [60, 68]. An early diagnosis of acute kidney injury is thus possible, and supportive interventions could be timely implemented, such as avoidance of nephrotoxic drugs and optimization of fluid management [62]. Second, biomarkers may inform the location and underlying etiology of AKI, such as differentiation between prerenal and intrinsic causes [62]. Third, biomarkers can help assess the severity and staging of AKI. Finally, biomarkers can provide information on prognosis and risk stratification for further complications [55].

However, these biomarkers have been only very limitedly applied in clinical settings [6, 55, 69]. Aside from the cost factors, the interpretive and practical issues need to be addressed and there exist no specific clinical recommendations. When should clinicians apply biomarker assays? Which one should they choose? What's the cut-off value? How can they interpret these data and make their decisions depending on the measurement results? Concerning this gap between existing knowledge and patient management, more research work requires to be accomplished in the future [55].

Acute kidney injury activates pathways of cell death, which contributes significantly to the severity of the syndrome [45]. Especially the injury and death of renal tubular cells are precipitating factors and major events during AKI [30]. As p53 plays an important role in regulating cellular life and death, we focused our research interest on roles of molecule p53 and its major negative regulator Mdm2 in renal tubular cells.

1.2 p53: guardian of genome

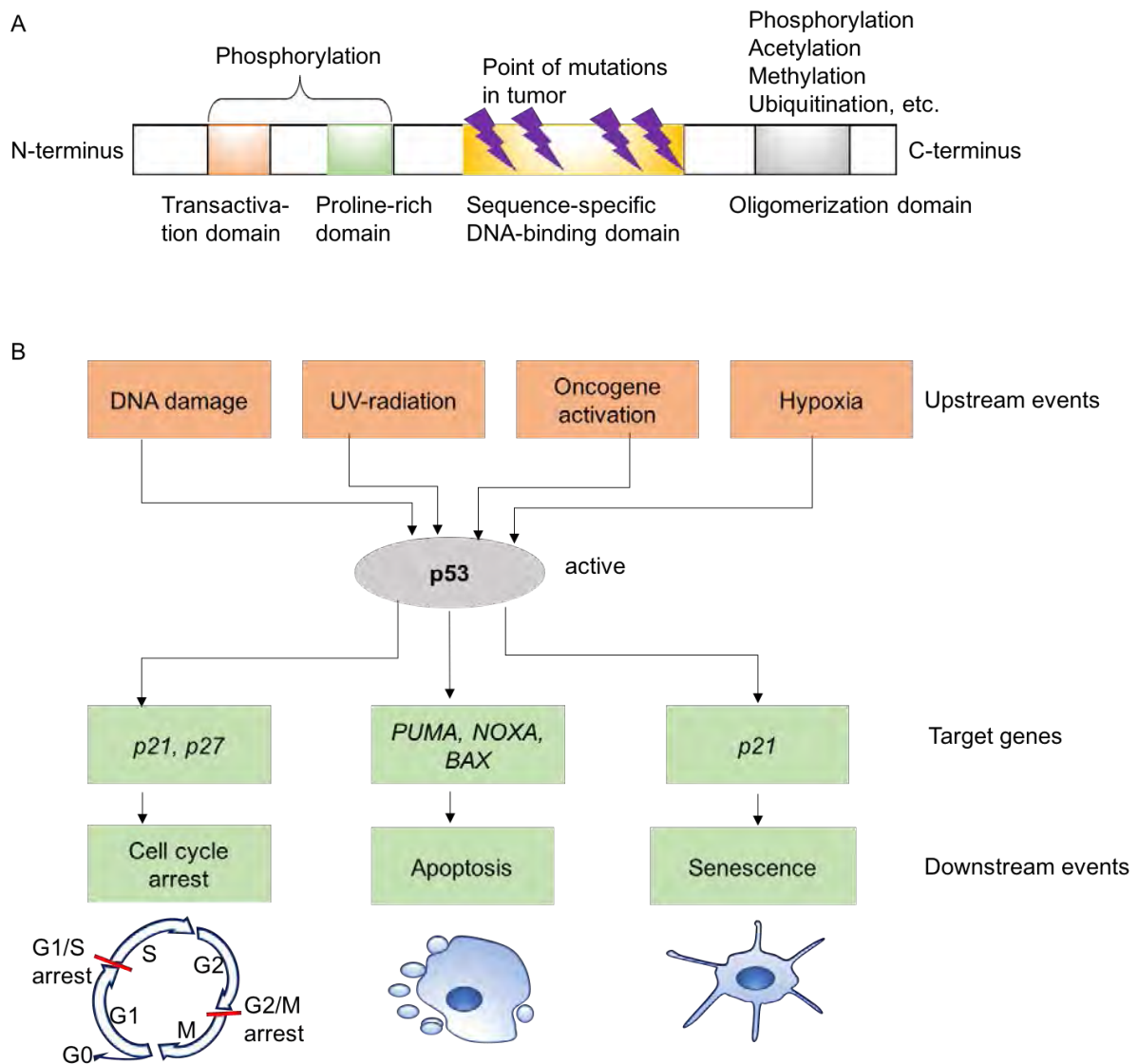
1.2.1 The protein p53

p53, well known as „guardian of genome” [70], has been rigorously studied since its identification and shed light on the understanding of cellular life and death. In 1979, p53 was found as a 54K Dalton protein in cells undergoing malignant transformation induced by simian virus 40 or adenovirus [71, 72]. Structural analysis reveals that human p53 protein consists of 396 amino acids and is encoded by TP53 gene in chromosome 17 [73]. As illustrated in Figure 4A, p53 protein contains structurally and functionally four domains [74]. First, a N-terminus transcriptional activation domain that interacts with its transcriptional machinery and its negative regulator Mdm2 [74]. Second, a proline-rich domain that is important for the apoptotic activity of p53. Third, central DNA-binding domain where mutations in cancers usually occur. Fourth, C-terminus oligomerization domain.

p53 is ubiquitously expressed in cells, and mainly acts as a transcription factor by activating a plethora of target genes. In response to cellular stress such as DNA damage, ionizing radiation and oncogene activation, p53 is activated and can induce three pathways [75] (Figure 4B):

- 1) cell cycle arrest, to ensure time for DNA repair and prevent cells from dividing incorrectly;
- 2) cell death, such as caspase-dependent apoptosis, to selectively destroy stressed cells and protect against tumor formation;
- 3) senescence, an irreversible cell-cycle arrest that stops damaged cells from dying [76].

Which scenario occurs, depends ultimately on the extent of injury: cell cycle progression is stopped if the injury is mild or moderate, whereas cells suffering a severe or sustained injury commit suicide when DNA damage cannot be repaired [77-79]. p53-dependent cell cycle arrest at G1/S checkpoint is mediated via induction of p21 [44].



reduced p53 level results in decreased cell death and increased proliferation, thereby providing advantageous conditions for tumor survival and progression [82, 83]. p53 was identified as a tumor suppressor protein in 1989, a decade after its discovery. Chromosome 17 deletions occur in over 75% of colorectal carcinomas, and p53 turns out to be a target of the deletions [84]. With further research, p53 mutation is also found in other solid tumors, namely in more than 50% of human cancers overall [85, 86], a higher rate than for any other known cancer-critical gene [76]. Most point mutations occur in the central DNA-binding domain with abrogation of p53 binding to its target DNA sequences, thereby blocking transcriptional activation of these genes [87]. In mouse models, p53-null mice spontaneously develop a variety of tumors including malignant lymphoma and sarcomas, indicating that p53 deficiency increases the susceptibility to neoplasm [88]. Another striking example is Li-Fraumeni syndrome, a rare autosomal dominant hereditary syndrome characterized by a high risk for various malignancies including sarcoma, leukemia, cancers of breast, brain and adrenal gland [89]. It is associated with germline mutation of *TP53* gene [90], which leads to loss of function of the tumor suppressor protein p53 [90, 91]. The finding of p53 provides new insights in cancer treatments, such as reactivating p53 to kill cancer cells. Due to such a great breakthrough in the life science, p53 was named “molecule of the year” in 1993 [92].

Normally, p53 is maintained at a low concentration in cells by its relatively short half-life (about 20 min) [87] and its negative regulator Mdm2 [93]. Furthermore, p53 activity is regulated by a variety of posttranscriptional mechanisms including phosphorylation, acetylation, sumoylation and glycosylation [94]. Under stress conditions, p53 is phosphorylated and cannot be degraded due to abrogation of p53-Mdm2 interaction. The level of p53 increases, leading to cycle arrest, apoptosis or senescence.

1.2.2 p53 and apoptosis

Activated p53 can induce apoptosis, directing cells to die. Apoptosis means “falling off” in Greek language, as leaves from a tree or petals from flowers [95]. It is a programmed cell death, through which cells destroy themselves in a highly regulated and controlled way. Cells undergoing apoptosis display characteristic morphological changes, including cell shrinkage, chromatin condensation (pykosis), nuclear fragmentation (karyorrhexis) and membrane blebbing with formation of apoptotic bodies [96]. Finally, they are engulfed and “eaten” by neighboring cells or macrophages, without leaking any cellular contents or causing a deleterious inflammatory response.

Apoptosis eliminates cells when they are no longer needed, irreversibly injured, or turn to be a threat to the organism [76]. In the human embryonic development, the individual fingers and toes separate because apoptosis of cells between them occurs. In homeostatic adult tissues, cell death and cell division must be kept in balance. Both excessive and insufficient apoptosis are associated with pathological processes: while accelerated apoptosis contributes to acute and degenerative disease, deficient apoptosis can give rise to tumorigenesis or autoimmune disorders [97].

The underlying biochemical mechanism for apoptosis is a caspase-mediated proteolytic cascade (Figure 5). Caspases are intracellular proteases that can cleave specific sequences in proteins, thereby activating signal transduction for cell death. There are initiator caspases (caspase 8,9) and executioner caspases (caspase 3,6,7), both normally exist as inactive precursors in cells and only activated during apoptosis [76]. Two best-understood apoptotic pathways are intrinsic and extrinsic pathways [81] with considerable crosstalk in between [22, 81]. The intrinsic pathway is mostly triggered by intracellular stress and starts from mitochondrial outer membrane permeabilization (MOMP). During MOMP, Cytochrome c, a protein that resides in the intermembrane space of mitochondria, is released into the cytoplasm, leading to activation of initiator caspase 9. MOMP is tightly controlled by BCL-2 family of proteins, including pro-apoptotic proteins such as BAX, BAK, PUMA and NOXA and anti-apoptotic proteins such as BCL and BCX. On the other hand, the extrinsic pathway is initiated by the binding of extracellular death ligands (FAS, TNF α) to their responsible death receptors on the surface of target cells, which recruits initiator caspase 8. In both intrinsic and extrinsic apoptotic pathways, executioner caspases are activated

by initiator caspases through proteolytic cleavage, thereby performing widespread intracellular protein cleavage that kill the cell.

p53 protein plays a key role in apoptosis. As a transcriptional factor, p53 upregulates genes that encode pro-apoptotic proteins PUMA, NOXA and BAX [93]. Moreover, p53 has transcriptionally independent activities such as transport of death receptors from the Golgi complex to cell surface, thereby engaging extrinsic pathway [98].

To date, there are numerous cell death modalities proposed based on morphology and signal transduction beyond apoptosis, such as necrosis and autophagy (Table 4). In contrast to apoptosis, cells undergo necrosis in response to extreme injuries or acute insults, such as trauma or toxins. Morphologically, necrotic cells swell instead of shrinking, they loss their membrane integrity, burst or disintegrate and spill out their cellular contents into extracellular space, causing an inflammatory response (Figure 6). Autophagy is a self-eating or self-cleaning process with massive vacuolization of the cytoplasm [99]. Autophagy can be a pro-survival mechanism that helps cells to survive, but can also induce cell death under certain circumstances [100]. The mechanism of autophagy is not fully understood and under current debate.

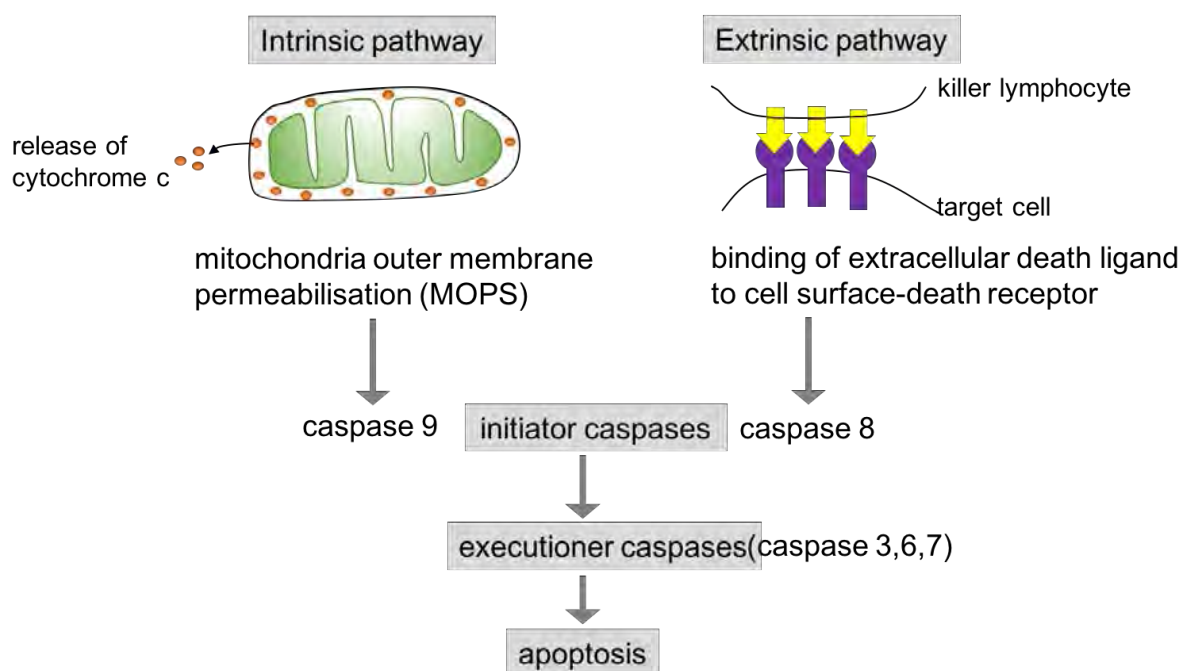
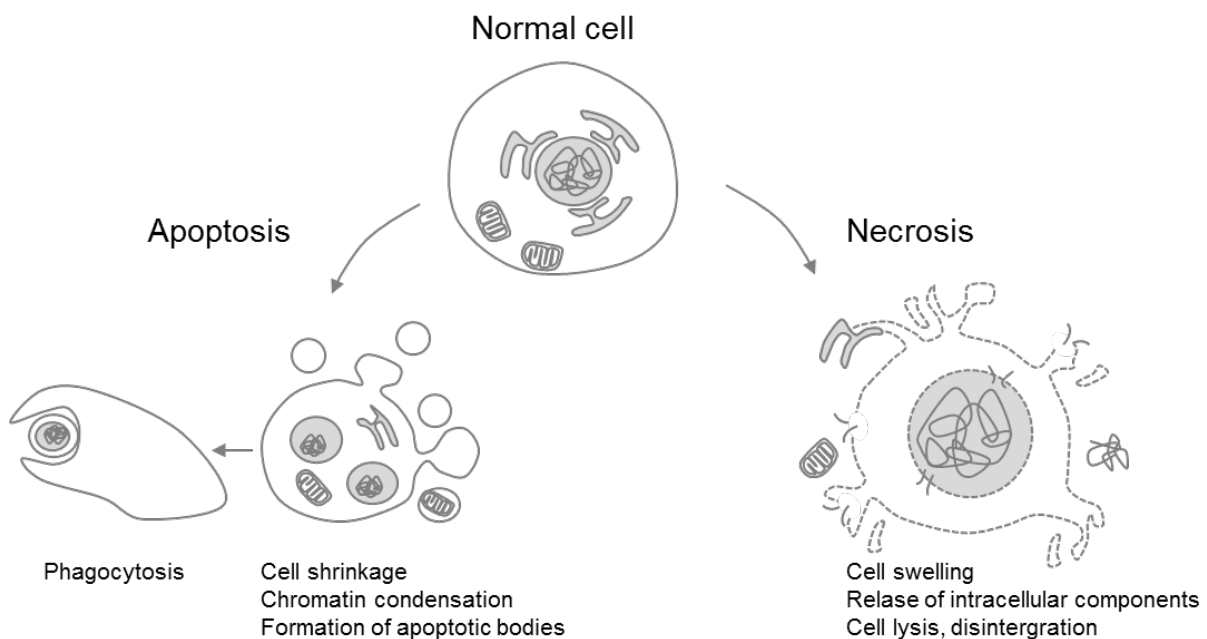


Figure 5: Intrinsic and extrinsic apoptotic pathways.

p53-induced apoptosis can engage intrinsic and extrinsic pathways. Intrinsic apoptotic pathway occurs in response to stress stimuli, and is initiated by mitochondria outer membrane permeabilisation (MOPS) with release of cytochrome C into cytoplasm. On the other hand, extrinsic apoptotic pathway is triggered by the binding of death ligand to their respective cell-surface receptors. Both pathways trigger a cascade of events, leading to activation of initiator and executioner caspases and cell death.

Table 4: Comparison of apoptosis, necrosis and autophagy

Cell death mode	Apoptosis	Necrosis	Autophagy
Activation	Moderate stress	Extreme, acute stress like trauma or toxins	Mild stress
Definition/Category	Programmed cell death	Programmed and not programmed cell death	“Self-eating” catabolic process involving lysosomes
Morphology	<ul style="list-style-type: none"> * Cell shrinkage * Membrane blebbing with maintained integrity * chromatin condensation, nuclear fragmentation * Apoptotic bodies formation 	<ul style="list-style-type: none"> * Cellular swelling * Loss of membrane integrity * Release of intracellular contents 	<ul style="list-style-type: none"> * Massive vacuolization of the cytoplasm * Increased quantity of autophagosomes formation
Inflammatory response	No	Yes	No
Destiny	Cell death: engulfed by neighboring phagocytes	Cell Death: ingested by macrophages	Survival or death

**Figure 6: Distinct morphological features of apoptosis and necrosis.**

Apoptotic cell shows nuclear fragmentation, while the cell membrane remains intact. The formatted apoptotic bodies are engulfed by a phagocytic cell. On the other hand, necrotic cell explodes, loses membrane integrity and releases its intracellular contents.

1.3 Mdm2: master inhibitor of p53

In 1987, Cahilly-Synder et al. identified *Murine Double Minute 2 (Mdm2)* gene as a strongly amplified DNA sequence present in a spontaneously transformed murine fibroblast cell line 3T3-DM [101]. *Mdm2* gene is found in double minutes, which are paired acentric chromatin bodies observed in abundant tumors [101]. *Mdm2* gene is evolutionarily conserved [102], located on chromosome 10 in mice and chromosome 12 in human [103]. Fakharzadeh et al. provided further *in vivo* evidence that *Mdm2* gene is tumorigenic, as *Mdm2*-overexpressing cells transfected in nude mice give rise to tumors rapidly [102].

1.3.1 The protein Mdm2

The murine *Mdm2* gene product is an intracellular protein with a molecular weight of 54 kDa [102]. Mdm2 protein consists of 489 amino acid [102], including a p53-binding domain, an acidic amino acid-rich domain, a zinc-finger-domain and a ring-finger-domain, as shown in Figure 7 [104, 105]. The ring domain of Mdm2 has E3 ligase activity, which is responsible for ubiquitination and degradation of proteins, including p53 and itself [106].

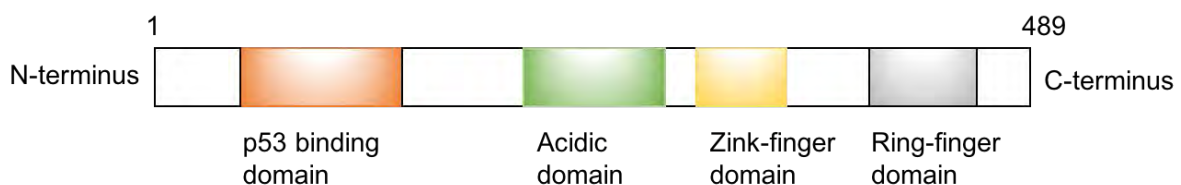


Figure 7: Schematic structure of Mdm2 protein.

From N- to C-terminus, the main motifs of Mdm2 protein are represented as p53 binding domain, acidic domain, Zink-finger domain and ring-finger domain. The numbers above the figure represent amino acid numbers. This figure is modified from Iwakuma et al., 2003 [104]

1.3.2 p53-Mdm2 autoregulatory feedback loop

Why can Mdm2 enhance transformation potential? Momand et al. revealed the reason, as they showed that Mdm2 can bind to the tumor suppressor protein p53 and inhibit p53-mediated cell cycle arrest, DNA repair and cell death [107]. In unchallenged cells, p53 and Mdm2 mutually regulate their levels tightly through an autoregulatory feedback loop (Figure 8). Mdm2 negatively regulates p53 in three ways:

- 1) Mdm2 functions as a E3 ubiquitin ligase and target p53 for proteasomal degradation.

- 2) Mdm2 chaperons p53 out of nucleus, namely out of the transcriptional center and causes loss of p53 function.
- 3) Mdm2 directly blocks the transcriptional activity of p53 by binding to its N-terminus transactivation domain and causing its configuration change [108].

The transcription of p53 target genes is thus diminished.

In turn, p53 activates the transcription of *Mdm2* gene by binding to its *P2* promoter. That is to say, p53 can upregulate its own inhibitor transcriptionally. During homeostasis, p53-Mdm2 autoregulatory feedback loop keeps both molecules in balance. In response to cellular stress, p53 and Mdm2 are posttranslationally modified such as with phosphorylation [93, 108], which blocks the p53- Mdm2 interaction. Also, Mdm2 can ubiquitinate itself upon DNA damage, resulting in auto-degradation [109]. The restoration of p53 results in consequent transcriptional activation of p53 target genes, leading to cell cycle arrest, cell death or senescence.

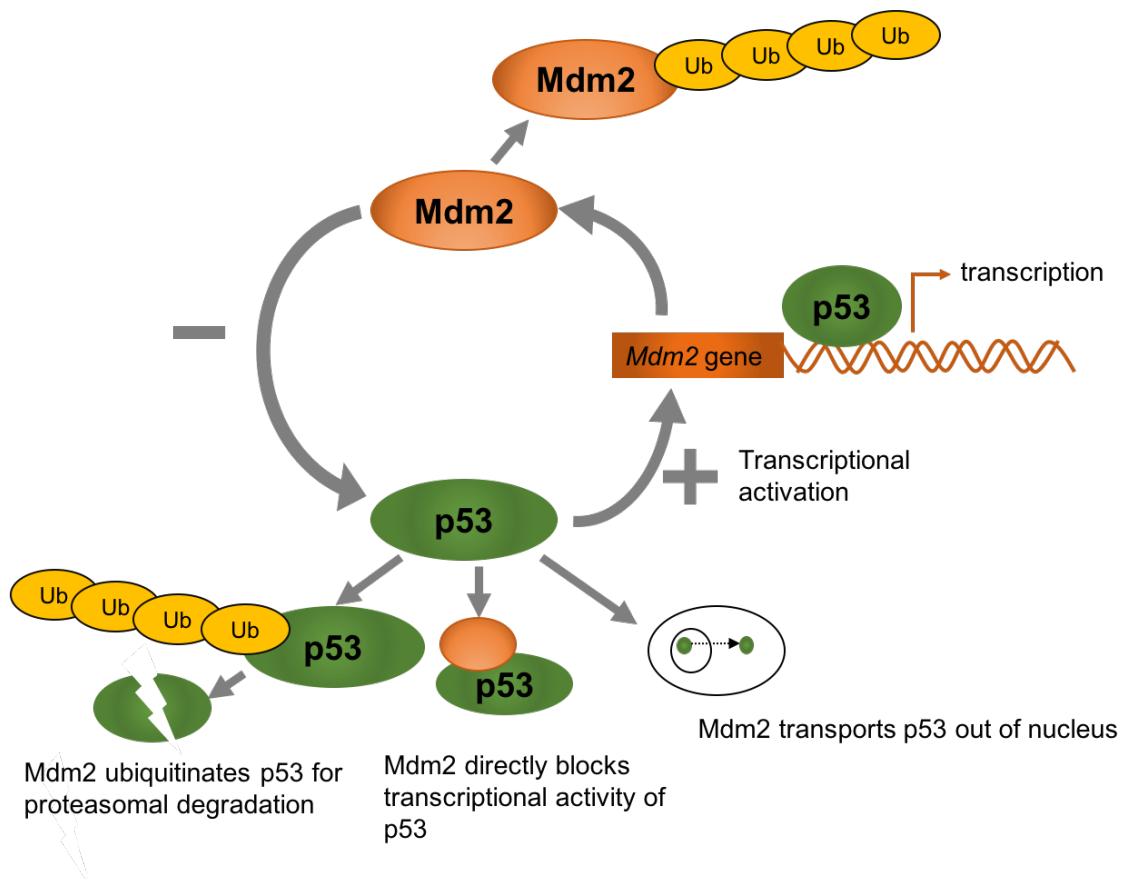


Figure 8: p53-Mdm2 autoregulatory feedback loop.

The E3-ubiquitin ligase Mdm2 negatively regulates p53 by ubiquitination, direct binding and nuclear export of p53. Mdm2 can also ubiquitinate itself for proteasomal degradation. In turn, p53 activates transcription of *Mdm2* gene, resulting in increased level of Mdm2. Thus, p53 and Mdm2 mutually regulate their levels through an autoregulatory feedback loop.

1.3.3 Biological functions of Mdm2

Mdm2 molecule exerts diverse biological functions in tumor development, embryogenesis, homeostatic adult tissues, inflammation and wound healing.

Mdm2-overexpression promotes tumorigenesis

Mdm2 is well known as an oncoprotein for its tumorigenic potential, as evidenced by numerous animal studies. Jones et al. generated transgenic mice that overexpress Mdm2 to 4-fold in comparison with control mice. Strikingly, all these transgenic mice develop tumors spontaneously, such as malignant lymphomas and sarcomas [110]. Also, mice with Mdm2-overexpression in mammary epithelium or skin are more susceptible to spontaneous tumor formation compared with control mice [111, 112]. Mechanistically, Mdm2-overexpression results in decreased activity of p53-mediated cell cycle control and cell death and increased proliferation. This provides growth advantages for tumor development.

In human sarcomas, Oliner et al. discovered significant *Mdm2* gene amplification and overexpression in more than third of 47 analyzed samples [103]. In human leukemias and lymphomas, overexpression of *Mdm2* gene was observed despite the absence of amplification [113]. Furthermore, Momand et al. examined over 3500 samples from 28 tumor types, and detected *Mdm2* amplification in 19 tumor types with an overall frequency of 7%. The highest frequency of *Mdm2* amplification was found in soft tissue tumors (20%), osteosarcomas (16%) and esophageal carcinomas (13%). [114].

Although both *Mdm2*- and *p53*-mutation were observed in abundant malignancies, they generally do not occur simultaneously within the same tumor sample [114]. In other words, Mdm2 is overexpressed predominantly in cancers with wild-type p53 [115]. The explanation is that *Mdm2* amplification or mutation is a growth advantage, only when p53 is wildtype and its activity can be inhibited by Mdm2-overexpression [116].

Mdm2 is essential for embryogenesis and homeostatic adult tissues

A complex network of growth stimulatory and differentiation signals is required during embryogenesis and organ formation [117]. To check the necessity of Mdm2 for embryonic development, transgenic mice with germline *Mdm2*-depletion were created. *Mdm2*-null mice die in early embryonic phase prior to implantation and present with developmental defects in histological analysis. Strikingly, these lethal phenotypes are

completely rescued by co-depletion of *p53*, as all *Mdm2/p53* double-null mice are viable and develop normally [118, 119]. These data indicate that Mdm2 is vital for the embryonic development, and loss of Mdm2 results in p53-overactivation which leads to unimpeded apoptosis and lethality.

Is Mdm2 also necessary for homeostatic adult tissues? To answer this question, Zhang et al. generated inducible *Mdm2* knockout mice. Strikingly, global *Mdm2* deletion induced by tamoxifen injection causes 100% lethality in both young adult mice (2-4 months old) and aged mice (16-18 months), and this phenotype is p53-dependent [120].

Experiments with hypomorphic and haploinsufficient mice provided further evidence for the necessity of Mdm2 in adult tissues. Mendrysa et al. created mice carrying a hypomorphic allele of *Mdm2* with a reduction of mRNA levels to approximately 30% in all tissues compared to wild-type mice. These genetically altered mice are viable and develop normally, but display relative to wild-type mice smaller body size, decreased body weight and lighter organs, especially in lymphoid organs such as spleen and thymus. This is consistent with major defects in lymphopoiesis presenting with markedly declined lymphocytes number in peripheral blood, spleen, thymus and bone marrow. Moreover, these mice are more sensible to ionizing radiation in comparison with wild-type mice. Interestingly, all these observed abnormalities are proofed to be p53-dependent, as crosses with *p53*-null mice completely rescue the deleterious phenotypes [121]. Terzian et al. generated haploinsufficient mice (*Mdm2*^{+/-}) which only have one functioning copy of the wild-type *Mdm2* allele, i.e. 50% of normal expression. These mice live an average life span but exhibit increased radiosensitivity in a p53-dependent manner, emphasizing the importance of sufficient Mdm2 level in response to DNA damage [122].

Mdm2 has a proinflammatory role

Mdm2 has also a p53-independent function in nuclear factor-kappa beta (NF-κB) signaling [115]. NF-κB proteins are transcription regulators that play a central role in inflammatory responses. NF-κB-dependent signaling pathway can be activated by various cell-surface receptors, such as Toll, Toll-like, IL-1 and TNF receptors. Activated NF-κB turns on transcription of numerous target genes that participate in inflammatory responses [76]. Mdm2 is a transcriptional target as well as a regulator of

NF- κ B signaling [123-125]. By facilitating NF- κ B signaling, Mdm2 has a proinflammatory role [123], which is evidenced by various *in vivo* studies.

For instance, in a lupus nephritis mouse model (*MRL-Fas^{lpr}* mice), disease progression is associated with increased *Mdm2* mRNA expression in the spleen and kidneys. Mdm2 inhibitor nutlin-3a ameliorates systemic inflammation, as documented by a reduction of plasma cells, production of lupus autoantibodies and expansion of T cells compared to control mice. Also, nutlin-3a prolongs survival of lupus mice. This study suggests that Mdm2 drives inflammation in systemic lupus erythematoses (SLE) and antagonizing Mdm2 may have therapeutic potential in SLE [126]. In another mouse model for lipopolysaccharide (LPS)-induced acute lung injury, Mdm2 antagonist nutlin-3a suppresses lung inflammation by suppressing NF- κ B DNA-binding activity in neutrophils and macrophages [127]. Moreover, MDM2 is overexpressed in cells in human atherosclerosis plaques [128], and nutlin-3 significantly attenuates NF- κ B-dependent inflammation in vascular smooth muscle cells [129].

Mdm2 fosters tissue repair and wound healing

Wound healing is a complex biological process which occurs after an injury [130]. Despite the differences of insults and organs, the wound repair process is similar in almost all tissues and consists of four overlapping but distinct phases: clotting, inflammation, reepithelialization and tissue remodeling [130, 131]. Mdm2 has a proliferative function by inhibiting p53-mediated cell cycle arrest and apoptosis [123]. The growth-promoting effect of Mdm2 is required for tissue repair and wound healing, which is elucidated by a study with skin epithelium-specific *Mdm2* knockout mice. Mice lacking *Mdm2* in epidermis develop an accelerated aging phenotype with progressive hair loss, decreased skin elasticity and thinning epidermis layer over time, compared with controls. In wound healing assay by a biopsy on the dorsum, these knockout mice exhibit slower wound healing process. Also, in hair growth assay by hair shaving, fur re-growth is delayed in knockout mice due to reduced tissue regenerative potential upon *Mdm2* deletion [132].

1.3.4 Mdm2 in the kidney

In developing mammalian kidneys, Mdm2 and p53 is highly expressed in all cell lineages including epithelial, mesenchymal and stromal compartments [133]. To check the role of Mdm2 in kidney development, Hilliard et al. created mice with conditional deletion of *Mdm2* in the ureteric bud epithelium (UB^{Mdm2^{-/-}}), which give rise to collecting duct system [117, 133]. These mice die soon after birth and show severe renal hypodysplasia, branching defects and nephron deficit caused by aberrant apoptosis and growth arrest due to p53 accumulation [133, 134]. In another study, Hilliard et al. reported that germline *Mdm2* deletion in nephron genitor cells (NPC) leads to perinatal lethality as well [135]. NPCs are housed in cap mesenchyme from metanephric mesenchyme and have self-renewing ability [117]. NPC^{Mdm2^{-/-}} mice display hypoplastic kidneys, NPC loss and nephron deficit with increased apoptosis and reduced proliferation due to unconstrained p53 activity [135]. The fatal phenotype of both UB^{Mdm2^{-/-}} and NPC^{Mdm2^{-/-}} mice is rescued by concomitant *p53* deletion, suggesting that Mdm2 is indispensable during nephrogenesis by restraining p53 activity [117, 133, 135].

Mdm2 mRNA expression in kidneys declines after birth [117]. Nevertheless, Mdm2 is consecutively expressed in podocytes and tubular epithelium in adult kidneys [136, 137] (Figure 9), but what for is not fully understood. To examine the role of Mdm2 in homeostatic podocytes, Thomasova et al. generated transgenic mice with podocyte-specific *Mdm2* knockout (*Mdm2^{-/-podocyte}*) [138]. These mice are vital and phenotypically indistinguishable from the wildtype until 3 weeks of age. With increased age, *Mdm2^{-/-podocyte}* mice develop evident focal segmental glomerulonephritis with progressive podocyte loss, accompanied by significant proteinuria and reduced lifespan. This detrimental phenotype is completely rescued by podocyte-double-knockout *Mdm2/p53^{-/-podocyte}*, indicating that Mdm2 is required for podocytes to maintain homeostasis by keeping p53 at low levels [138]. However, whether Mdm2 is also essential for renal tubular epithelial cells has not been investigated, which motivates us to accomplish further studies as described in this dissertation.

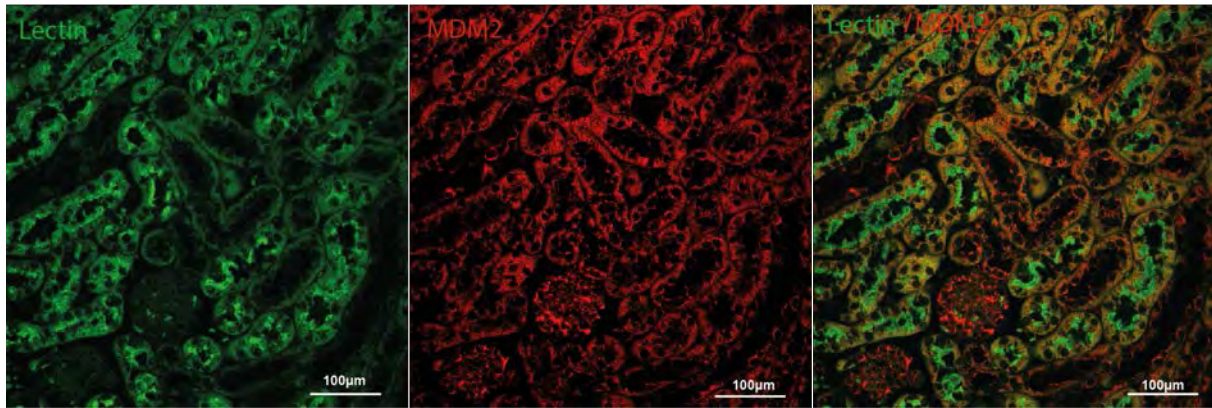


Figure 9: Mdm2 is strongly expressed in renal tubular cells.

Representative images of kidney sections of wildtype mice with C57BL/6 background, stained with Lectin tetragonolobus that marks living proximal tubular cells, Mdm2 immunofluorescence and the fusion of both (Lectin/Mdm2). With permission of Dr. Dana Thomasova [139].

Mdm2 drives inflammation by facilitating NF- κ B signaling in kidney disease, vice versa, Mdm2 inhibitor can dampen inflammatory response in kidneys. For instance, in a mouse model of adriamycin induced focal segmental glomerulosclerosis, treatment with Mdm2 antagonist nutlin-3a significantly attenuates disease progression compared to control mice, as evidenced by reduction of intrarenal cytokine and chemokine expression, glomerular macrophage and T cell amounts, and serum creatinine and blood urea nitrogen levels [137]. Also, in experimental rapidly progressive glomerulonephritis, either pre-emptive or delayed Mdm2 blockade with nutlin-3a shows protective effects by dampening NF- κ B dependent inflammation [140].

In acute kidney injury, Mdm2 acts like a double-edged sword in mediating both harmful and beneficial effects [141]. Mdm2 fosters inflammation by facilitating NF- κ B signaling in the early stage of AKI, but promotes renal regeneration by limiting p53-mediated cell death in the later stage of AKI [136]. Kidney repair following ischemic, septic or toxic injury is conceptually similar to epithelial regeneration in other organs including skin wound repair [130, 136]. Adaptive repair after AKI is predominately mediated by regeneration of surviving tubular epithelial cells, which finally leads to restoration of physiological nephron structure and function [142]. Treatment with Mdm2 antagonist nutlin-3a attenuates inflammation, but aggravates acute kidney injury in the healing phase, as the growth stimuli of surviving cells are suppressed by p53 activation [136].

1.4 Targeting p53-MDM2 interaction: clinical potential

Human MDM2 protein represents an attractive therapeutic target for cancer therapy [143]. Antagonism of MDM2 results in restoration of p53 activity, which leads to cell cycle arrest, apoptosis and subsequently suppression of tumor growth. Among different approaches of releasing p53 from MDM2 control, inhibition of MDM2-p53 interaction appeared the most progressed strategy [144, 145]. Using the crystallographic structures of MDM2 and p53, the first potent and selective small-molecule MDM2 antagonist nutlin was identified by Vassilev et. al in 2004 [146]. As shown in Figure 10, Nutlin has a strong affinity to MDM2 and binds to its hydrophobic pocket of N-terminus, thereby blocking the interaction of MDM2 and p53 specifically [146]. There are nutlin-1, nutlin-2 and nutlin-3, whereas nutlin-3 possess the most potent binding activity and most commonly used in cancer research [146, 147]. The anti-cancer effects of nutlin is evidenced by numerous *in vivo* and *in vitro* studies. For instance, nude mice bearing human cancer xenografts showed successful tumor-growth inhibition and tumor regression after 3 weeks treatment with nutlin injection [148]. Importantly, nutlin requires wild-type p53 in cancer cells for their effectiveness [144].

However, nutlin was found to have poor bioavailability and high toxicity, which prevented its translation to the clinic [145]. Recently, new nutlin-derivatives with optimization in bioavailability and potency were discovered, some of which have advanced into clinical trials for treatment of human cancers [145, 149, 150], such as the most developed compound RG7112 [151-153].

Nevertheless, potential adverse effects of MDM2 inhibitors are important issues to be addressed. One key concern is drug safety regarding the toxicity on normal tissues [144]. The desired anti-proliferative and pro-apoptotic effects of MDM2 antagonist in cancer can also affect healthy organs and tissues, especially those with a high proliferative index such as hematopoietic system and intestinal epithelium. For instance, grad 4 neutropenia and thrombocytopenia were observed in 30% and 15% of patients in the clinical trial of RG7112 in liposarkoma respectively [154, 155]. Also, long-term toxicities of exposure to MDM2 inhibitors are not examined [145]. Another concern is acquired resistance of tumor cells to cancer drugs [144]. Taken together, the clinical potential of small molecule MDM2 antagonist is promising, yet remains to be further studied.

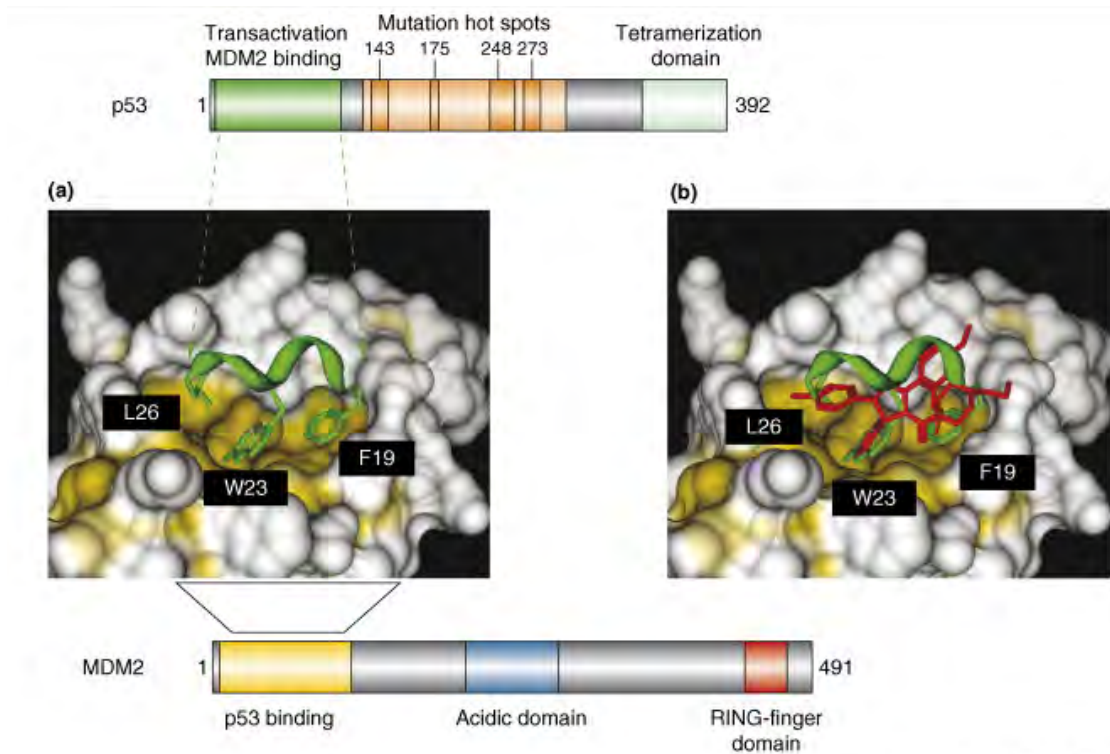


Figure 10: Nutlin inhibits p53-MDM2 interaction

(a) Crystallographic structure of p53-MDM2 binding illustrates that the three amino acid residues of the p53 protein (green) are inserted into a deep pocket of MDM2 (yellow). (b) Nutlin-2 (red) mimics the three amino acid residues of p53 (green) and binds to the pocket of MDM2 (yellow), thereby efficiently blocking the p53-MDM2 binding. Picture taken from Vassilev *et al.*, 2007 [144] with permission (licence number 4335880094078, licence date Apr 25, 2018).

2 Research hypothesis

Renal tubular cells are a central component in the pathophysiology of acute kidney injury (AKI): they are not only passive victims, but also active participants by mediating sterile inflammation. Tubular cells also contribute to the kidney regeneration after injury. Despite the ongoing debates, one well-recognized theory is that tubular cells dedifferentiate and proliferate to replenish the lost cells and restore the functional integrity of the nephron. A maladaptive repair, however, can lead to kidney fibrosis and chronic kidney disease, which are serious long-term complications of AKI.

Murine Double Minute 2 (Mdm2) is a key negative regulator of p53. During acute kidney injury, Mdm2 plays dual roles: on one hand Mdm2 promotes inflammation in the early stage, which aggravates AKI; on the other hand Mdm2 fosters regeneration in the later stage, which is beneficial for the healing after AKI [136].

However, the role of Mdm2 in homeostatic renal tubular cells is not fully understood. Renal tubular cells constitutively express high levels of Mdm2 under physiological conditions [136], but what for is unknown. Studies published to date have not investigated the role of Mdm2 in unchallenged tubular cells of adult healthy kidneys in a tissue-specific manner. Moreover, MDM2-antagonists such as nutlin and its analogs are extensively researched for anti-cancer therapy, which can however suppress Mdm2 levels in kidneys with potential side effects. In this background, we studied the role of Mdm2 in quiescent renal tubular cells with the following hypothesis:

Mdm2 and its negative regulation of p53 is essential for the homeostasis of renal tubular epithelial cells. Deletion of *Mdm2* can lead to p53-upregulation, causing disorders and even death of renal tubular cells.

3 Materials and Methods

3.1 Materials

3.1.1 Instruments

Pipettes

Serological pipettes 5ml, 10ml, 25ml	BD, Heidelberg, DE
Pipette Pipetman	Gilson, Middleton, WI, USA
Multichanal pipette	Eppendorf AG, Hamburg, DE
Pipette Easypet	Eppendorf AG, Hamburg, DE
Pipette Pipetus	Hirschmann Laborgeräte, DE
Pipetting aid Pipetus-classic	Hirschmann Laborgeräte, DE
Pipette tips 1 - 1000 µl TypGilson	Peske, Aindling-Arnhofen, DE
Pipette tips epT.I.P.S	Eppendorf AG, Hamburg, DE

Balances

Analytic Balance, BP 110 S	Sartorius, Göttingen, DE
Mettler PJ 3000	Mettler-Toledo, Greifensee, CH

ELISA

ELISA reader Tecan, GENios Plus	Tecan, Crailsheim, DE
ELISA Micoplate Strip Washer ELx50	BioTek, Bad Friedrichshall, DE

Centrifuges

Centrifuge Heraeus, Minifuge T	VWR Internation, Darmstadt, DE
Centrifuge Heraeus, Sepatech Biofuge A	Heraeus Sepatech, Osterode, DE
Centrifuge 5415 C	Eppendorf, Hamburg, DE
Centrifuge 5418 C	Eppendorf, Hamburg, DE
Universal 16	Hettich, Bäch, CH

RNA isolation, gel electrophoresis, cDNA and Real-time PCR

Homogenizer Ultra Turrax T25	IKA GmbH, Staufen, DE
Nano drop	PEQLAB Biotechnology, Erlangen DE
Electrophoresis gel chamber MiniVE	Amersham, Glattbrugg, CH
Electrophoresis voltage power PAC 3000	BioRad, Munich, DE
LightCycler 480 Real-Time PCR System	Roche, Basel, CH
Adhesive Foil	Roche, Basel, CH

LightCycler 480 Multiwell-Plate 96 Roche, Basel, CH

Histology and Microscopes

Microtome HM 340E	Microm, Heidelberg, DE
Tissue processors	Leica Microsystems, Wetzlar, DE
Light microscope Leitz DM IL	Leica Microsystems, Wetzlar, DE
Light microscope Zeiss Axioplan 2	Carl-Zeiss AG, Oberkochen, DE
LSM 510 confocal microscope	Carl-Zeiss AG, Oberkochen, DE
Libra 120	Carl-Zeiss AG, Oberkochen, DE
CCD camera	Tröndle, Moorenwies, DE
Axiocam HR	Carl-Zeiss AG, Oberkochen, DE
JEOL 1200 EX electron microscope	JEOL, Tokyo, Japan

Miscellaneous

Disposable cuvettes 1,5ml	Brand, Gießen, DE
Eppendorf tubes 1,5ml	TPP, Trasadingen, CH
Falcons 15ml, 50ml	BD, Heidelberg, DE
Thermomixer 5436	Eppendorf, Hamburg, DE
Vortex Genie 2™	Bender & Hobein AG, Zürich, CH
pH meter WTW	WTW GmbH, Weilheim, DE

3.1.2 Materials for animal experiments

Doxycycline	Sigma-Aldrich, Steinheim, DE
Sucrose	B. Braun, Melsungen, DE

Blood sample collection

EDTA	Biochrom, Berlin, DE
Isofluran Forene	Abbott, Chicage, USA
Mikropipetten 20µl	Blau, Wertheim, DE

Kidney isolation

Formaldehyde	ThermoFischer, Waltham, USA
RNA-later	Qiagen GmbH, Hilden, DE
Embedding cassettes	Simport, St.-M.-de-Beloeil, CA

3.1.3 Materials for molecular biology methods

DNA isolation

QIAamp DNA Mini Kit	Qiagen GmbH, Hilden, DE
---------------------	-------------------------

Proteinkinase K Merck, Darmstadt, DE

RNA isolation

PureLink® RNA Mini Kit Qiagen GmbH, Hilden, DE
 RNase free Spray Gene Choice, Frederick, USA
 RNase-Free® DNase Set Qiagen, Hilden, DE
 β-Mercaptoethanol Carl Roth, Karlsruhe, DE
 100 % Ethanol Merck, Darmstadt, DE

Gel electrophoresis

Agarose powder Invitrogen, Karlsruhe, DE
 Ethidium bromide Roth, Karlsruhe, DE
 RNA loading buffer Sigma-Aldrich, St. Louis, USA
 10x MOPS buffer 200 mM MOPS, 50 mM sodium acetat, 10 mM EDTA, 50 mM sodium acetate, adjust pH to 7.0 with 1 N NaOH, solved in 1 L water
 1 x TBE buffer 108g Tris, 55g boric acid, 5.84g EDTA, solved in 10 L water

cDNA Synthesis

Nano drop PEQLAB Biotechnology, Erlangen DE
 Thermomixer 5436 Eppendorf, Hamburg, DE
 Superscript II (Reverse transcriptase) Invitrogen, Karlsruhe, DE
 Linear Acrylamid Ambion, Darmstadt, DE
 0,1M DTT Invitrogen, Karlsruhe, DE
 25 mM dNTPs GE Healthcare, München, DE
 5x First Strand Buffer Invitrogen, Karlsruhe, DE
 Diethyl pyrocarbonate (DEPC) Sigma-Aldrich, St. Louis, USA
 RNAsin® Promega, Fitchburg, USA
 Hexanucleotide-Mix Roche Life Science, Basel, CH

Real time polymerase chain reaction (RT-PCR)

Primer Metabion GmbH, Planegg, DE

Table 5: Primers used for PCR

Gene	Primer sequence	
18s	Forward primer	5'-GCA ATT CCC CAT GAA CG-3'
	Reverse primer	5'-AGG GCC TCA CTA AAC CAT CC-3'
Mdm2	Forward primer	5'-TGT GAA GGA GCA CAG GAA AA -3'
	Reverse primer	5'-TCC TTC AGA TCA CTC CCA CC -3'
Cre	Forward primer	5'-GCA TAA CCA GTG AAA CAG CAT TGC TG-3'
	Reverse primer	5'-GGA CAT GTT CAG GGA TCG CCA GGC G-3'
Pax8	Forward primer	5'-CCA TGT CTA GAC TGG ACA AGA-3'
	Reverse primer	5'-CTC CAG GCC ACA TAT GAT TAG-3'
p53	Forward primer	5'-CTA GCA TTC AGG CCC TCA TC-3''
	Reverse primer	5'-TCC GAC TGT GAC TCC TCC AT-3'
p21	Forward primer	5'-CGGTGTCAGAGTCTAGGGGAn-3'
	Reverse primer	5'-ATCACCAGGATTGGACATGG-3'
Puma	Forward primer	5'-CACCTAGTTGGGCTCCATTT-3'
	Reverse primer	5'-ACCTCAACGCGCAGTACG-3'
Kim-1	Forward primer	5'-TGG TTG CCT TCC GTG TCT CT-3'
	Reverse primer	5'-TCA GCT CGG GAA TGC ACAA-3'
Ngal-1	Forward primer	5'-TGA ACT TCT GAA AAC GGCT-3
	Reverse primer	5'-AGC AGC AAG GGC ACA AT-3'
Timp-2	Forward primer	5'-CGT TTT GCA ATG CAG ACG TA-3'
	Reverse primer	5'-GAA TCC TCT TGA TGG GGT TG-3'
Tgf-beta	Forward primer	5'-GGA GAG CCC TGG ATA CCA AC-3'
	Reverse primer	5'-CAA CCC AGG TCC TTC CTA AA-3'
Fibronectin	Forward primer	5'-GGA GTG GCA CTG TCA ACC TC-3'
	Reverse primer	5'-ACT GGA TGG GGT GGG AAT-3'
Collagen 1a1	Forward primer	5'-ACA TGT TCA GCT TTG TGG ACC-3'
	Reverse primer	5'-TAG GCC ATT GTG TAT GCA GC-3'
Collagen 4a1	Forward primer	5'-GTC TGG CTT CTG CTG CTC TT-3'
	Reverse primer	5'-CAC ATT TTC CAC AGC CAG AG-3'
α-Sma	Forward primer	5'-ACTGGGACGACATGGAAAAG-3'
	Reverse primer	5'-GTTCAAGTGGTGCCTCTGTCA-3'

10x Taq buffer without detergent	Fermentas, St. Leon-Rot, DE
SYBR Green Dye detection	Applied Biosystems, Norwalk, USA
BioStab PCR Optimizer	Bitop, Witten, DE
10 x PE-buffer	ThermoFisher, Waltham, USA
1,25mM dNTPs	Metabion GmbH, Planegg, DE
Taq-DNA-Polymerase	New England BioLabs, Ipswich, USA
Diethyl-Pyrocarnat (DEPC)	Sigma-Aldrich, St. Louis, USA
SYBR Green	Roche, Mannheim, DE
Creatinine FS kit	DiaSys, GmBH, Holzheim, DE
Urea FS kit	DiaSys, GmBH, Holzheim, DE

3.1.4 Materials for histological methods

PAS stain

Periodic acid-Schiff (PAS)	Sigma-Aldrich, St. Louis, USA
Xylene	Merck, Darmstadt, DE

Immunohistochemistry and immunofluorescence

Unmasking solution	Vector Laboratories, Burlingame, USA
Avidin/biotin blocking kit	Vector Laboratories, Burlingame, USA
Avidin/biotin complex reagent	Sigma-Aldrich, St. Louis, USA
Tris-hydrochlorid	Sigma-Aldrich, St. Louis, USA
Nickel (II)-chloride	Sigma-Aldrich, St. Louis, USA
Hydrogen peroxide (H ₂ O ₂)	Sigma-Aldrich, St. Louis, USA
DAB	Sigma-Aldrich, St. Louis, USA
DAB staining solution	200 ml TRIS-HCL (37°C), 4ml DAB, 1ml NiCl ₂ , 500 µl 3% H ₂ O ₂
Methyl green	Sigma-Aldrich, St. Louis, USA
Vecta Mount mounting medium	Vector Laboratories, Burlingame, USA

Antibodies

Anti-mouse Mdm2 (rabbit)	Abcam, Cambridge, UK
Anti-mouse p53 (rabbit)	Vector Laboratories, Burlingame, USA
Anti-mouse Ki-67 (rabbit)	Dako Deutschland GmbH, Hamburg, DE
Anti-mouse cleaved caspase-3 (rabbit)	Cell signaling Technology, USA
<i>Lotus Tetragonolobus Lectin</i>	Vector Laboratories, Burlingame, USA
Tamm-Horsfall protein	Santa Cruz, CA, USA

Anti-mouse Aquaporin 2 (rabbit)
DAPI
Cell death detection (TUNEL) kit

Abcam, Cambridge, UK
Sigma-Aldrich, St. Louis, USA
Roche, Mannheim, DE

Electron microscope

Glutaraldehyde
Paraformaldehyde
Sodium cacodylate (buffer 7.4)
Propylene oxide
Embed-812
Uranyl acetate
Lead(II) nitrate

Sigma-Aldrich, St. Louis, USA
Sigma-Aldrich, St. Louis, USA
Sigma-Aldrich, St. Louis, USA
Sigma-Aldrich, St. Louis, USA
EM Sciences, Hatfield, USA
Sigma-Aldrich, St. Louis, USA
Sigma-Aldrich, St. Louis, USA

3.1.5 Softwares

Microsoft Office 365
Graphpad Prism 6
Endnote X8
Adobe Illustrator CC 2017
Software LSM

Microsoft, WA, USA
GraphPad Software, Inc., CA, USA
Thomson- Reuters, NY, USA
Adobe Systems Incorporated, USA
Carl Zeiss, Oberkochen, DE

3.2 Animal experiments

3.2.1 Animal housing

All mice were raised in poly-propylene cages under standard conditions with the room temperature of $22\pm 2^{\circ}\text{C}$ and 12 hours light and dark cycle. Maximal 5 mice were housed in each cage. All mice were supplied with water and standard chow diet (Sniff, Soest, Germany) *ad libitum* for the entire duration of the study. Cages, bedding, nestles, food, and water were sterilized by autoclaving before contact with mice. Transferring and separating the young animals was always performed in a sterile environment. The regulations of *Deutsches Tierschutzgesetz* and *the European Directive 2010/63/EU* were strictly followed all the time. All animal handlings and experiments were performed with approval of the *Regierung von Oberbayern*.

3.2.2 Generation of *Pax8rtTA-Cre;Mdm2^{flox/flox}* mouse line

We generated inducible tubular cell-specific *Mdm2* knockout mice *Pax8rtTA-Cre;Mdm2^{flox/flox}*. This novel mouse model allows us to specifically study the roles of *Mdm2* in tubular epithelium *in vivo*.

Transgenic animals are nowadays widely used in the scientific research to explore functions of certain genes in complex biological processes such as embryogenesis or cancer, or to establish disease models. Different genetic alteration strategies in experimental animals are compared in Table 6. In traditional gene-knockout model, gene of interest is deleted in all cells, thus not specific for a certain cell lineage. In contrast, conditional gene-knockout targets a specific cell type and allows a more precise investigation of the gene functions in the organism. Moreover, with inducible gene knockout system, gene of interest is only deleted upon induction, thereby circumventing any developmental abnormalities or neonatal lethality caused by gene knockout. Also, this provides an exquisite way to study on adult organ physiology. The inducible system, in which the investigators can turn genes on and off when and where they choose, is therefore a breakthrough in the methodology of life science research [156].

Table 6: Comparison of different gene alterations in transgenic animals

Gene-knock-out	Traditional gene-knockout	Non-selective gene deletion in the germline
	Conditional gene-knockout	Tissue-specific gene deletion with high selectivity, e.g. by using Cre/loxP or CRISPR/Cas9 system
	Inducible gene-knockout	Gene deletion only upon induction, e.g. by using tetracycline-dependent (Tet) system
Gene knock-down		The genome of the organism is unchanged. The gene expression is decreased by interfering RNA or inhibitors.
Gene knock-in		An additional gene of interest is inserted in the germline

Here, we exploited Cre/loxP and Tet (tetracycline-dependent) system to generate tubular cell-specific *Mdm2*-knockout mice. Cre recombinase (cause recombination) is an enzyme originally found in the bacteriophage *P1*, a virus which infects and replicates in a bacterium. Cre is required by bacteriophage *P1* for integration and excision of its own DNA into the chromosome of infected bacterium [157, 158]. *LoxP* (locus of crossing over of *P1* phage) is a short DNA motif acting as the recognition site for Cre recombinase. Enzymatically, Cre catalyzes DNA recombination between two *loxP* sites, resulting in removal of DNA-sequence from the chromosome [158]. To generate inducible tissue-specific knockout mice, we crossed transgenic mice carrying *Cre recombinase* gene under the control of *Pax8* promoter (*Pax8-rtTACre*) and mice with *Mdm2* gene flanked by loxP (*Mdm2^{fllox/fllox}*) (Figure 11). Promoter *Pax8* is highly expressed in all proximal, distal tubules and the whole conducting system of both fetal and adult kidney [159, 160], but almost absent in other organs except for the thyroid gland [160, 161]. The *Pax8-rtTACre* mice were kindly provided by T. Huber (University of Freiburg, Freiburg, Germany), and *Mdm2^{fllox/fllox}* mice were from laboratory of G. Lozano (University of Texas, Huston, USA). Both mice lines were characterized and described before [161, 162].

The crossbreeding yielded double-transgenic mice *Pax8rtTA-Cre;Mdm2^{fllox/fllox}* which were born at expected Mendalian ratios. These transgenic mice developed normally and were phenotypically indistinguishable from the wildtype mice. *Mdm2^{fllox/fllox}* littermates lacking the *Pax8rtTA-Cre* transgene served as controls. *Pax8rtTA-Cre;Mdm2^{fllox/fllox}* mice express Cre recombinase under control of *Pax 8* promoter in a tetracycline-dependent manner.

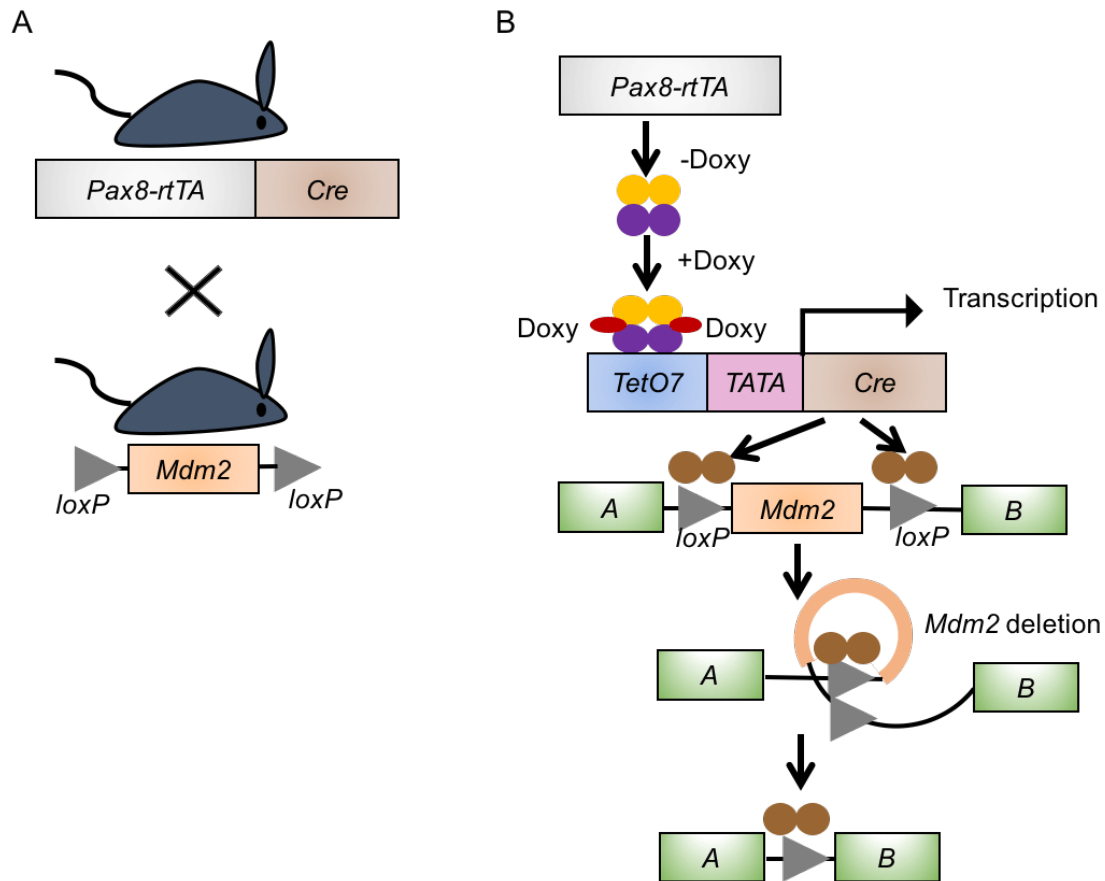


Figure 11: Generation of tubular cell-specific *Mdm2* knockout mice.

A. We crossbred *Pax8-rtTA*Cre mice and *Mdm2^{flox/flox}* mice to generate double-transgenic *Pax8rtTA-Cre;Mdm2^{flox/flox}* mice. B. *Pax8rtTA-Cre;Mdm2^{flox/flox}* mice expresses reverse tetracycline-dependent transactivator (*rtTA*) in all renal tubular epithelial cells under the control of *Pax8* promoter. In absence of the inducer doxycycline (doxy), no genetic alteration occurs in *Pax8rtTA-Cre;Mdm2^{flox/flox}* mice and the *Mdm2* alleles should have wild-type activity [156]. Upon doxycycline induction, doxycycline forms a complex with *rtTA* dimers which specifically binds to *tet operon* (*TetO*), leading to activation of a minimal promoter (*TATA*) and transcription of *Cre recombinase*. *Cre* recognizes both *loxP* sites flanking *Mdm2* gene and causes recombination, resulting in *Mdm2* gene excision. This picture is modified from Lewandoski et al., 2001 [156].

3.2.3 Doxycycline treatment regime

To induce *Cre* recombinase expression and subsequent *Mdm2* deletion in tubular cells, we subjected experimental and control mice to different doxycycline treatment regimes (2mg/ml in drinking water supplemented with 5% sucrose):

1) Continuous treatment regime: both *Pax8rtTA-Cre;Mdm2^{flox/flox}* and control mice were administered with doxycycline continuously for 4, 8 and 11days in three groups. Each group consisted of 4-6 mice that were matched in sex, age and weight.

2) Intermittent treatment regime: both *Pax8rtTA-Cre;Mdm2^{flox/flox}* and control mice were administered with doxycycline for only 2 days and then with pure water for 5 days before they were induced again, repeated for 4 weeks.

3.2.4 Genotyping

Mouse genotype was determined with DNA samples obtained from 2 mm tissues of mouse tail tips. Gene sequences to be determined were amplified by PCR and evaluated by gel electrophoresis. Genotyping was performed in three steps:

- 1) DNA isolation: The mouse tissues were lysed in proteinase-K buffer at 56°C under constant shaking for 4 hours, so that proteins were hydrolyzed and genomic DNA were exposed. The genomic DNA were eluted after serial steps of centrifugation and purification with DNA kit (Qiagen GmbH, Hilden, DE) as per manufacturer's instructions.
- 2) Polymerase chain reaction (PCR): Genes of interest were amplified by PCR, namely wild-type and floxed *Mdm2*, *Pax8* and *Cre*. 0.5 µl of the isolated DNA was mixed with 1 µl of each 1:10 diluted forward and reverse primers and a master mix of 2.5 µl of 10 × PE buffer, 4.0 µl of 1.25 mM dNTPs, 5 µl of PCR optimizer, 0.2 µl of Taq polymerase and 13.0 µl of H₂O to a total volume of 27.2 µl. For *Mdm2* genotyping, wildtype as well as floxed *Mdm2* were examined with the respective primers (Figure 12). Samples with distilled water instead of mouse DNA served as negatives controls.
- 3) Gel electrophoresis: The evaluation of the amplicons was carried out by agarose gel electrophoresis (Figure 12). Expected bands length:

<i>Pax8rtTA</i>	640 bp
<i>Cre recombinase</i>	300 bp
<i>Mdm2</i> Wildtype	342 bp
<i>Mdm2 flox</i>	474 bp

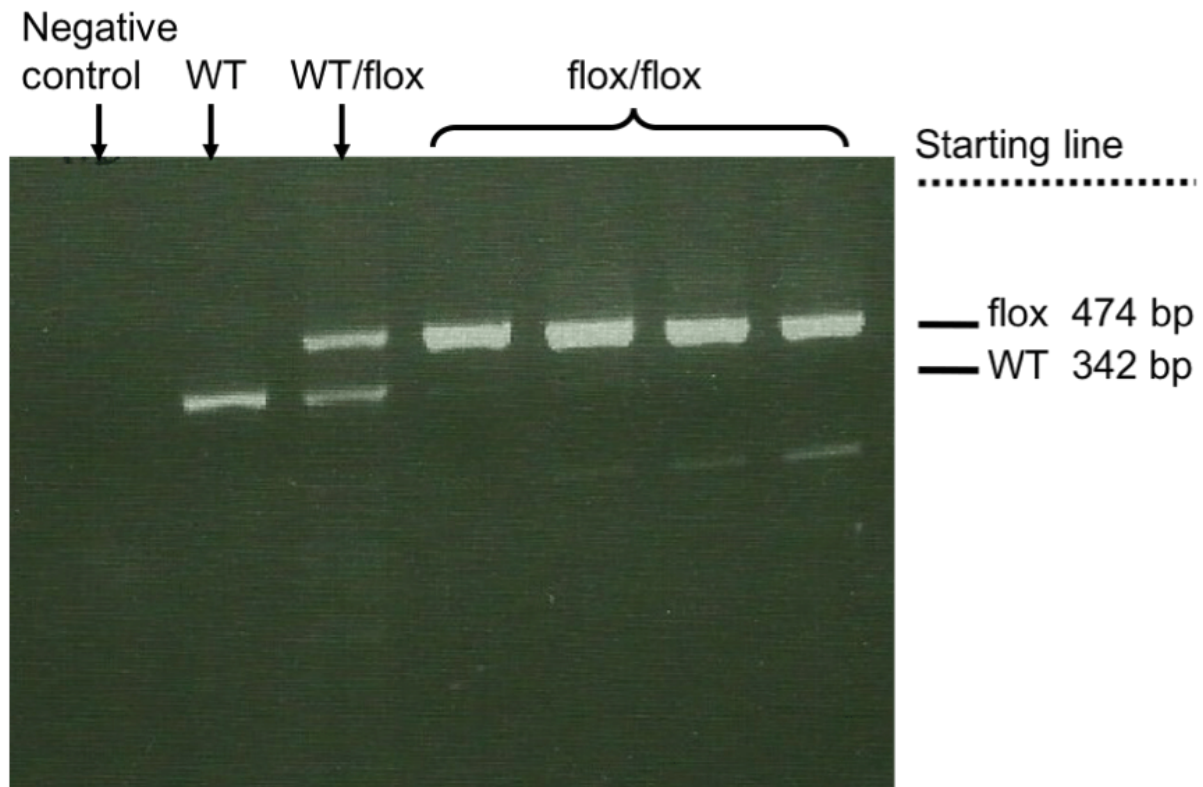


Figure 12: Genotyping for wild-type and floxed *Mdm2* gene

Wild-type *Mdm2* gene as well as floxed *Mdm2* gene were examined for mouse genotyping. Evaluation of DNA samples relies on the reading of the bands on gel electrophoresis. In the picture from left to right: negative control, $Mdm2^{wt/wt}$, $Mdm2^{wt/flox}$ and $Mdm2^{flox/flox}$ for the last 4 bands. WT: wild-type.

3.2.5 Blood sample collection

Mice were anesthetized using 2.5 % isoflurane in oxygen with a flow rate of 2 L/h. Blood were taken from retrobulbar plexus using micro lancet and collected into EDTA-containing centrifuge tubes (10 μ l of 0.5 M EDTA solution for 200 μ l of blood). Blood samples were subsequently centrifuged at 8000 rpm for 5 minutes. The collected plasma was stored at -20°C until further use.

3.3 Molecular biological methods

3.3.1 RNA isolation

RNA isolation from mice kidneys was performed with RNA isolation kit (PureLink® RNA Mini Kit, Qiagen GmbH). Kidneys were extracted from sacrificed mice, immediately preserved in RNA-later solution and stored at -20°C until processed for RNA isolation. Because a stable enzyme RNase exists ubiquitously and can split up RNA, we used disposable gloves and RNase-free water during the whole procedure to avoid RNA degradation by RNase. There were two main steps for RNA isolation:

- 1) Lysis and homogenization: Lysis buffer (600 µL) containing guanidine isothiocyanate and 1% β-mercaptoethanol (10 µL/mL) were freshly prepared. Next, kidney tissues were homogenized in lysis buffer with blade homogenizer for 30 seconds at speed level 4. The homogenate was centrifuged at 6000 rpm for 5 minutes. 550 µL of supernatant were transferred into a DEPC-treated RNase-free tube. Subsequently, 550 µL 70 % ethanol was added to the tube and mixed gently, until visible precipitate was dispersed. The whole mixture was then transferred into a RNA column.
- 2) RNA purification: We proceeded RNA isolation by steps of binding, washing and elution of RNA as per manufacturer's instruction. The chemical chloroform and centrifugation processes led to separation of the mixture in 3 layers: the upper layer contained RNA, the middle layer contained DNA and the lowest layer contained proteins. RNA in watery supernatant was separated from other two layers and then precipitated with ethanol. Finally, the membrane of spin cartridge with bound RNA was dried to get rid of ethanol and RNA was eluted in RNase-free water.

Next, the amount, purity and integrity of the isolated RNA were checked as described below, and RNA samples were kept on ice for immediate downstream application or stored at -80°C for long-term storage.

3.3.2 RNA quantification and purity check

The isolated RNA samples were quantified with Nano drop based on the principle of absorption spectroscopy. DNA and RNA molecules absorb ultraviolet light with an

absorption maximum at wave length of 260 nm, so that their concentration can be determined by a spectral photometer according to Beer-Lambert law (Figure 13):

$$E(\lambda) = -\lg\left(\frac{I_0}{I_1}\right) = e_\lambda \times c \times d$$

In case of Nano drop, 2 μ L of RNA sample was added in a quartz cuvette in a measurement chamber of a spectral photometer, and ultraviolet light with a wave length of 260 nm was emitted from one side the of cuvette. On the other side of cuvette, the intensity of transmitted UV was detected (Figure 13). The more light absorption in the cuvette, the higher is the concentration of RNA.

The contamination of nucleic acid with proteins can be checked with $OD_{260\text{ nm}}/OD_{280\text{ nm}}$ ratio (OD: optical density), as proteins have an absorption maximum at wave length of 280 nm. Only if the OD ratio is between 1.8 and 2.0, the RNA or DNA samples were considered as approximately protein-free and of acceptable quality.

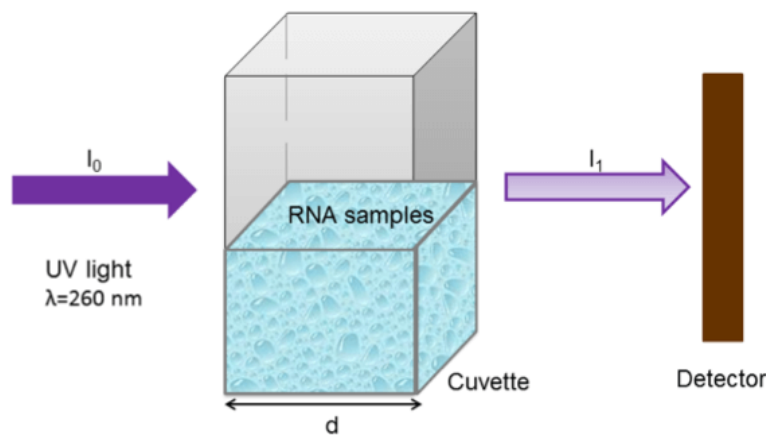


Figure 13: Principle of Nano drop.

I_0 : intensity of entering UV-light, I_1 : intensity of transmitted UV-light, λ : wave length, d : thickness of cuvette. According to Beer-Lambert law, i.e. $E(\lambda) = -\lg(I_0/I_1) = e_\lambda \times c \times d$ (E : extinction coefficient or optical density, c : concentration of RNA samples), concentration of RNA samples can be calculated. This figure is modified from BASIC Experimentelle Doktorarbeit, 2010 [163].

3.3.3 RNA integrity check

If necessary, RNA quality check for its integrity was carried out by agarose gel electrophoresis, which was commonly used for separation and analysis of nucleic acids. Nucleic acids are negative charged molecules and migrate from cathode to anode in the electric field through the porous agarose gel at different rates, which are largely dependent on their molecular mass.

A RNA denaturing gel consisting of agarose and MOPS buffer was placed in a buffer-filled electrophoresis chamber. RNA samples were dissolved in 3 μ L DEPC-treated water, 2 μ L 10xMOPS buffer, 10 μ L formamide, 4 μ L formaldehyde 37% and 1 μ L ethidium bromide. Ethidium bromide was used for detecting nucleic acids, because it intercalates with base pairs of nucleic acids and fluoresces under ultraviolet light. Next, RNA samples, markers and tracking dye (bromophenol blue) were added into wells of the agarose gel and an electrical field with approximately 80 volts was charged for 1 hour. Bands on the gel were visualized on a gel documentation device under a UV lamp and printed out (Figure 14). Single bright bands in the agarose gel indicated good quality of RNA samples, whereas smears in the gel revealed loss of RNA integrity.

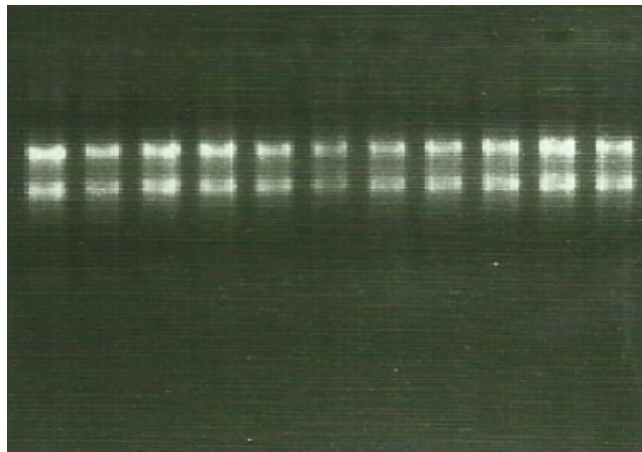


Figure 14: RNA integrity check with gel electrophoresis.

3.3.4 cDNA synthesis

The isolated RNA samples were as next converted to cDNA (complementary DNA), because only DNA but not RNA can be amplified by PCR. To do so, reverse transcriptase (RT) II from Invitrogen was used, which is a modified version of MMLV (Moloney murine leukemia virus-)-RT. Reverse transcriptase was originally found in retroviruses such as HIV. As a RNA-dependent DNA-polymerase, reverse transcriptase can transcribe RNA to complementary, double-stranded DNA and integrate virus genome into host genome.

To conduct cDNA conversion, RNA samples were diluted with RNase-free water to reach a concentration of 1 μ g/20 μ L. Next, Master Mix was prepared as a mixture of 4 μ L of 5x first strand buffer, 0.4 μ L of 25 mM dNTP, 1 μ L of 0.1 M DTT, 0.25 μ L of linear acrylamide, 0.215 μ L of Hexanucleotide, 0.5 μ L of 40U/ μ L RNAsin, 0.435 μ L of Super-

script or ddH₂O in the case of negative control. To start reverse transcription, 6.8 µl of Master Mix was added to each diluted RNA sample to a total volume of 20 µl, and the tubes were incubated on a thermal shaker at 42°C for 1.5 hours. The enzymatic reaction was ended by heating the tubes at 85°C for 5 minutes to denature the enzymes. The cDNA samples were diluted 1:10 and stored at -20°C until used for real-time PCR.

3.3.5 Real-time quantitative polymerase chain reaction (RT-PCR)

Polymerase chain reaction (PCR) was carried out as a central part of molecular biology methods. With the technique of PCR, small amount of DNA can be exponentially amplified *in vitro* and therefore easily detected in a sufficient amount. To do so, DNA polymerase, nucleotides, primers specific for genes of interest, SYBR Green and appropriate buffer system were required. Taq DNA polymerase was commonly used for PCR because it is heat-resistant, as it was originally found in a bacteria species named *Thermus aquaticus* that lives in hot springs and tolerates high temperature up to 100°C. SYBR Green was applied for DNA detection, as it intercalates with double-stranded DNA and fluoresces under light stimulation. The increase of fluorescence signal from cycle to cycle is directly proportional to the increase of the amplified DNA. 2 µl of the 1:10 diluted cDNA samples were mixed with 10 µl of SYBR green master mix, 0.6 µl of each 1:10 diluted forward primer and reverse primer, which are specific for the gene of interest, 0.16 µl of Taq polymerase and 6.64 µl of distilled water to a total volume of 20 µl. RT minus and ddH₂O served as negative controls.

Real-time quantitative PCR was performed in a programmed thermal cycler (Light Cycler 480). Each amplification cycle consisted of three steps and was repeated for 45 cycles:

- 1) Denaturation at 95°C: denaturation and complete separation of double-stranded DNA to single-stranded DNA;
- 2) Annealing at 60°C: gene-specific primers (Table 5) bind complementary to single-stranded DNA and represent the starting point of amplification;
- 3) Elongation at 72°C: Taq polymerase works in its optimal temperature. It begins at 3' end of primer and adjoins nucleotides to form a new, complementary DNA fragment.

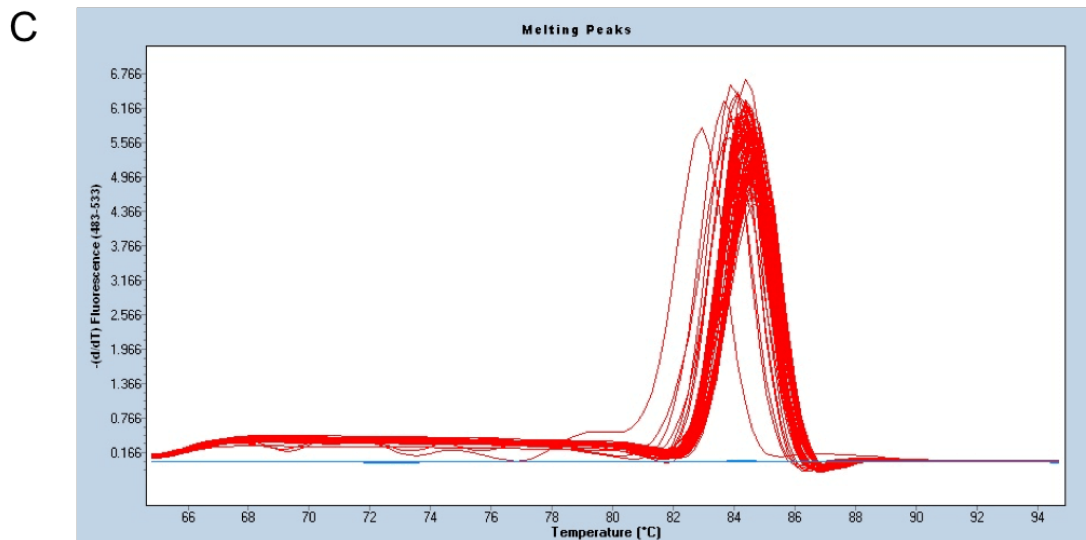
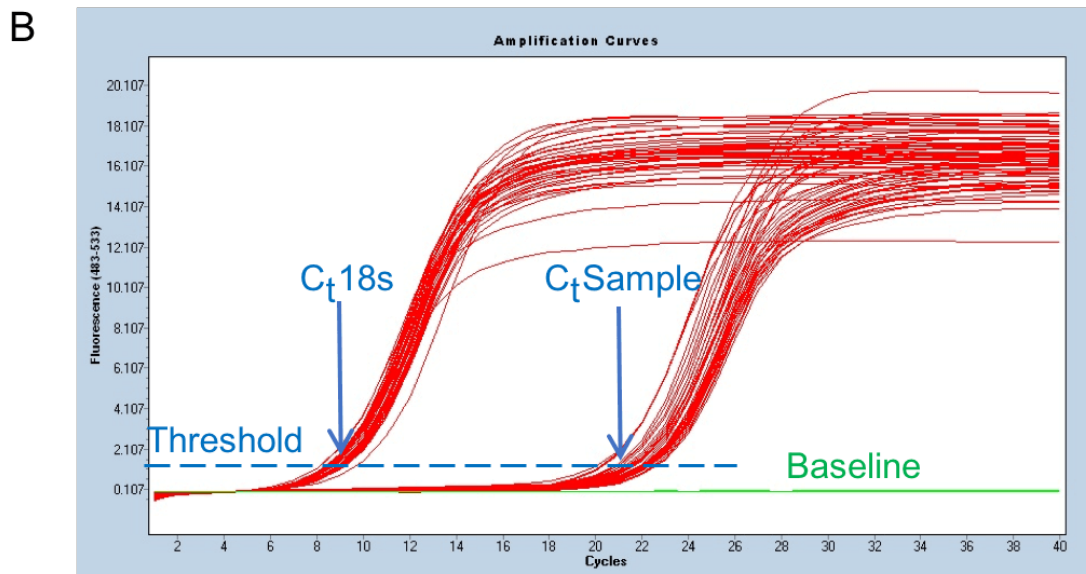
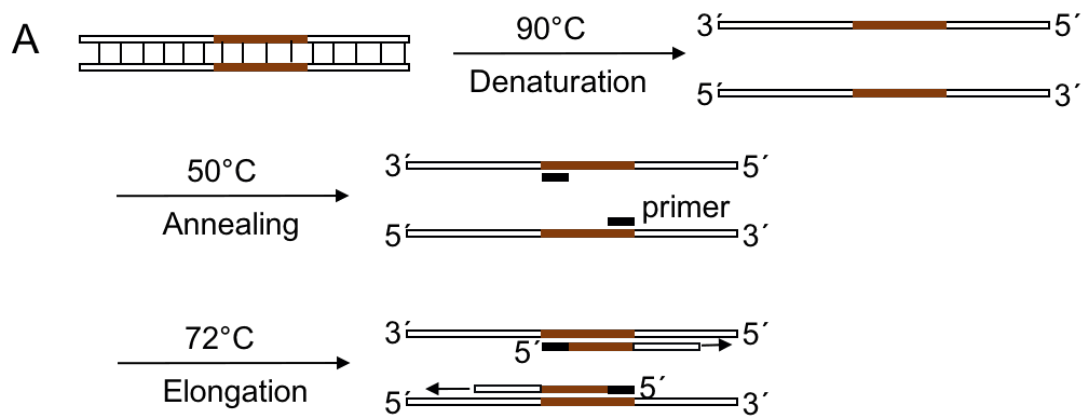


Figure 15: Principle of real-time quantitative PCR

A. Each amplification cycle of PCR consisted of denaturation, annealing and elongation. This picture is modified from BASICS Experimentelle Doktorarbeit, 2010 [163]. B. Example amplification curves of cDNA samples. C. Example melting curves for quality check.

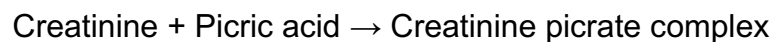
The RT-PCR results were illustrated on amplification curves (Figure 15), as fluorescence signal was plotted against the number of cycles on a logarithmic scale. To quantify gene expression, C_t value was introduced and defined as the number of cycles at which the fluorescence exceeds the threshold. ΔC_t was calculated by subtracting C_t value of a housekeeping gene from C_t value of gene of interest ($\Delta C_t = C_{t\text{Sample}} - C_{t18s}$). 18s gene is constitutively expressed in all cells and used as the housekeeping gene in our experiments. In this way, the variation in amount and quality of different samples could be normalized. The calculation was performed as follows:

$$R = 2^{-(C_{t\text{Sample}} - C_{t18s})}$$

The melting curves were generated at the end of RT-PCR and analyzed for each sample to detect unspecific products and primer dimers (Figure 15).

3.3.6 Creatinine measurement

Plasma creatinine levels were measured with Creatinine FS kit based on Jaffe reaction, which is a colorimetric method firstly described by German biochemist Max Jaffe (1841-1911) in 1886. In Jaffe reaction, creatinine reacts with picric acid in an alkaline solution and forms an orange-red complex:



As the color change is directly proportional to creatinine concentration, creatinine levels can be determined by the difference in absorbance of the complex at defined times. Although Jaffe reaction is non-specific for creatinine, it is till now the most widely used method in clinical chemistry for creatinine analysis.

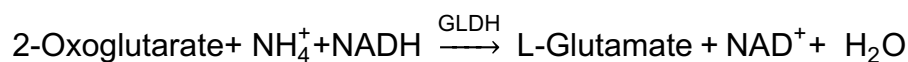
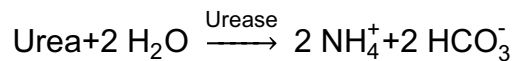
As instructed by the manufacturer, we prepared serial dilutions of the standard and mono reagent by mixing 4 parts of reagent 1 (R1, sodium hydroxide) and 1 part of reagent 2 (R2, picric acid). Next, 10 μl of each defrozen plasma sample and standards were added to a 96-well flat bottom plate (Nunc maxisorb plate), followed by adding the mono reagent (200 μl) to each well. We incubated the reaction mixture at 20-25°C for 60 seconds and read the absorbance A_1 at 492 nm by using an ELISA plate reader. After 120 seconds, absorbance was measured again as A_2 . The change in absorbance (ΔA) was defined as $\Delta A = [(A_2 - A_1) \text{ sample or standard}] -$

[(A2 – A1) blank]. Finally, calculation of creatinine concentration in the samples was performed as follows:

$$\text{Creatinine (mg/dl)} = \frac{\Delta A \text{ sample}}{\Delta A \text{ standard}} \times \text{Concentration of standard (mg/dl)}$$

3.3.7 BUN measurement

Plasma BUN levels were measured using Urea FS kit. The principle of the measurement is an enzymatic UV test with urease and GLDH:



GLDH: Glutamate dehydrogenase

According to manufacturer's instructions, we prepared serial dilutions of standard which is provided in the kit. Mono reagent was made as a mixture of 4 parts of reagent 1 (R1, containing TRIS, 2-Oxoglutarate, ADP, urease and GLDH) and 1 part of reagent 2 (R2, NADH) provided in the kit. Next, 2 µl of each of plasma sample and standards were added to a 96-well flat bottom plate (Nunc maxisorb plate), followed by adding the mono reagent (200 µl) to each well. We incubated the reaction mixture at 25°C for 60 seconds and read the absorbance A1 at 360 nm by using an ELISA plate reader. After 120 seconds, absorbance was measured again as A2. The change in absorbance (Δ A) was defined as Δ A = [(A2 – A1) sample or standard] – [(A2 – A1) blank]. Finally, calculation of urea concentration in the samples was performed as follows:

$$\text{Urea (mg/dl)} = \frac{\Delta A \text{ sample}}{\Delta A \text{ standard}} \times \text{Concentration of standard (mg/dl)}$$

Urea was converted to BUN as:

$$\text{BUN (mg/dL)} \times 2.14 = \text{Urea (mg/dL)}$$

3.4 Histological methods

3.4.1 Histological sections

To study the microscopic structures and pathology, histological sections of mice kidneys were carried out with the following steps:

- 1) Fixation: The isolated kidney tissues were fixed in 4% neutral-buffered formalin overnight to preserve tissues from degradation. Formalin can cross-link basic amino acids of proteins irreversibly and maintain the structural integrity of cells and subcellular components.
- 2) Processing and embedding: Kidney tissues were deprived of water by incubating in gradually more concentrated alcohol baths, followed by using a hydrophobic clearing agent xylene to remove the alcohol. Then the tissues were embedded in lipophilic paraffin which replaced xylene and solidified. The paraffin blocks were cooled down and sliced into 4 μm sections using a microtome.
- 3) Deparaffinization and rehydration: The sections were deparaffinised with xylene, the rehydrated by incubating in a graded series of ethanol (100%, 95%, 70% and 50%) and washed with distilled water.

3.4.2 Periodic acid-Schiff (PAS) staining

The periodic acid-Schiff (PAS) staining was performed for routine kidney histology in our studies. After deparaffinization and rehydration, the sections were incubated in periodic acid solution (2 % in distilled water) for 10 minutes and then washed with distilled water. Next, the sections were incubated in Schiff solution for 20 minutes and then washed with tap water. This was followed by dehydration by incubating sections in serials of alcohol solutions with increased concentration. Finally, the microscope slides were closed with glass coverslips.

3.4.3 Immunohistochemistry

Immunohistochemistry was used to visualize certain antigens by specific antigen-antibody-reaction. Tissue antigens of interest in our experiments included Mdm2, p53, caspase 3 and Ki-67. Also, living proximal and distal tubular cells as well as collecting ducts were identified with appropriate antibodies, i.e. lectin, THP and aquaporin. Here, indirect method with avidin-biotin-complex (ABC) was applied: firstly pri-

Primary antibodies target the tissue antigens of interest, then secondary antibodies labelled with biotin bind Fc regions of primary antibodies. Finally, the marker substance ABC with reporter enzymes is added, detecting secondary antibodies and stains with a brown color (Figure 16). Multiple secondary antibodies can bind a single primary antibody, thus generating signal amplification by increasing the number of chromogenic substrates per antigen. ABC method has the highest sensitivity in immunohistochemistry, because of the strong affinity between avidin and biotin and the immense signal amplification.

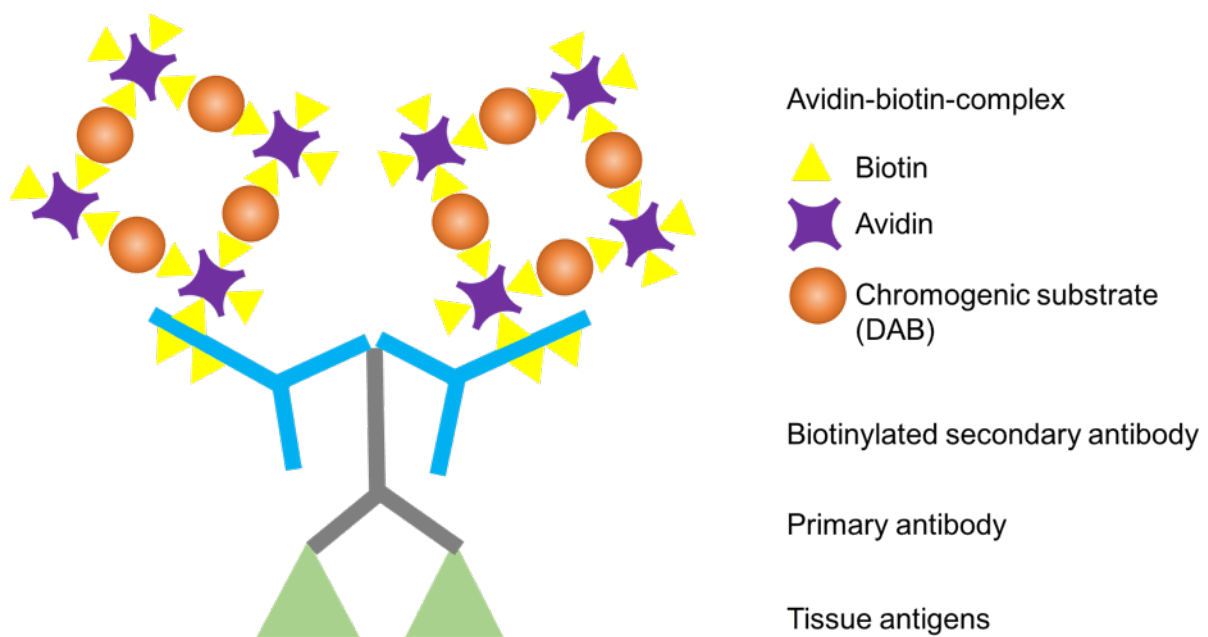


Figure 16: Avidin-biotin-complex method for immunohistochemistry staining.

For immunohistochemical staining, 2 μm paraffin sections were deparaffinized, rehydrated and washed with PBS (2x7 minutes). Prior to antibody staining, the endogenous peroxidase contained in the sections was blocked by incubating sections in H_2O_2 and methanol mixture (20 ml of 30% H_2O_2 in 180 ml of methanol) for 20 minutes, followed by washing with PBS (2x7 minutes). As fixation process with formalin could lead to cross-links of proteins, the epitope conformation of antigens could have changed and the antibody may not bind the specific antigens. To unmask the antigens, the sections were placed into a mixture of 3 ml of antigen-masking solution and 300 ml of H_2O , and heated in a microwave (4 x 2.5 minutes). This was followed by washing with PBS (2x7 minutes). After the sections were cooled to room temperature, the endogenous biotin contained in the sections was blocked with avidin for 15

minutes. This was followed by a quick wash of the sections and incubation with biotin for 15 minutes, then washed again with PBS (2 x 7 minutes).

To reduce non-specific binding and background staining to minimum, the sections were incubated in 10% goat serum for 10 minutes, blocking the reactive sites to which the primary or secondary antibodies may otherwise bind. The sections were subsequently incubated with diluted primary antibodies for 1 hour at room temperature or overnight at 4°C in a wet chamber, and then washed with PBS for 7 minutes. This was followed by incubation with the respective diluted biotinylated secondary antibody for 30 minutes at room temperature, and washing with PBS for 7 minutes. The ABC substrate solution (15 µl of reagent A and 15 µl of reagent B to 1 ml of PBS) for secondary antibodies was then added, incubated for 30 minutes in a wet chamber at room temperature and then washed again with PBS. Immediately afterwards, sections were washed with TRIS hydrochloride for 5 minutes. Next, the reporter enzyme DAB solution was added for 1 to 10 minutes to stain. DAB was oxidized in the presence of hydrogen peroxide, producing a brownish product that was easily observed. The stain intensity was controlled with microscope. This was followed by counterstaining with methylene green to increase the color contrast. The sections were washed with 96% ethanol (2 x 10 seconds), followed by washing with 100% ethanol (3 x 10 seconds) to remove excess stain. Finally, a drop of VectaMount mounting medium was added and the slides were covered with cover lids. Negative controls were performed for each immunostaining by incubating with the respective isotype antibody instead of the primary antibody.

3.4.4 Immunofluorescence

Immunofluorescence relies on fluorescent instead of chromogenic detection. The evaluation was performed on LSM 510 confocal microscope and LSM software. TUNEL/DAPI staining was conducted to detect apoptotic cell death and nuclei respectively. TUNEL (TdT-mediated dUTP nick-end labeling) is a sensitive method to identify DNA strand breaks ("nicks") generated during endonucleolysis, which is a key biochemical event of apoptosis. These DNA fragmentations can be labelled with TdT (terminal deoxynucleotidyl transferase) in an enzymatic reaction and subsequently detected with fluorochrome-labelled deoxynucleotides which fluoresce in green. DAPI (4',6-diamidino-2-phenylindole) was applied to label DNA in nuclei, as it binds to A-T rich regions of double-stranded DNA and fluoresces in blue.

TUNEL/DAPI immunofluorescent staining was carried out as following: First, formalin-fixed, paraffin-embedded kidney sections were dewaxed by washing in xylene for 5 minutes and rehydrated through a graded series of ethanol (100%, 96%, 70%) for 2 minutes, followed by washing with PBS (2 x 7 minutes). Second, the sections were incubated with proteinase K (50 µg/ml in Tris/HCl) for 10 minutes. Next, 50 µl enzyme solution was added to each section, followed by incubation for 1 hour at 37°C. Finally, each section was added with 1-2 drops mounting medium containing DAPI, closed with coverslips and analyzed by confocal microscopy.

3.4.5 Histopathological evaluations

Tubulus damage Score

To evaluate the severity of the tubulus damage in PAS-stained kidney sections, tubulus damage score was carried out as an established, semi-quantitative method. Three major aspects were analyzed during scoring:

- 1) Tubular injury (cellular swelling, vacuolization and loss of brush border etc.),
- 2) Cast formation,
- 3) Tubular dilation.

For each PAS-stained kidney section, 25 representative fields were analyzed under light microscope with 200 x magnification. The scoring was performed for each aspect as follows:

Score	Damage level
0	None
1	≤ 10%
2	21% to 40%
3	41% to 60%
4	61% to 80%
5	81% to 100%

3.4.6 Transmission Electron Microscopy

Transmission electron microscope permits the visualization of cellular ultrastructure inclusive subcellular components with a much higher resolution (0.2 nm) than light microscope (200 nm). A beam of high voltage accelerated electrons is transmitted

through the sample and detected by the camera, creating a unique image of the sample.

For transmission electron microscope, the extracted kidneys were cut into 1x1 mm cubes and immediately immersed in fixation solution containing 3% glutaraldehyde and 1% paraformaldehyde in PBS. This was followed by post-fixation in 2% glutaraldehyde and 2% paraformaldehyde in sodium cacodylate buffer (pH 7.4) for 24 hours. The fixation was completed by incubation in phosphate cacodylate-buffered 2% OsO₄ for 1 h. Next, dehydration was carried out by incubating kidneys in graded ethanol and lastly in propylene oxide. The kidneys were embedded in Embed-812 resin and sliced into ultrathin sections (~90-nm thick). The sections were stained with uranyl acetate and Venable's lead citrate and evaluated under the JEOL model 1200EX electron microscope. The image taking was performed by Prof. Dr. Helen Liapis at Washington University in St. Louis, Missouri, USA.

3.5 Statistical analysis

All Data are presented as mean \pm SEM (standard error of the mean). SEM was calculated as follows:

$$\bar{x} = \frac{\sum_{i=1}^n x_i}{n}$$
$$s = \sqrt{\frac{\sum_{i=1}^n (x_i - \bar{x})^2}{n-1}}$$
$$\text{SEM} = \frac{s}{\sqrt{n}}$$

\bar{x} : sample mean, n: size of the sample, s: standard deviation , SEM: standard error

The statistical significance was calculated using the bilateral Student's t-test, and a p-value of <0.05 was considered statistically significant. p <0.05, p <0.01 and p <0.005 were marked with *, ** and *** respectively. Survival rates were presented in Kaplan-Meier's survival curve.

4 Results

4.1 *Mdm2* expression is reduced exclusively in renal tubular epithelial cells of *Pax8rtTA-Cre;Mdm2^{flox/flox}* mice treated with doxycycline (*Mdm2^{-/-tubulus}*)

We crossbred *Mdm2^{flox/flox}* mice and *Pax8rtTA-Cre* mice to generate a new conditional gene knockout mouse line *Pax8rtTA-Cre;Mdm2^{flox/flox}*. Theoretically, upon induction with tetracycline or its derivative doxycycline, *Pax8rtTA-Cre;Mdm2^{flox/flox}* mice express Cre recombinase under the control of tubular cell-specific *Pax8* promoter. Cre recombinase then recognizes *loxP* sites, which flank exon 4 and 5 of *Mdm2* gene, thereby enzymatically causing *Mdm2* gene deletion in all tubular cells in proximal tubules, distal tubules and collecting ducts.

The genotype of tubular cell-specific *Mdm2* knockout mice was verified by PCR and electrophoresis of DNA samples isolated from mouse tissues. We proceeded to examine if tubular cell-specific *Mdm2* knockout indeed occurred upon doxycycline induction, in other words, if doxycycline dependent Cre/*loxP*-system worked successfully in our new mouse models.

We fed 5-week-old *Pax8rtTA-Cre;Mdm2^{flox/flox}* mice with 2mg/ml doxycycline in drinking water continuously for 4, 8 and 11 days respectively. Their littermates *Mdm2^{flox/flox}* mice served as controls. At the end of treatment, experimental and control mice were sacrificed and their kidneys were extracted for analysis. mRNA from total kidneys was isolated and quantified by real-time PCR. As demonstrated in Figure 17, intrarenal *Mdm2* mRNA expression of knockout mice exhibited a progressive decrease with the length of doxycycline treatment, compared with control mice. While on day 4 there was no change in *Mdm2* mRNA level in kidney tissues of knockout mice, a significant decrease of *Mdm2* mRNA expression was evident on day 8 (39% reduction) and on day 11 (49% reduction), compared with control mice.

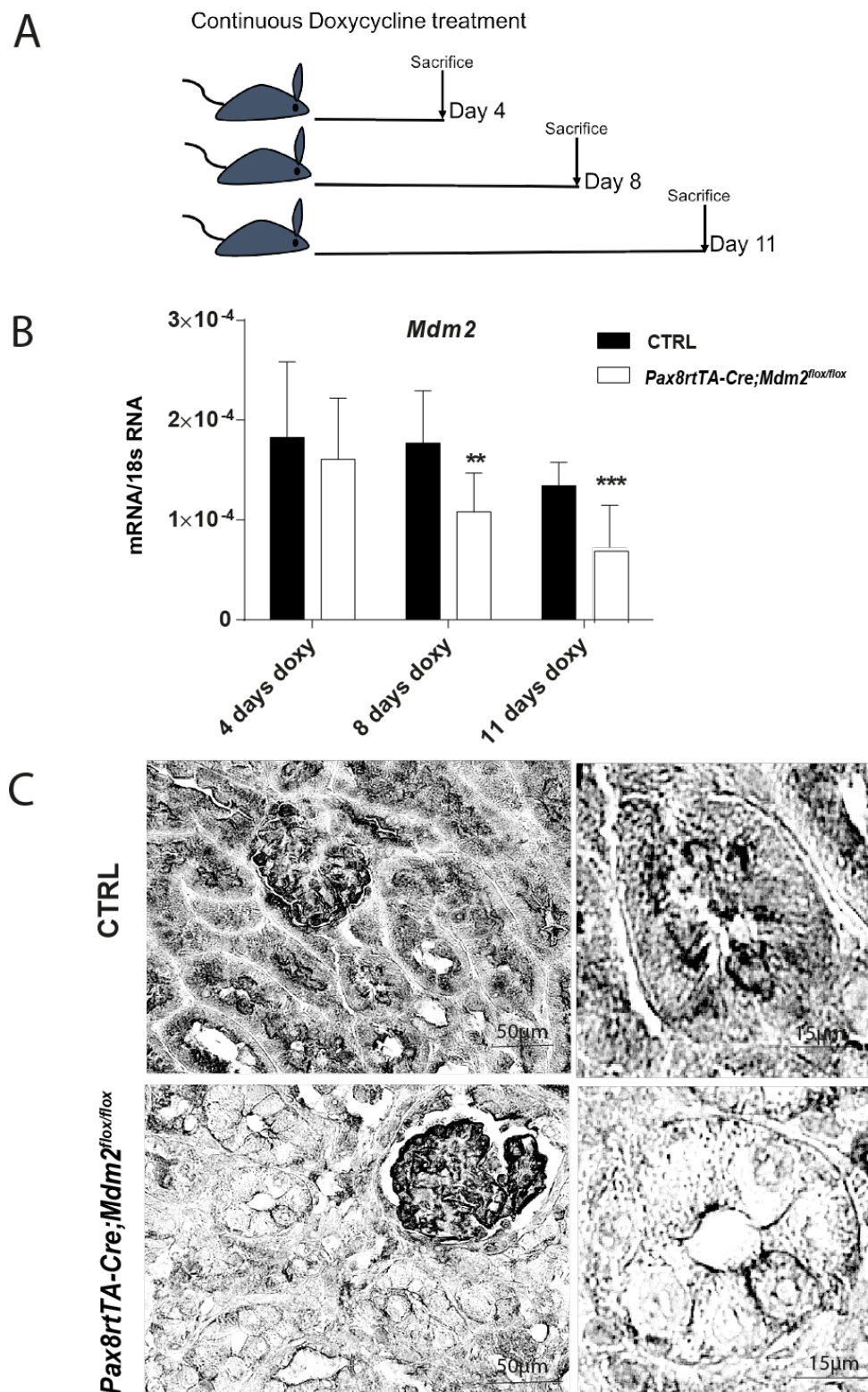


Figure 17: *Mdm2* expression was reduced in *Pax8rtTA-Cre; Mdm2^{flox/flox}* mice treated with doxycycline.

A: Schematic view of continuous doxycycline treatment regime. Experimental and control mice were treated with 2mg/mL doxycycline for 4, 8 and 11 days. B: Real-time PCR detected progressive decrease of *Mdm2* mRNA levels in kidney lysates of *Pax8rtTA-Cre; Mdm2^{flox/flox}* mice upon doxycycline induction (n=5-6 mice/group). Data are means \pm S.E.M. * $P < 0.05$, ** $P < 0.01$, *** $P < 0.005$. C: *Mdm2* immunostaining was diminished in tubular epithelial cells, while staining of podocytes and other cell types within the kidney remained intact. The selectivity of *Mdm2* knockout in renal tubular cells was confirmed.

Next, intrarenal expression of Mdm2 protein was determined by immunohistochemistry with Mdm2 antibody in kidney sections. Consistent with PCR results, there was diminished Mdm2 protein detected in renal tubular cells of *Pax8rtTA-Cre;Mdm2^{flox/flox}* mice treated with doxycycline, compared with control mice (Figure 17). In contrast, the glomeruli and mesenchymal tissues within the kidney remained unchanged in all sections, which authenticated the selectivity of *Mdm2* knockout in renal tubular epithelial cells of *Mdm2^{-tubulus}* mice.

Taken together, genotype of *Pax8rtTA-Cre;Mdm2^{flox/flox}* mice was confirmed, and real-time quantitative PCR detected decreased intrarenal *Mdm2* mRNA expression in *Pax8rtTA-Cre;Mdm2^{flox/flox}* mice treated with doxycycline. Furthermore, Mdm2 immunostaining of kidney sections showed that Mdm2 protein was depleted exclusively in renal tubular cells of knockout mice (referred as *Mdm2^{-tubulus}* in the following text). Hence, tubular cell-specific *Mdm2* knockout was successful in *Pax8rtTA-Cre;Mdm2^{flox/flox}* upon doxycycline induction.

4.2 Continuous tubule-specific *Mdm2* depletion results in acute kidney injury

We characterized the phenotype of *Pax8rtTA-Cre;Mdm2^{flox/flox}* mice treated with doxycycline continuously. To study the concrete biological effects of tubular cell-specific *Mdm2* depletion in mice, following aspects in transgenic mice were analyzed:

- 1) Clinical parameters such as urine production, body weight and life span;
- 2) Serum creatinine and urea for assessment of renal function;
- 3) Intrarenal mRNA expression of p53 and its effector genes, as well as tubulus damage markers by real-time PCR;
- 4) Histopathological evaluations of kidney sections by light microscopy, and ultrastructural analysis by electron microscopy.

We observed that *Mdm2^{-/-tubulus}* mice experienced severe deterioration of kidney function, upregulation of tubulus damage markers in kidneys and acute tubular injury with progressive cellular loss in the histology. These pathological processes together were in line with acute kidney injury. Also, continuous doxycycline treatment caused rapid lethality in *Mdm2^{-/-tubulus}* mice, but did not affect their control littermates. We conclude that tubular cell-specific *Mdm2* knockout results in acute kidney injury.

4.2.1 Oliguria, weight loss and shortened life span

With the length of doxycycline treatment, *Mdm2^{-/-tubulus}* mice became moribund, developed oliguria and weight loss. By contrast, all *Mdm2^{flox/flox}* control mice lacking *Cre* transgene remained active and healthy throughout the entire time course of doxycycline treatment. Moreover, *Mdm2^{-/-tubulus}* mice showed a significant shortened life span compared with their control littermates, as demonstrated in Kaplan-Meier survival curve (Figure 18). The first *Mdm2^{-/-tubulus}* mouse died already on day 6 of doxycycline treatment, and the majority of knockout mice died between day 7 and day 10. Furthermore, no knockout mouse survived longer than 14 days. The high mortality of experimental mice is presumably attributable to the development of devastating acute kidney injury, because no other tissue but tubular epithelium in the kidney is affected by *Mdm2* knockout.

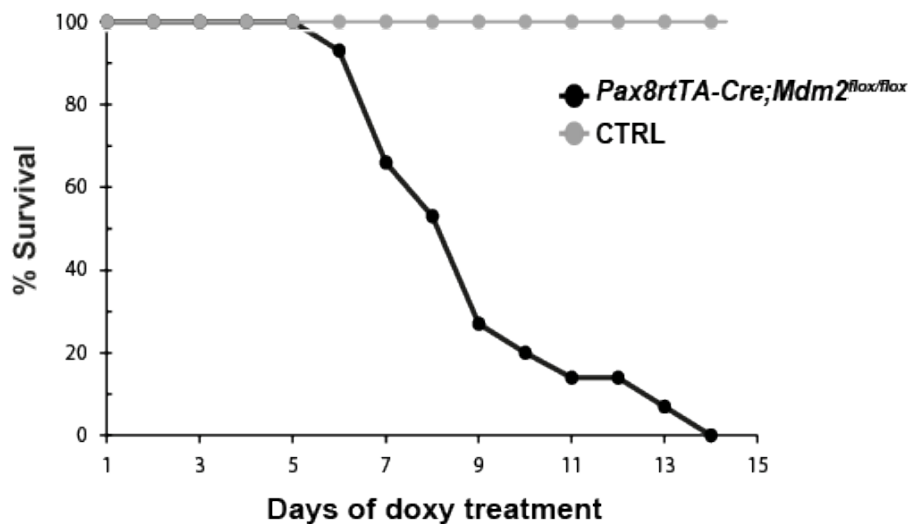


Figure 18: Kaplan-Meyer survival curve of *Mdm2^{-/-tubulus}* and control mice.

While all *Mdm2^{flox/flox}* control mice survived through doxycycline treatment, *Pax8rtTA-Cre;Mdm2^{flox/flox}* mice treated with doxycycline died rapidly from day 6 and survived no longer than 14 days. Data are based on n=17 mice/group.

4.2.2 Impaired renal function

We measured creatinine and urea concentration in serum to assess kidney function. Blood samples were collected from retrobulbar venous plexus of mice at the end of doxycycline treatment before they were sacrificed.

As illustrated in Figure 19, serum creatinine and urea concentration of *Mdm2^{-/-tubulus}* mice displayed a progressive increase with the length of doxycycline treatment, compared with control mice. Whereas on day 4 the kidney function of *Mdm2^{-/-tubulus}* mice was normal, serum creatinine of *Mdm2^{-/-tubulus}* mice increased by twofold on day 8 and by fivefold on day 11 compared with control mice (Figure 19). Also, serum BUN showed a fivefold and sixfold elevation on day 8 and day 11 respectively, in comparison with control mice (Figure 19). Furthermore, glomerular filtration rate (GFR) of *Mdm2^{-/-tubulus}* mice decreased rapidly from day 4, and the knockout mice were critically oliguric on day 8, compared with their control littermates which had constant GFR during the whole doxycycline treatment (data not shown, published in [139]).

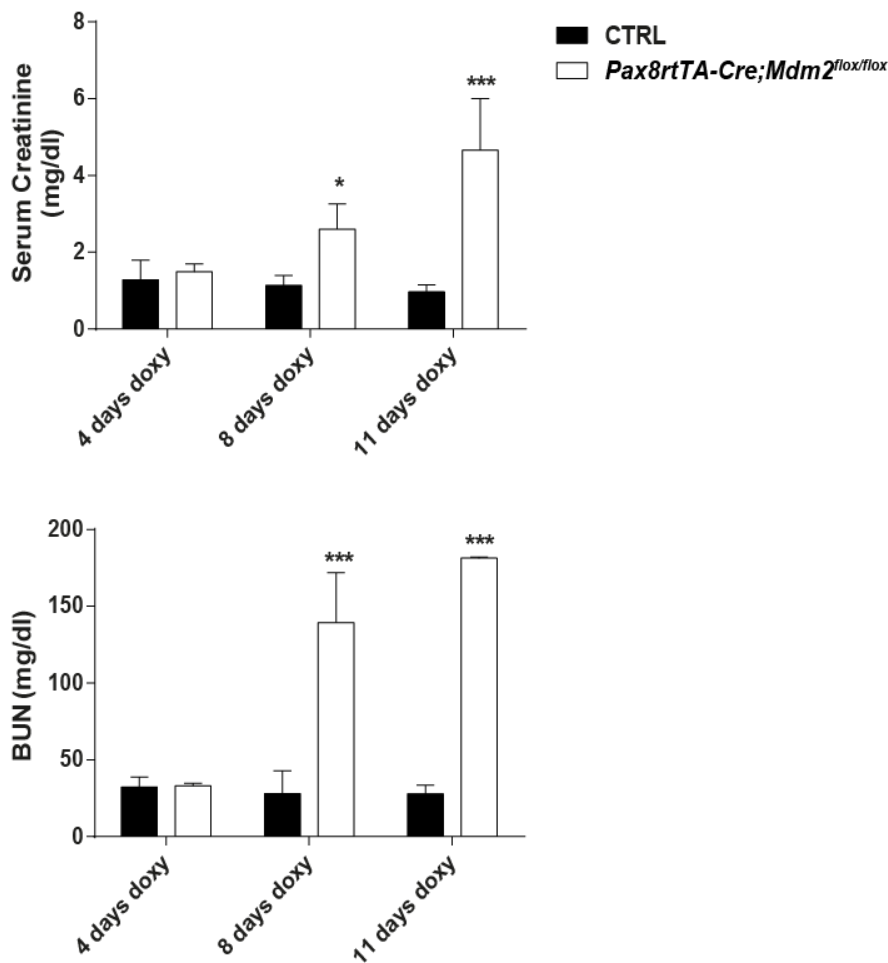


Figure 19: Serum creatinine and urea concentration.

Pax8rtTA-Cre;Mdm2^{flox/flox} mice treated with doxycycline underwent a progressive deterioration of renal function, as detected by significantly increased levels of serum creatinine and BUN compared with control mice (n=5-6 mice in each group). Data are means \pm S.E.M. * $P < 0.05$, ** $P < 0.01$, *** $P < 0.005$.

4.2.3 Upregulation of *p53*, *p21* and *Puma* in the kidney

We further examined with real-time quantitative PCR, whether or not stabilization of *p53* molecule occurred in response to *Mdm2* deletion through their autoregulatory feedback loop in *Mdm2^{-/-tubulus}* mice kidneys. As illustrated in Figure 20, intrarenal *p53* mRNA level in *Mdm2^{-/-tubulus}* mice elevated by 65% on day 8 of doxycycline treatment, compared with their control littermates.

Additionally, we measured mRNA expression of *p53* downstream genes *p21* and *Puma*. *p21* gene encodes a 21-kDa protein that is constitutively expressed at low levels under physiological conditions [45, 164]. *p21* protein inhibits cycline-dependent kinase (Cdk) that is a necessary enzyme in the cell cycle progression, thereby causing the cell cycle arrest at checkpoint G1/S or G2/M [44]. *Puma* (*p53*-upregulated mediator of apoptosis) encodes pro-apoptotic protein of BCL-2 family, and is a key

apoptotic transcriptional target gene of p53. Mice lacking *Puma* show profound defects in apoptotic processes in many tissues, thus “no Puma, no cell death” [165-167]. Strikingly, intrarenal *p21* and *Puma* mRNA level of *Mdm2*^{-/-tubulus} mice increased substantially on day 8 of doxycycline treatment respectively, compared with control mice (Figure 20). The elevation of *p21* and *Puma* mRNA was sixfold and threefold on day 11. Together, *Mdm2* depletion resulted in upregulated mRNA levels of *p53* and its target genes *p21* and *Puma* in renal tubular epithelial cells. Also, increased p53 protein expression was detected by immunostaining as described in 4.2.8.

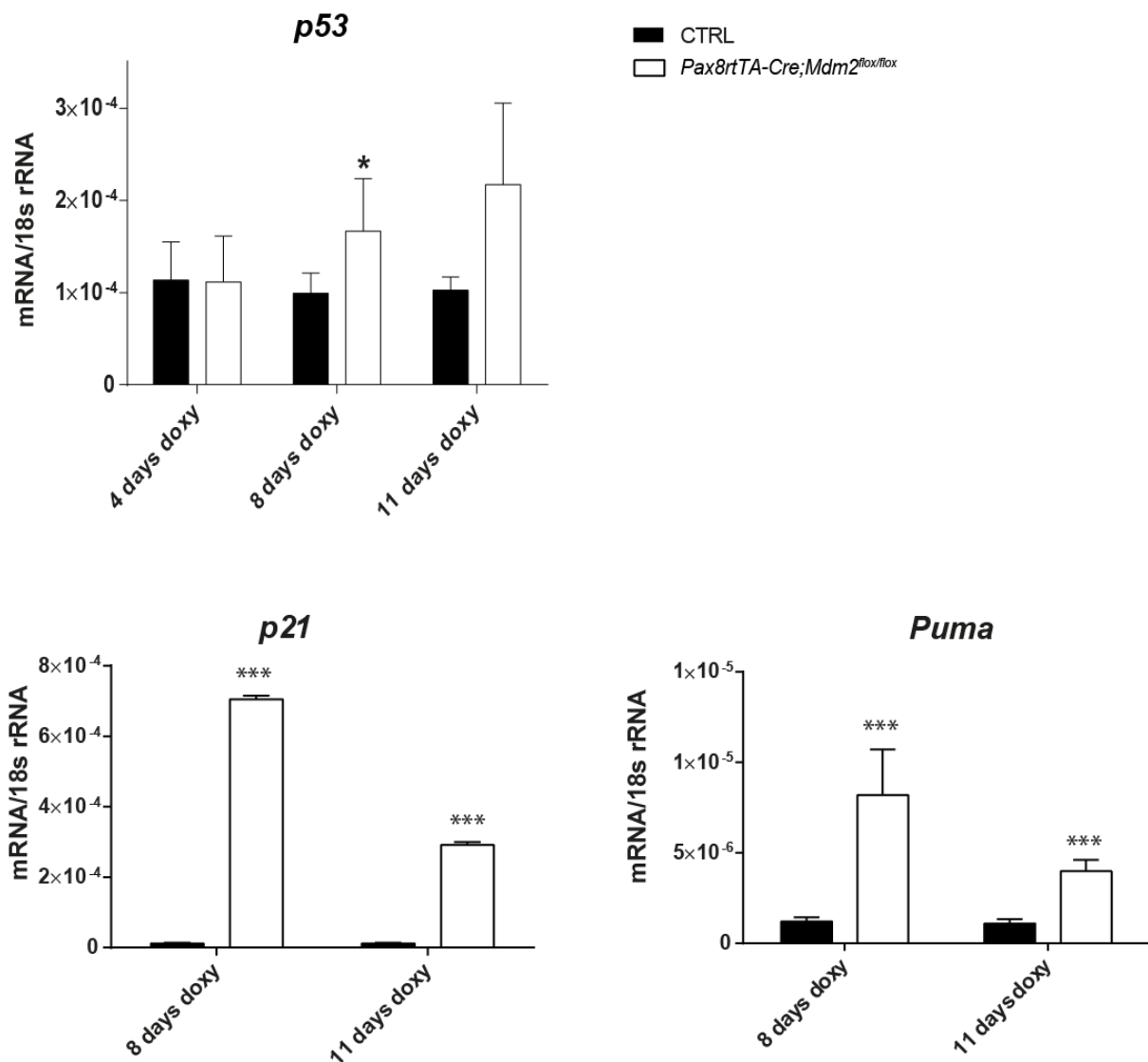


Figure 20: Upregulation of *p53*, *p21* and *Puma* in renal tubules lacking *Mdm2*.

Mdm2^{-/-tubulus} mice showed no change of *p53* mRNA expression on day 4 of doxycycline treatment, but a significant increase on day 8 and day 11 compared to control mice. Furthermore, mRNA levels of *p53* target genes *p21* and *Puma* elevated markedly from day 8 of doxycycline treatment (n=5-6 mice/group). Data are means ± S.E.M. **P*<0.05, ***P*<0.01, ****P*<0.005.

4.2.4 Upregulation of tubulus damage markers in the kidney

As mentioned in introduction 1.1.3, serum creatinine and BUN are standardly used parameters to assess kidney function, but not highly specific or sensitive for acute kidney injury. Also, serum creatinine is a late marker, as loss of more than 50% of kidney function must occur before serum creatinine rises [168]. Kidney-specific biomarkers aiming to recognize AKI faster have emerged during the last decade. Some of these biomarkers have shown good performance in early diagnosis and prognosis prediction of AKI in clinical trials, and their translation into clinical practice is promising.

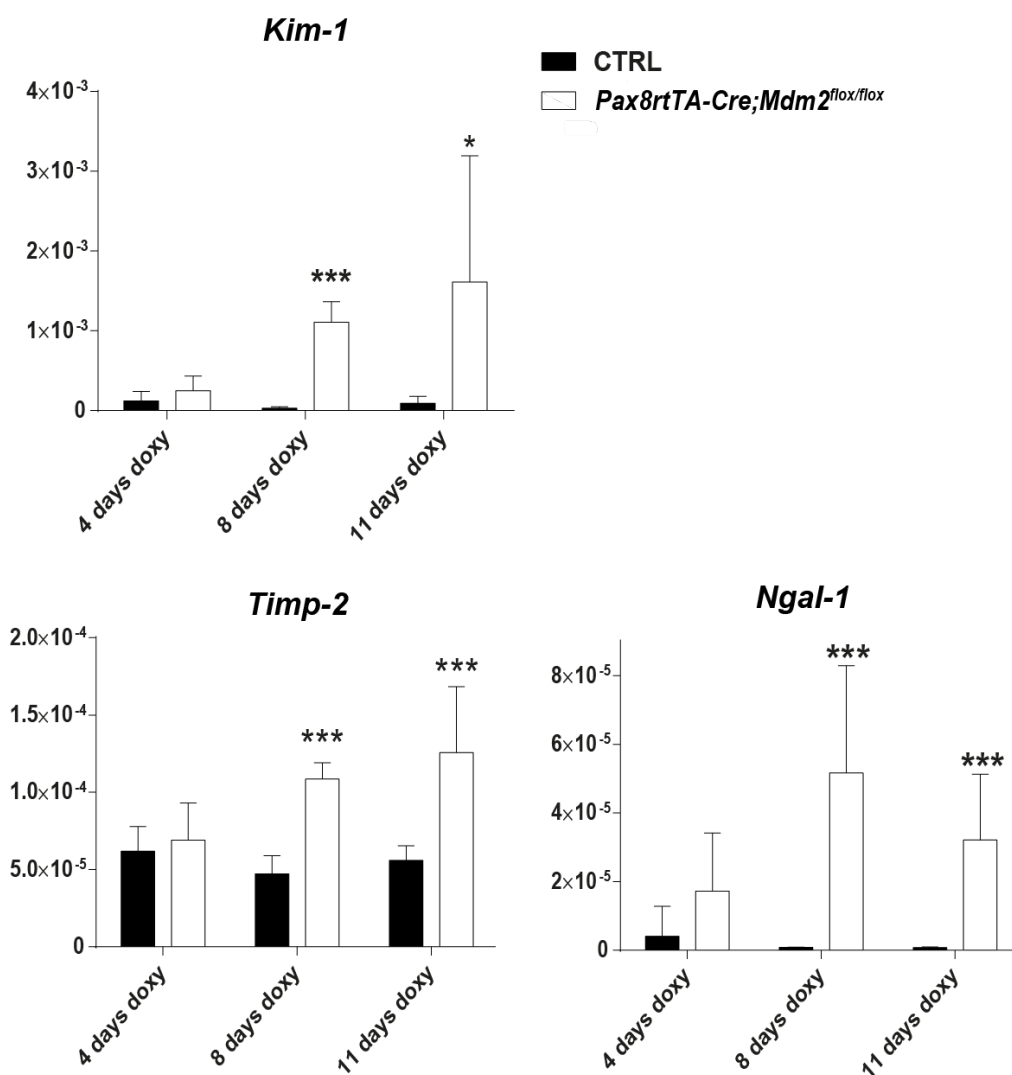


Figure 21: Upregulation of tubulus damage markers in *Mdm2^{-/-tubulus}* mice kidneys.

Kim-1, Timp-2 and Ngal-1 are newly identified biomarkers for tubulus damage with high sensitivity. Their mRNA levels in kidney lysates of *Mdm2^{-/-tubulus}* mice increased progressively with the length of doxycycline treatment, in comparison with controls (n=5-6 mice/group). Data are means \pm S.E.M. * P <0.05, ** P <0.01, *** P <0.005.

Here, we screened a series of tubulus damage biomarker in kidney lysates of *Mdm2*^{-/-tubulus} mice, including Kim-1, Timp-2 and Ngal-1. Strikingly, intrarenal mRNA levels of *Kim-1*, *Timp-2* and *Ngal-1* in *Mdm2*^{-/-tubulus} mice were substantially upregulated from day 8 of doxycycline treatment compared with control mice, as shown in Figure 21. On day 11, the elevation of *Kim-1*, *Timp-2* and *Ngal-1*mRNAs was measured as 15-fold, 2-fold and 15-fold respectively.

The data are consistent with progressively impaired kidney function, as documented by increased serum creatinine, BUN and decreased GFR in *Mdm2*^{-/-tubulus} mice. Marked upregulation of tubulus damage markers suggest further the ongoing injury in renal tubular epithelium upon Mdm2 deletion/p53 activation.

4.2.5 Acute tubular injury under light microscope

To further investigate structural abnormalities in *Mdm2*^{-/-tubulus} mice kidneys, we performed periodic acid-Schiff (PAS) staining of kidney sections and analyzed them under light microscope. Kidney sections of *Mdm2*^{-/-tubulus} mice appeared normal on day 4 of doxycycline treatment, but showed apparent pathological features such as tubular epithelial cells swelling and vacuolization on day 8 (Figure 22). On day 12, kidney sections of knockout mice revealed widespread severe tubular damage, including massive tubular dilatation, cast formation and cellular loss with exfoliation of tubular cells into lumen. On the contrary, no pathology in control mice kidneys was detected.

We also performed semi-quantitative tubulus damage score (described in method 3.4.5) for PAS-stained kidney sections of *Mdm2*^{-/-tubulus} mice. As shown in Figure 22, the score for each category (tubular injury, cast formation and tubular dilatation) increased with the length of doxycycline treatment.

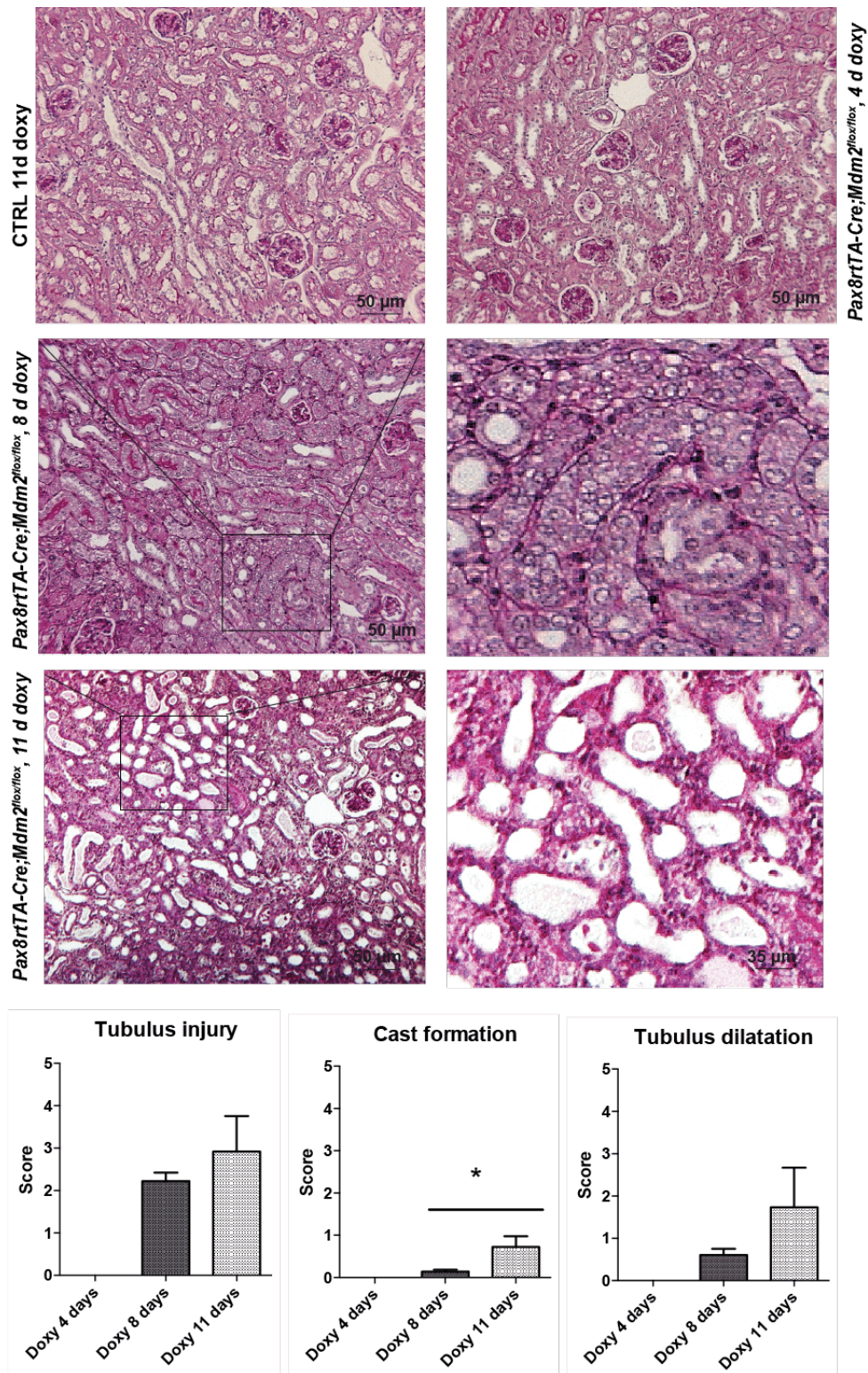


Figure 22: Acute tubular injury in *Mdm2*^{-tubulus} mice kidneys.

Representative images of PAS-stained kidney sections of *Pax8rtTA-Cre;Mdm2*^{flox/flox} mice treated with doxycycline for 4, 8 or 11 days displayed tubular injury with progressive severity, compared to controls mice. While on day 4 no tubular damage was evident, on day 8 pronounced tubular cells swelling and vacuolization was detected. On day 11, severe tubular injury with massive tubular dilation, cast formation and exfoliation of tubular cells into lumen was observed. Images are shown at a magnification of x 200. Semiquantitative scoring of tubulus injury, cast formation and tubulus dialation in *Mdm2* knockout mice kidneys is depicted below the PAS-images.

4.2.6 Cellular loss in proximal tubules, distal tubules and collecting ducts

With measurement of biomarkers and histopathological analysis, we detected that the severity of tubular cell damage increased with the length of doxycycline treatment. Further, we investigated the survival rate of tubular cells upon *Mdm2*-knockout-induced injury. To do so, we stained kidney sections of experimental and control mice with the following compounds:

- 1) *Lotus Tetragonolobus* Lectin, identifying living proximal tubular cells;
- 2) Tamm-Horsfall protein (THP) identifying living distal tubular cells;
- 3) Aquaporin identifying living collecting ducts.

As shown in Figure 23, staining in proximal and distal tubules as well as in collecting ducts of knockout mice kidneys was progressively diminished, compared to controls. This suggests that cellular demise occurred in renal epithelium in the absence of *Mdm2*.

To quantify the cellular survival rate, tubules with intact staining patterns was counted under microscope. The bar charts in Figure 23 illustrated a significant reduction in percentage of living cells in all tubular compartments from day 8 of doxycycline treatment. Moreover, the proximal tubules were the most affected site by cellular loss, compared with distal tubules and collecting ducts. On day 8 of doxycycline treatment, 53% of proximal tubular cells survived. On day 11, merely 26% of proximal tubular cells were viable; in other words, 73% of proximal tubular cells underwent cell death caused by *Mdm2* deletion. The percentage of cellular loss in distal tubules and collecting ducts on day 11 were 29% and 21%, respectively.

Together, tubular epithelial cells underwent spontaneous cell death upon *Mdm2*-depletion, predominantly in proximal tubules.

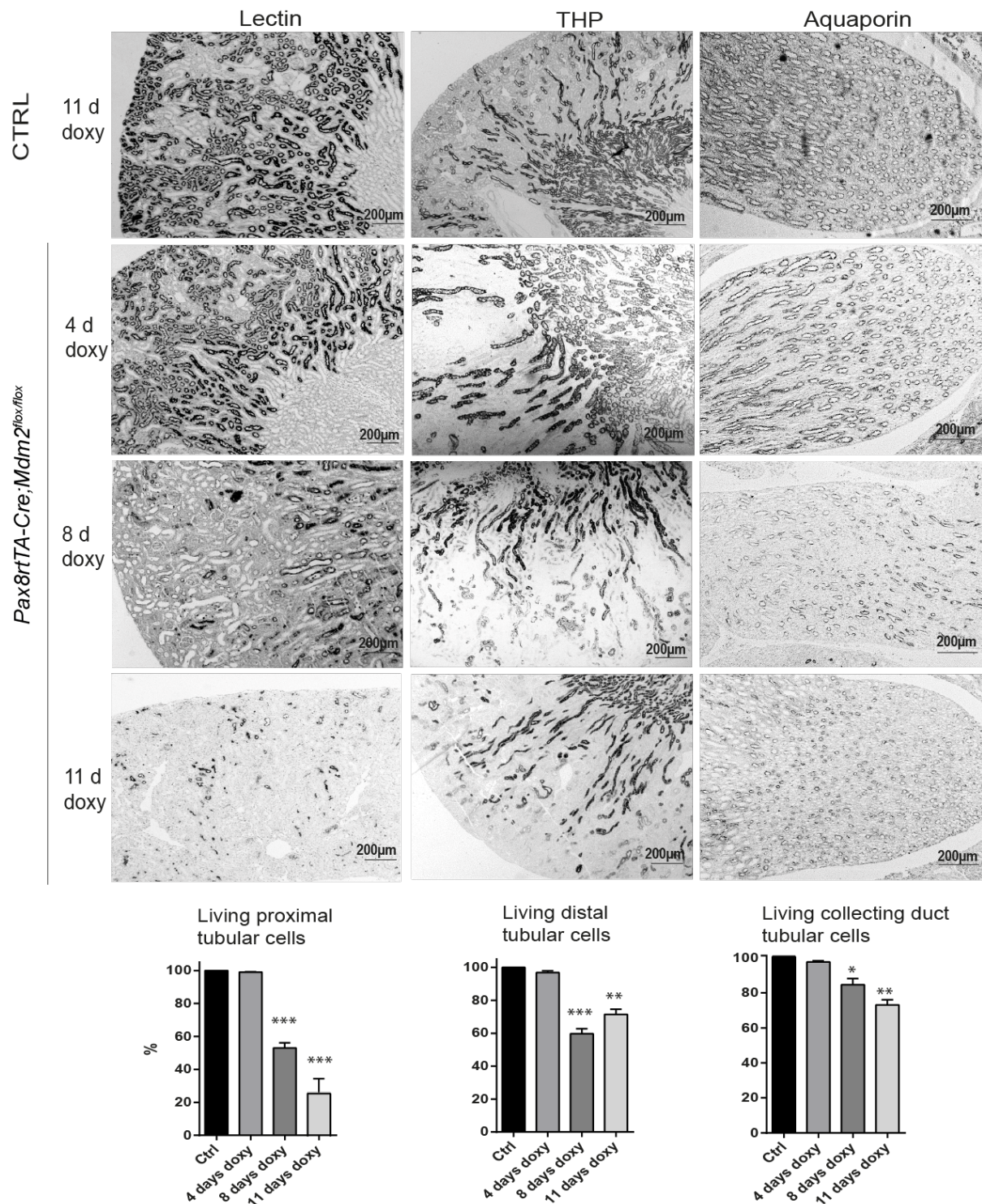


Figure 23: Cellular loss in renal tubules of $Mdm2^{-/-tubulus}$ mice.

Representative images of kidney sections from $Mdm2^{-/-tubulus}$ and control mice, stained with *Lotus Tetragonolobus* Lectin, Tamm-Horsfall protein (THP) and Aquaporin, which identified living tubular cells in proximal, distal tubules and collecting ducts respectively. Tubules with intact staining patterns decreased progressively with length of doxycycline treatment in $Mdm2^{-/-tubulus}$ mice kidneys, compared to control mice. Images are shown at a magnification of x 100. The quantitative evaluation of kidney sections is depicted in the percentage of living tubular cells. Proximal tubules suffered the most cellular loss, compared with distal tubules and collecting ducts. Data are means \pm S.E.M, n=5-6 mice/group. * $P < 0.05$, ** $P < 0.01$, *** $P < 0.005$.

4.2.7 Ultrastructural pathology of tubular cells under electron microscope

Following the histopathological analysis of kidney sections by light microscopy, we further checked ultrastructural changes in renal tubular epithelial cells with *Mdm2* depletion by electron microscopy. As shown in Figure 24, tubular cells lacking *Mdm2* exhibited multiple ultrastructural abnormalities. The first apparent pathological feature was cytoplasmic swelling without membrane blebbing, which emerged on day 4 of doxycycline treatment and became prominent on day 8. Also, mitochondria appeared swollen and displayed loss of cristae with their transformation into vacuoles. Moreover, the nuclei were edematous with intact nuclear membrane, but did not show signs of consolidated chromatin which is characteristic for apoptosis. Taken together, these morphological patterns under electron microscope indicate that tubular epithelial cells experienced a stage of asphyxia upon *Mdm2* depletion/p53 activation. With the injury persistent, tubular cells could not compensate for intracellular damage and started dying from the cytoplasm with dead mitochondria. Eventually, complete disintegration of tubular epithelial cells was observed on day 11 of doxycycline treatment, along with rupture of plasma membrane and release of nuclei and other cytoplasmic organelles into the tubular lumen.

Together, tubular cells upon *Mdm2* depletion showed pathological changes in ultrastructure such as cytoplasmic swelling and mitochondria degradation with vacuoles. However, characteristic morphologic features of apoptosis were not detected by electron microscopy in *Mdm2*^{-/-tubulus} mice kidneys [96].

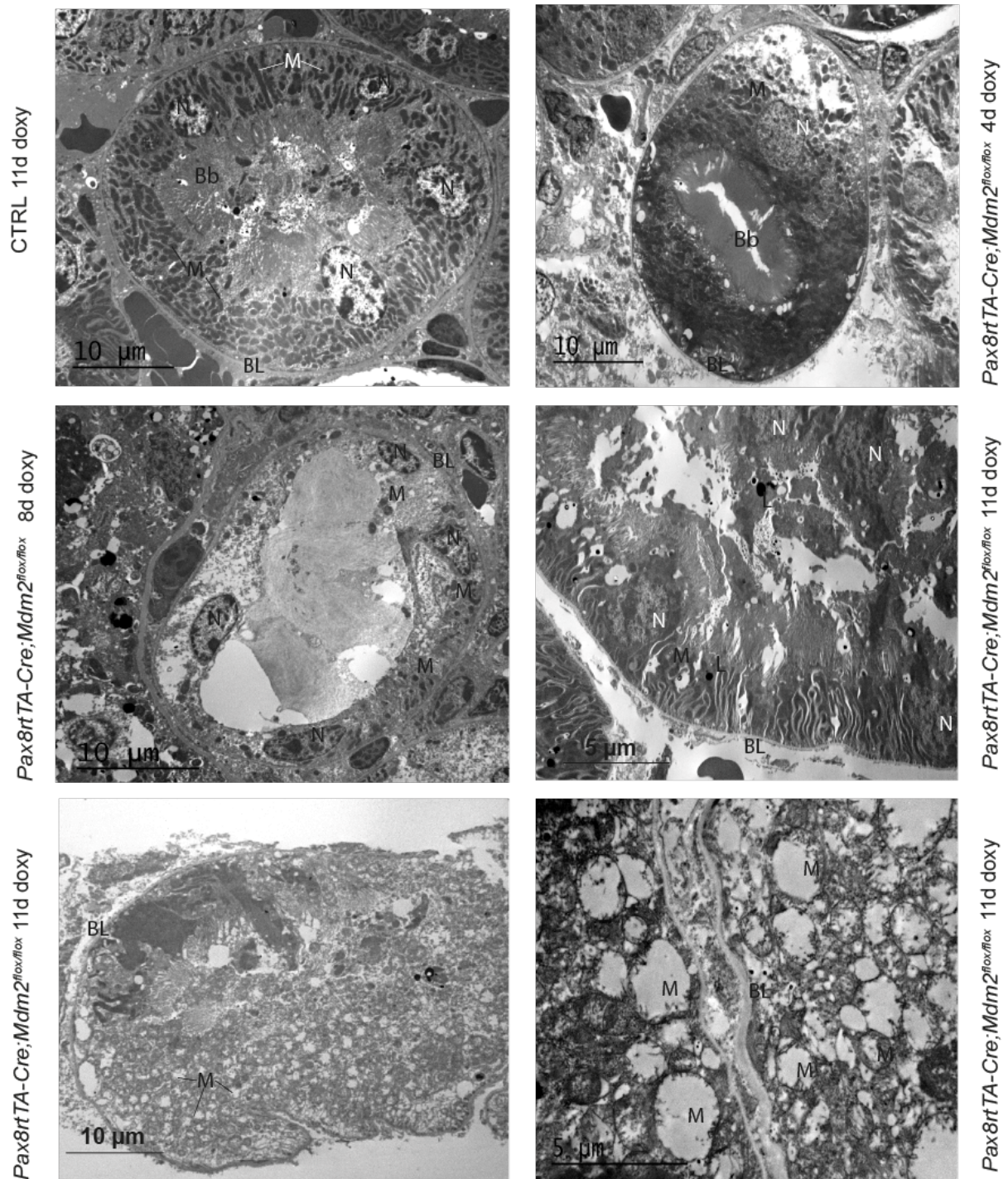


Figure 24: Ultrastructural pathology in tubular cells of *Mdm2*^{-/-tubulus} mice.

Electron microscopy detected cytoplasmic swelling of tubular cells on day 4 of continuous doxycycline treatment, which exacerbated on day 8. With persistent Mdm2 depletion, nuclei became edematous but nuclear membrane remained intact, and mitochondria lost cristae which transformed into vacuoles. On day 11, tubular cells completely disintegrated with rupture of cytoplasmic membrane, degradation of mitochondria and release of cellular contents into the tubular lumen. Images are shown in 1500–12000 magnification (successively low–medium–high). Bb, brush border; BL, basal lamina; L, lysosome; M, mitochondria; N, nucleus.

4.2.8 Apoptosis and proliferation assays with immunostaining

How did tubular epithelial cells die in the absence of *Mdm2*? Was apoptotic pathway activated in response to p53 activation? To answer these questions and to study the mechanism for cellular loss, we performed apoptosis analysis with various immunostaining methods for kidney sections of experimental and control mice. We applied p53 and cleaved caspase 3 (also referred as activated caspase 3) immunohistochemical staining as well as TUNEL immunofluorescence staining (Figure 25 and Figure 26). Tubular compartment of *Mdm2*^{-/-tubulus} mice kidneys stained increasingly with p53 antibodies, suggesting a progressively enhanced expression of p53 protein in tubular cells upon *Mdm2* depletion. By contrast, p53 expression remained constantly undetectable in tubular cells of control mice, as p53 protein is kept at low levels under physiological conditions. The data confirmed again that *Mdm2* depletion results in p53 activation in renal tubular cells, which is in line with PCR results.

However, only marginal expression of caspase 3 was identified by immunostaining in tubular cells of *Mdm2*^{-/-tubulus} mice. Caspase 3 is an executioner caspase and activated in both p53-induced intrinsic and extrinsic apoptotic pathways. Also, TUNEL staining, which detects DNA fragmentation and is considered as “gold standard” to investigate apoptosis *in situ* [96], showed just modest positivity in tubular cells. The activation level of caspase-3 did not correlate with p53 activation level and the extent of the tubular damage, indicating that rather secondary cell apoptosis occurred.

Additionally, we checked the proliferation activity in renal epithelium by Ki-67 immunohistochemistry and immunofluorescence (Figure 25 and Figure 26), as Ki-67 is a marker for cellular proliferation or hypertrophy. Marked Ki-67 activation in tubular cells where the *Mdm2* deletion was incomplete was observed, suggesting that surviving tubular cells reentered into cell cycle, proliferated or hypertrophied upon injury in order to compensate for the cellular loss. Nonetheless, tubular cells could not compensate for *Mdm2*-deletion/p53-activation mediated cell death through enhanced regenerative activity.

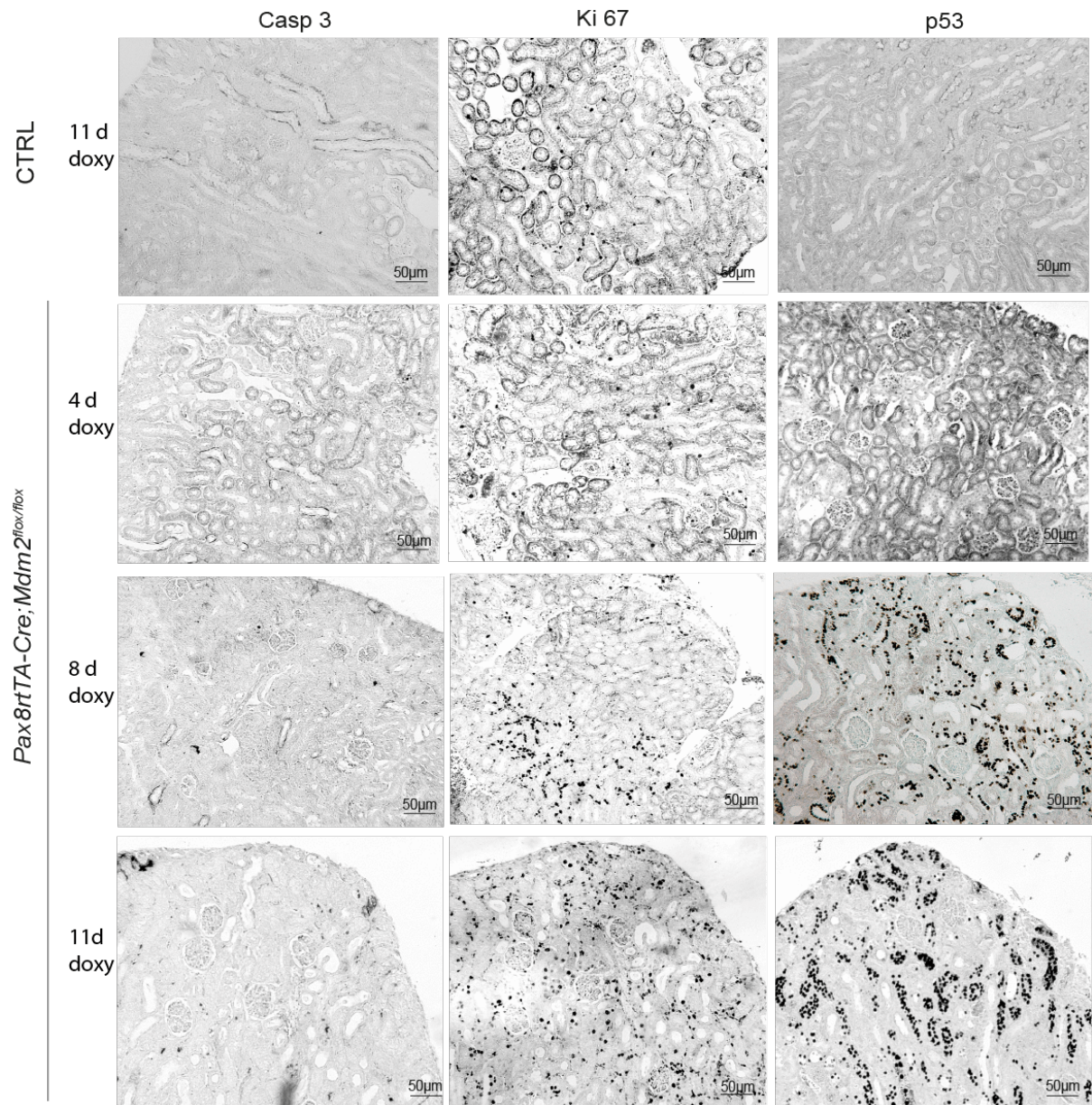


Figure 25: Caspase-3, Ki-67 and p53 immunostaining in kidney sections.

Representative images of kidney sections of *Mdm2*^{-/-tubulus} and control mice, stained with caspase 3, Ki-67 and p53 respectively. Caspase 3 (marker for apoptosis) staining was only marginal in tubular cells of *Mdm2*^{-/-tubulus} mice. By contrast, Ki-67 (marker for proliferation) and p53 (marker for cell cycle arrest, cell death and senescence) was increasingly expressed in tubular cells lacking *Mdm2*. On day 11 of doxycycline treatment, Ki-67 and p53 was substantially upregulated in tubular cells of *Mdm2*^{-/-tubulus} mice, compared to control mice kidneys. All images are shown at a magnification of $\times 100$.

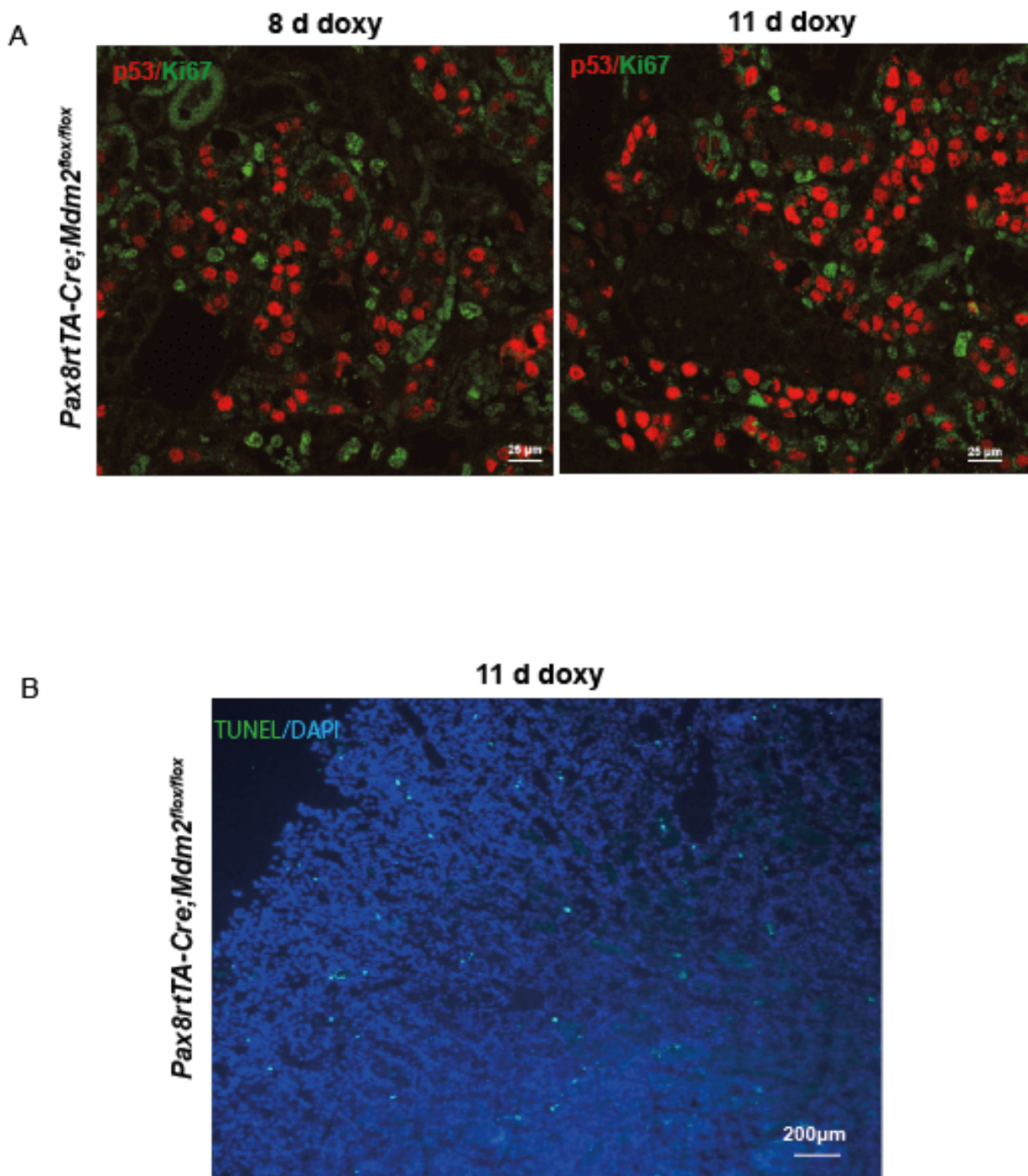


Figure 26: p53/Ki-67 and TUNEL immunofluorescence in kidney sections.

A. Representative images of kidney sections from *Pax8rtTA-Cre;Mdm2^{flx/flx}* and control mice treated with doxycycline for 8 and 11 days, stained with p53 (red) and Ki-67 (green) simultaneously. Both p53 and Ki-67 were markedly upregulated in tubular cells of knockout mice, but no co-localization of Ki-67 and p53 positive cells was detected. Images are shown at a magnification of x200. B. Representative images of kidney sections from knockout mice subjected to 11 days doxycycline treatment, stained with TUNEL/DAPI. TUNEL (TdT-mediated dUTP nick-end labeling) identifies DNA strand breaks generated typically during apoptosis, and DAPI (4',6-diamidino-2-phenylindole) labels nuclei. Only a few tubular cells were positively stained with TUNEL. Image is shown at a magnification of x100.

4.3 Intermittent tubule-specific *Mdm2* depletion results in kidney fibrosis

To avoid the rapid lethality in *Mdm2* tubule-specific knockout mice upon continuous doxycycline treatment, we applied an intermittent doxycycline administration regime as described in Materials and Methods. The discontinuous treatment regime was also used as a strategy in other studies to overcome the problem of early lethality, because transgene expression is reversible and drops sharply when treatment is stopped. Thus, mice have time to recover from the detrimental effects of gene deletion [161]. Previously, Valentin-Vega *et al.* reported that intestinal epithelium as a tissue with high turn-over capacity can fully compensate for *Mdm2*-deletion/p53-activation mediated cell death over time [169]. The possible compensation mechanism is negative selection against *Mdm2*-null cells, and enhanced proliferation of cells with retained *Mdm2* activity due to loss of Cre recombinase. Additionally, intestinal stem and progenitor cells multiply to increase crypt fissions and thus intestine growth [169]. We investigated if this phenomenon would occur to tubular epithelial cells as well, which have low turn-over during homeostasis but are highly proliferative in response to injury.

Over the course of the 4-week-long discontinuous doxycycline treatment, all *Pax8rtTA-Cre;Mdm2^{flox/flox}* mice appeared healthy and active. However, a deterioration of renal function was detected in knockout mice (Figure 27). After 4 cycles of intermittent doxycycline administration, both serum creatinine and urea of knockout mice were elevated by twofold in comparison with controls. Furthermore, intrarenal mRNA levels of tubular damage markers *Kim-1*, *TIMP-2* and *Ngal-1* in knockout mice increased significantly by 60-fold, 2.5-fold and 30-fold respectively, compared to control mice.

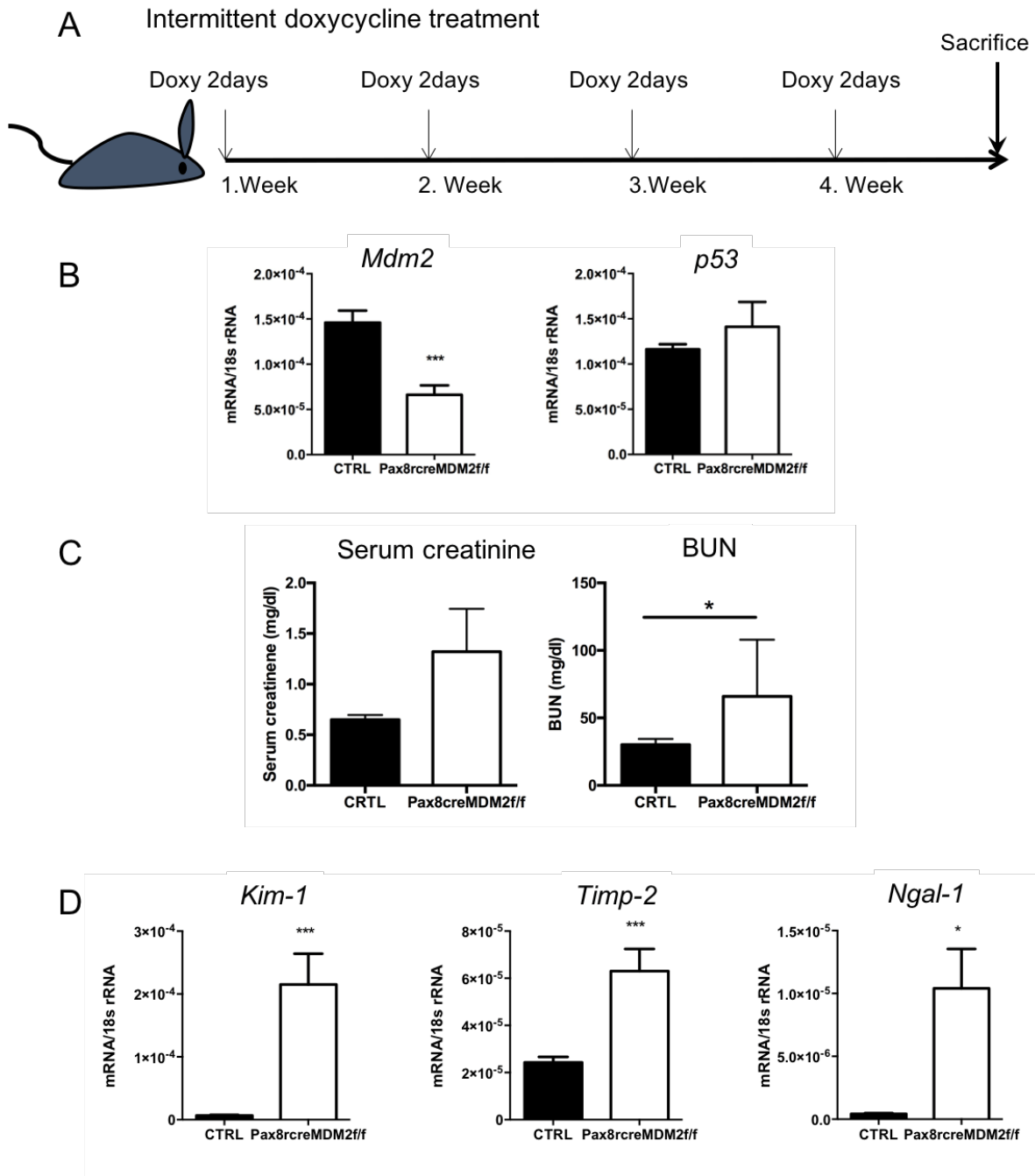


Figure 27: *Pax8rtTA-Cre;Mdm2^{fllox/fllox}* mice subjected to intermittent doxycycline treatment showed impaired kidney function and upregulated tubulus damage markers.

A. Schematic view of discontinuous doxycycline treatment regime: experimental and control mice were administered with 2mg/mL doxycycline for only 2 days and then with pure water for 5 days, repeated for 4 weeks. B. Intrarenal mRNA levels of *Mdm2* and *p53* in knockout and control mice. C. Knockout mice showed a deterioration of kidney functions compared to control mice. D. mRNA expression of tubulus damage markers *Kim-1*, *TIMP-2* and *Ngal-1* significantly increased in kidney lysates of knockout mice, compared to control mice. N=5-6 mice/group. Data are means \pm S.E.M. * $P < 0.05$, ** $P < 0.01$, *** $P < 0.001$.

Notably, the macroscopic appearance of kidneys isolated from *Mdm2*^{-tubulus} mice was pale and fibrotic, and multiple nodules on the organ surface were visible and palpable. We further analyzed kidney sections of experimental and control mice under light microscope. As shown in Figure 28, PAS staining revealed focal tubular damage and increased extracellular matrix in knockout mice kidneys. Furthermore, Masson's tri-chrome staining confirmed overproduction of fibrotic tissue in kidneys. Additionally, immunochemical staining showed moderate p53 accumulation in kidneys, with especially high expression in the medullar region.

We subsequently screened expression of fibrosis markers in kidney lysates of knockout mice, namely Tgf-beta 1, fibronectin1, collagen 1a1, collagen 4a1 and a-Sma. Transforming growth factor beta 1 (Tgf-β1) is a central mediator of kidney fibrogenic process by stimulating the synthesis of extracellular matrix within the kidney [170]. Fibronectin is a glycoprotein in extracellular matrix. Collagen 1a1 belongs to type I collagen that exists in most connective tissues. Collagen 4a1 is a subunit of type IV collagen, which is the major structural component of basement membrane. Alpha smooth muscle actin (a-Sma) is commonly used as a marker of myofibroblast formation. Strikingly, all these tested pro-fibrotic genes except *a-Sma* were significantly upregulated in kidneys of *Pax8rtTA-Cre;Mdm2*^{flox/flox} mice subjected to intermittent doxycycline treatment (Figure 29). mRNA levels of *Tgf-beta 1*, *fibronectin*, *collagen 1a1* and *collagen 4a1* significantly increased by 2-fold, 8-fold, 13-fold and 2-fold respectively.

In summary, unlike intestinal epithelium, tubular epithelium cannot completely compensate for the cell loss due to *Mdm2* deletion/*p53* activation. Instead, the repair process after injury was incomplete and kidney fibrosis occurred. With impaired kidney function and sustained parenchymal damage, *Pax8rtTA-Cre; Mdm2*^{flox/flox} mice did not fully recover from *Mdm2* depletion, but progressed into chronic kidney disease.

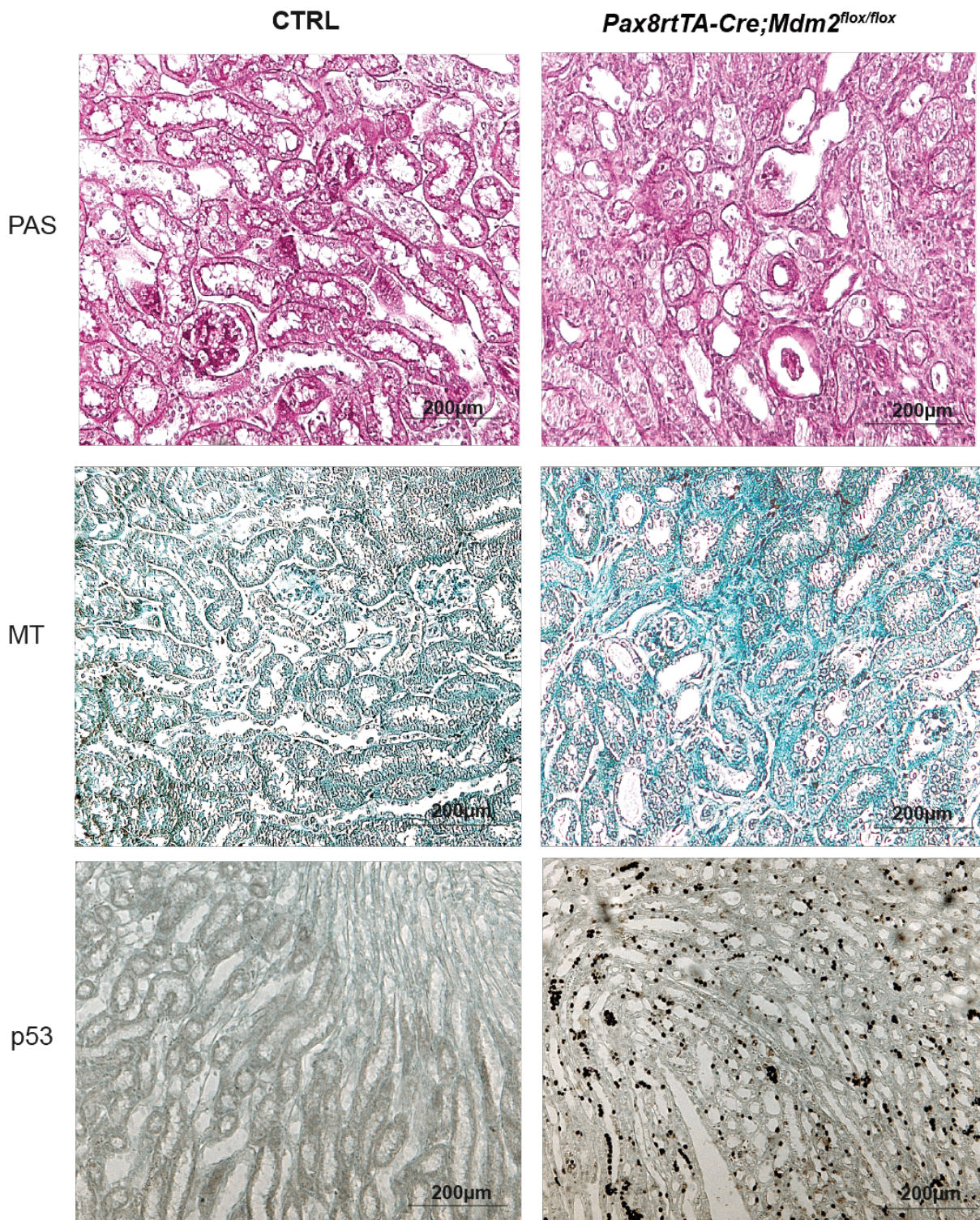


Figure 28: Intermittent *Mdm2* depletion in tubular cells results in kidney fibrosis.

Representative images of kidney sections from *Pax8rtTA-Cre;Mdm2^{lox/lox}* and control *Mdm2^{lox/lox}* mice subjected to discontinuous doxycycline treatment for 4 weeks. Kidney sections were stained with PAS, Masson's trichrome and p53 antibody. PAS and Masson's trichrome staining revealed overproduction of extracellular matrix and fibrotic tissues in knockout mice kidneys. Immunochemical staining detected p53 activation in knockout mice kidneys, especially in the medullar region. All images are shown at a magnification of x 200.

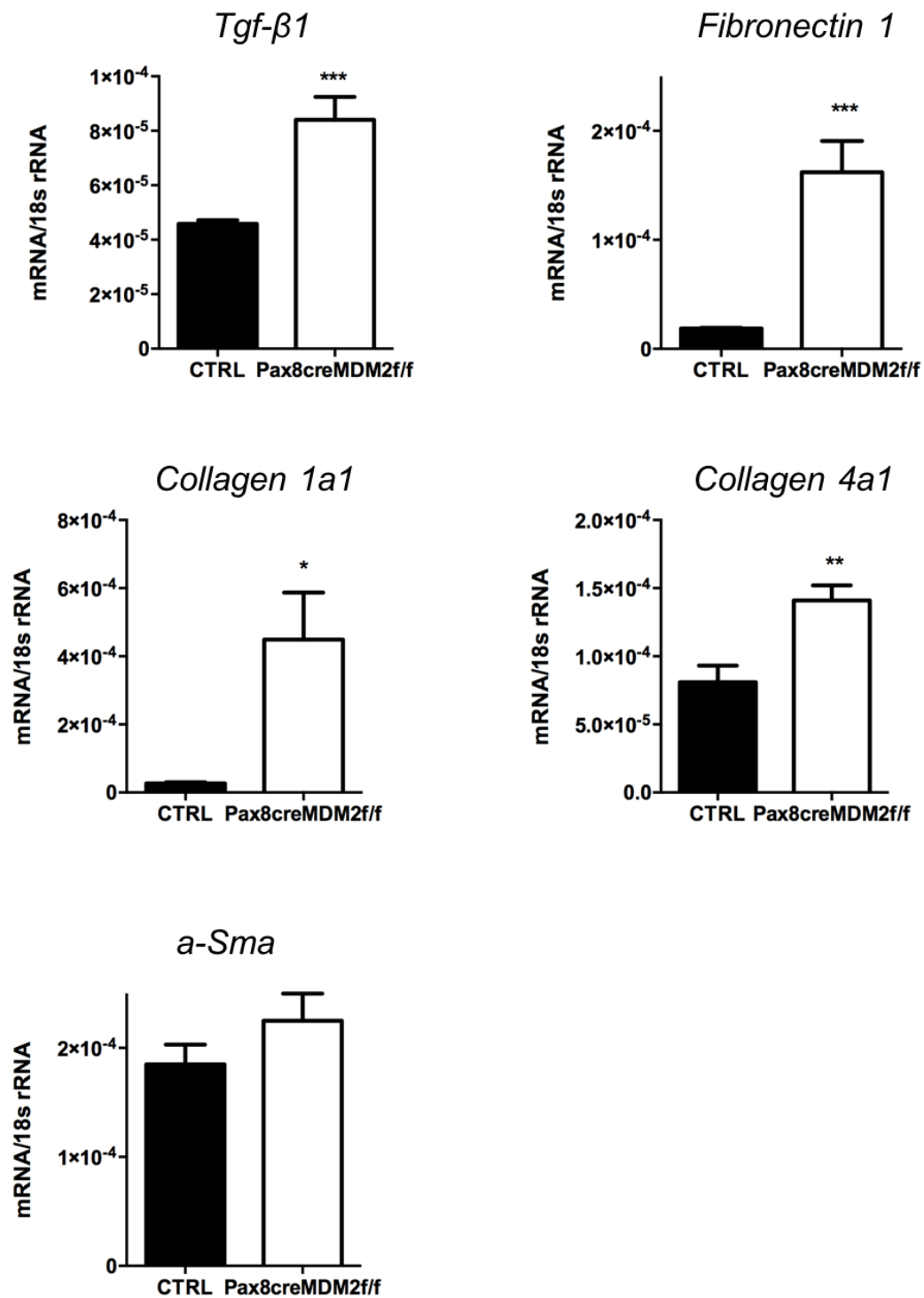


Figure 29: Upregulation of fibrosis markers in kidney lysates of *Pax8rtTA-Cre; Mdm2^{flox/flox}* mice subjected to intermittent doxycycline treatment.

Increased intrarenal mRNA levels of *Tgf-beta 1*, *fibronectin1*, *collagen 1a1* and *collagen 4a1* were detected in knockout mice, compared to control mice. No significant difference of *a-SMA* mRNA expression between experimental and control mice. N=5-6 mice/group. Data are means \pm S.E.M. * $P < 0.05$, ** $P < 0.01$, *** $P < 0.005$.

4.4 Summary of results

We induced *Mdm2* deletion in renal epithelium of *Pax8rtTA-Cre;Mdm2^{flox/flox}* mice by continuous doxycycline administration (*Mdm2^{-/-tubulus}*) for 4, 8 and 11 days. The tubule-specific *Mdm2*-knockout was successful and confirmed by real-time PCR and immunohistochemistry. With increasing doxycycline treatment time, *Mdm2^{-/-tubulus}* mice showed a progressive reduction of intrarenal *Mdm2* mRNA levels compared with control mice. Also, *Mdm2* immunostaining was diminished in renal epithelium of *Mdm2^{-/-tubulus}* mice but remained intact in glomerulus and other cell types within the kidney, thus corroborating the selectivity of *Mdm2* deletion in tubular cells.

With the length of doxycycline treatment, kidney function of *Mdm2^{-/-tubulus}* mice was progressively deteriorated as detected by elevated serum creatinine and BUN levels. Clinically, *Mdm2^{-/-tubulus}* mice developed oliguria, weight loss and had a shortened life span. Moreover, mRNA expression of *p53* and its effector genes *p21* and *Puma* as well as tubular damage markers *Timp-2*, *Kim-1* and *Ngal-1* was upregulated. Under light microscope, kidney sections of *Mdm2^{-/-tubulus}* mice exhibited profound tubular damage from day 8 of doxycycline treatment, which was characterized by tubular cell injury, casts formation, tubular dilatation and progressive cell loss. Under electron microscopy, tubular cells of *Mdm2^{-/-tubulus}* mice displayed ultrastructural pathology, including cytoplasm swelling and mitochondria degradation on day 8, and complete disintegration of tubular cell structure with rupture of plasma membrane on day 11 of doxycycline treatment. Taken together, *Mdm2* deletion in renal tubular epithelium results in p53-activation mediated cell death and acute kidney injury.

Besides, we applied intermittent doxycycline administration regime on *Mdm2^{-/-tubulus}* mice, to circumvent the rapid lethality of continuous doxycycline induction. Within the experimental period of 4 weeks, all *Mdm2^{-/-tubulus}* mice survived and appeared normal. However, impaired renal function of the knockout mice was detected and histopathology of their kidneys revealed pronounced kidney fibrosis with overproduction of extracellular matrix. Furthermore, renal mRNA levels of fibrosis markers *Tgf- β* , *fibronectin 1*, *collagen1a1* and *collagen 4a1* of *Mdm2^{-/-tubulus}* mice increased markedly. This suggests that tubular cells can only partially compensate for the cellular loss due to *Mdm2* deletion, unlike intestinal epithelium that can fully compensate for *Mdm2* deficiency. We conclude that *Mdm2* is indispensable for the survival and homeostasis of renal tubular cells.

5 Discussion

Mdm2 is the key negative regulator of tumor suppressor p53. Mdm2 downregulates p53 activity in three ways: it targets p53 with ubiquitination for proteasomal degradation, it transports p53 out of nucleus and it blocks the p53 activity by direct binding. In turn, p53 upregulates Mdm2 activity by transactivation of its gene expression. Thus, p53 and Mdm2 titrate their levels exquisitely in an autoregulatory feedback loop.

Despite extensive research of Mdm2 in cancer therapy, the function of Mdm2 in homeostatic kidneys remains not well explored. Previously, our research group corroborated the requirement of Mdm2 in unchallenged podocytes [138]. *Mdm2*-deletion in podocytes leads to p53-overactivation mediated cellular loss and focal segmental glomerular sclerosis [138]. In this study, we focused on the role of Mdm2 in quiescent renal tubular cells, which represent a distinct cell type in comparison to podocytes. Tubular cells exert important physiological functions of secretion and reabsorption of small molecules, and play a key role in the pathophysiology of acute kidney injury. With ischemic injury, tubular cells are extremely susceptible to oxygen depletion and thus become a main victim of AKI. Also, they contribute to sterile inflammation during AKI via releasing proinflammatory cytokines and expressing TLRs. Besides, tubular cells with their substantial regenerative capacity contribute to tissue recovery after AKI.

We had hypothesized that resting renal tubular cells require MDM2 to maintain their homeostasis. Without MDM2, tubular cells undergo p53-mediated cell death. To test this hypothesis, we generated tubule-specific *Mdm2*-knockout mice and induced *Mdm2* deletion with doxycycline treatment (*Mdm2*^{-/-tubulus}). By continuous induction, *Mdm2*^{-/-tubulus} mice displayed reduced life expectancy and rapid deterioration of renal function. Moreover, significant increase of mRNA levels of tubular damage markers, pronounced cellular injury and cell death in the renal tubular compartment of *Mdm2*^{-/-tubulus} mice were detected. All these pathological changes developed in homeostatic kidneys and were in line with acute kidney injury.

Furthermore, by intermittent induction of *Mdm2*-knockout, tubular epithelium could not completely compensate for the cell loss by proliferation of tubular cells with retained *Mdm2* activity due to loss of Cre recombination, unlike the intestinal epithelium [169]. Instead, mesenchymal healing occurred and kidney fibrosis with overproduc-

tion of extracellular matrix was observed. To our knowledge this is the first study that examined the role of Mdm2 in quiescent tubular cells of adult healthy kidneys in a tissue-specific manner.

Aside from the phenotypical characterization of tubule-specific *Mdm2*-knockout mice, we have derived the following conclusions from this study:

1. Mdm2 is indispensable for the homeostasis of renal tubular cells in adult healthy kidneys. In unchallenged renal tubular cells, *Mdm2* deletion results in spontaneous tubular cell death and acute kidney injury. Our hypothesis is confirmed.
2. Tubular epithelium lacking *Mdm2* cannot compensate for the cell loss due to *Mdm2* deletion. Inadequate tissue repair after *Mdm2*-deletion/*p53*-activation mediated acute kidney injury leads to chronic nephropathy.
3. MDM2 inhibitors (such as family of nutlins and their derivatives) as new cancer therapeutics can have dose-limiting detrimental effects on healthy kidneys. Special caution such as regular monitoring of kidney function is thus required, when MDM2 inhibitors are systemically administered.

5.1 Mdm2 is required for the homeostasis of renal tubular cells

We demonstrated that tubular cell-specific *Mdm2* deletion results in spontaneous cell death and acute kidney injury, which underscores the non-redundant role of Mdm2 for tissue homeostasis and survival. The importance of Mdm2 in negatively regulating p53 activity during embryogenesis is emphasized by *Mdm2*-null mice. Loss of *Mdm2* leads to embryonic lethality, which is completely rescued in the absence of p53 [118, 119, 171]. Mechanistically, *Mdm2* deletion results in p53 activation and p53-mediated cell cycle arrest and cell death. As embryonic development requires an exquisite balance of apoptosis and proliferation, *Mdm2*-null embryos are not viable due to uncontrolled apoptotic cell death.

Recently, a growing body of studies has investigated the role of Mdm2 during organogenesis in a tissue-specific manner, e.g. by engineering conditional knockout mice with Cre/loxP system. Mostly, mice display deleterious phenotypes upon specific *Mdm2*-deletion in tissues, ranging from embryonic lethality [172, 173], morphological and functional abnormalities [174, 175] to compensation of the tissues for *Mdm2* loss [169] (Table 7). All tissues experience p53 activation in the absence of *Mdm2*, however, the severity of the phenotypical defects differs from tissue to tissue [106].

For example, mice lacking *Mdm2* in the central nervous system die very soon after birth and present with dome-shaped head and hydranencephaly [176, 177]. Loss of *Mdm2* in cardiomyocytes in mice causes heart failure and embryonic lethality [82]. Also, *Mdm2* deletion in lens epithelial cells results in aphakia and neonatal lethality of unknown reasons [178]. Moreover, Mice with *Mdm2*-deletion in smooth muscle cells (SMC) of intestines die rapidly after inactivation of *Mdm2* and exhibit severe lesions in the SMC-containing layers of the intestinal wall [179]. Removing *Mdm2* in the oocytes results in impaired fertility, irregular menstruation and small ovaries [174, 175]. Conditional inactivation of *Mdm2* in erythroid progenitor cells disrupts the primitive erythropoiesis. Such knockout mice are non-viable and show dramatically reduced number of erythrocytes, most of which undergo apoptotic cell death [173]. As for skeletal development, *Mdm2* deletion causes pronounced impairment of bone formation and embryonic lethality [172]. Strikingly, all these deleterious phenotypes are proved to be p53-dependent. In contrast, intestinal epithelial cells can bypass *Mdm2* loss with time due to their high proliferative capacity and overgrowth of cells that retain *Mdm2* activity [169].

Table 7: Phenotypes of mice with tissue-specific *Mdm2*-knockout

Tissues	Genotype	Phenotype	Refs
CNS	<i>Mdm2</i> ^{FM/FM} ; <i>Nestin-Cre</i>	Neonatal lethal; domed-head and hydrocephaly	[176, 177]
Heart	<i>Mdm2</i> ^{FM/-} ; <i>αMyhc-Cre</i>	Embryonic lethal; heart failure	[82]
Lens	<i>Mdm2</i> ^{FM/FM} ; <i>Le-Cre</i>	Neonatal lethal; eyeless	[178]
Smooth muscle	<i>Mdm2</i> ^{FM/FM} ; <i>Sm22-CreER</i> ^{T2}	Rapid lethality after <i>Mdm2</i> inactivation; severe cellular loss of intestinal SMCs	[179]
Ovary	<i>Mdm2</i> ^{FM/-} ; <i>Zp3-Cre</i>	Impaired fertility, small ovaries	[174, 175]
Blood	<i>Mdm2</i> ^{flox/flox} ; <i>EporGFP-Cre</i>	Embryonic lethal; erythropoietic defects	[173]
Bone	<i>Mdm2</i> ^{flox/-} ; <i>Col3.6-Cre</i>	Embryonic lethal; impaired bone formation	[172]
Intestine	<i>Mdm2</i> ^{FM/FM} ; <i>Villin-Cre</i>	Intestinal abnormalities, which disappear with age	[169]
Kidney	<i>Mdm2</i> ^{flox/+} ; <i>αHoxb7-Cre</i>	Perinatal lethal, severe renal hypodysplasia	[133]
	<i>Mdm2</i> ^{flox/flox} ; <i>Six2-GFP::Cre</i> ^{tg/+}	Perinatal lethal, hypodysplastic kidneys	[135]
	<i>Mdm2</i> ^{flox/flox} ; <i>Nphs2-Cre</i>	Focal segmental glomerulonephritis	[138]

CNS: central nervous system; SMC: smooth muscle cells; *Mdm2*^{FM}: exons 5 and 6 of *Mdm2* gene are flanked by loxP sites; *Mdm2*^{flox}: exons 7 and 9 of *Mdm2* gene are flanked by loxP sites; Cre: Cre recombinase; GFP: green fluorescent protein.

Tissue-specific promoters: *Nestin*: promotor specific for neurons; *αMyhc* (α -myosin heavy chain): promoter specific for cardiomyocytes; *Le*: promotor specific for lens epithelial cells; *Sm22*: promoter specific for smooth muscle cells; *Zp3* (Zona pellucida glycoprotein 3): promoter specific for growing oocytes; *Epor* (endogeneous erythropoietin receptor promoter): promoter specific for erythroid progenitor cells; *Col3.6*: promoter specific for osteoblasts; *Villin*: promoter specific for epithelial cells of small and large intestines; *αHoxb7* (*Homobox B7*): promoter specific for ureteric bud and mesonephric duct; *Six2*: promoter specific for nephron progenitor cells; *Nphs*: podocin promoter specific for podocytes.

To explore the redundancy of *Mdm2* in kidney development, Hiliard *et al.* engineered mice with conditional *Mdm2*-knockout in the ureteric bud epithelium (UB^{*Mdm2*^{-/-}}) and nephron progenitor cells (NPC^{*Mdm2*^{-/-}}) respectively. None of these mice survive after birth and display aberrant nephrogenesis and hypodysplasia. Moreover, Thomasova *et al.* deleted *Mdm2* in podocytes in mice (Podocyte^{*Mdm2*^{-/-}}), which are viable but develop focal segmental glomerulonephritis with time. All these phenotypes are rescued by concomitant *p53* deletion, demonstrating that *Mdm2* and its negative regulation of *p53* is a prerequisite for kidney development and long-term survival of kidneys as

well. However, there is to date no published data about the role of Mdm2 in renal tubular cells, which motivated us to conduct this study.

In consistence with above mentioned mouse experiments, our data fortify the fact that Mdm2 has a non-redundant role in homeostatic tissues. We explored the significance of Mdm2 function, also in a tissue-specific manner by generation of tubule-specific knockout mice using Cre/loxP system. Different from those studies, we focused on the role of Mdm2 in adult tissues instead of during embryonic development. Using conditional gene expression system, we could study adult organ physiology in transgenic mice by exerting strict control on transgene expression and circumventing any developmental defects [161]. Our data demonstrated that also within adult kidneys under physiological conditions, proper level of Mdm2 is required to maintain homeostasis. Renal epithelium experiences cellular injury and cell death upon *Mdm2* deletion, leading to acute kidney injury associated with high mortality.

Further on, our findings are in line with another study conducted by Zhang *et al.*, who generated a tamoxifen-inducible mouse line *Mdm2^{FM/-};CAG-CreER* [120]. Zhang *et al.* aimed to identify the effects of global *Mdm2* loss on adult tissues and thus address the question, whether Mdm2 inhibitors have adverse effects on normal tissues. Tamoxifen injections were administered in transgenic mice at young adult age (2-4 months) and at advanced adult age (16-18 months) as well. All these mice, regardless of age, became moribund within 1-2 days after daily tamoxifen injection for 3 consecutive days and were sacrificed. Necropsies of knockout mice show evident morphological abnormalities in all examined tissues including kidneys, which exhibit tubule dilation and protein cast. However, kidney functional parameter BUN remains normal, suggesting that the renal phenotypical defects are not severe enough to cause functional change within this time period. The requirement of Mdm2 during the whole life span of the mouse has been thus confirmed [120].

Similarly, Ringshausen *et al.* generated a tamoxifen-inducible, switchable p53 mouse model *Mdm2^{-/-}; p53^{KI/-}* to determine the effects of global *Mdm2* loss in adult mice [94]. In the absence of tamoxifen, the knock-in allele p53^{KI} is in a non-functional state. Upon tamoxifen injection, p53 activity is rapidly restored. In this way, the embryogenic lethality of *Mdm2*-null mice is circumvented and *Mdm2^{-/-}; p53^{KI/-}* mice can develop normally and live to adulthood. After reactivation of systemic p53 activity through daily tamoxifen injection, these adult *Mdm2*-null mice die within 6 days. Analysis of the

harvested organs of *Mdm2*^{-/-}; *p53*^{KI/-} mice reveals profound damage with atrophy and widespread apoptosis in radio-sensitive organs, i.e. thymus, spleen, bone marrow and intestines. However, the radio-insensitive organs, including kidney, are morphologically not affected by unbuffered p53 activity, which differs from our and Zhang's findings. Nevertheless, the kidneys display upregulation of *p53* target genes such as *p21* and *Puma*, suggesting that kidneys are still affected by restoration of p53 to a certain extent [94]. It is to note that the results of Ringshausen *et al.* should be interpreted cautiously, because *Mdm2*^{-/-}; *p53*^{KI/-} mice only express one copy of *p53* upon tamoxifen induction, which does not faithfully mimic the clinical conditions of tumors that express two wild type *p53* alleles [120]. In contrast, our study allows upregulation of both wild type *p53* alleles upon *Mdm2* deletion, thus more authentic to the aforementioned clinical situation.

Last but not least, our results are in accordance with experiments with haploinsufficient and hypomorphic mice as well. Haploinsufficient mice (50% of wild type *Mdm2* expression) and hypomorphic mice (30% of wild type *Mdm2* expression) exhibit increased radiosensitivity, the latter also with small body size and hematopoietic defects [121, 122]. This indicates that alterations of Mdm2 levels alone are sufficient to cause detrimental effects due to Mdm2 suppression/p53 activation [106].

In summary, our study provides first *in vivo* evidence that Mdm2 is required for homeostasis in unchallenged tubular epithelial cells of healthy adult kidneys. Tubule-specific *Mdm2* knockout results in spontaneous cell death and acute kidney injury. This observation fits into the big picture that Mdm2 plays a key role in restraining p53 at a low level in homeostatic tissues. This is not only important for understanding renal physiology, but also clinically relevant for evaluating the potential toxicities of Mdm2 inhibitors on healthy kidney tissues.

5.2 Tubular cells cannot fully recover from *Mdm2*-deletion induced injury

We also applied intermittent doxycycline treatment regime on *Mdm2*^{-/-tubulus} mice, to avoid rapid lethality observed during continuous doxycycline induction. Surprisingly, *Mdm2*^{-/-tubulus} mice survived within the whole experimental period and appeared normal. However, kidneys of *Mdm2*^{-/-tubulus} mice exhibited pronounced interstitial fibrosis with overproduction of extracellular matrix, as detected by PAS and Masson trichrome's stain under light microscope. Kidney function parameter BUN was elevated by 2-fold compared to control mice. Moreover, renal mRNA expression of profibrotic markers was significantly enhanced compared to control mice, including *Tgf-beta*, *fibronectin*, *collagen1a1* and *collagen 4a1*. Further on, *Mdm2*^{-/-tubulus} mice displayed significantly increased intrarenal mRNA level of *p53* and enhanced p53 immunostaining in kidneys in comparison with control mice. Taken together, the data suggest that tubular cells cannot fully compensate for cell death due to *Mdm2* depletion/p53 activation; instead, kidney scarring and renal fibrosis occurred.

In contrast, Valentin-Vega *et al.* reported that intestinal epithelial cells lacking *Mdm2* can compensate for cellular loss with time [169]. Transgenic mice *Mdm2*^{flox/flox}; *Villin-Cre* lacking *Mdm2* in the intestinal epithelium (*Mdm2*^{-/-intestines}) were born viable but displayed multiple adverse phenotypes early in life: significantly lower body weight compared to their control littermates, hyperplasia of intervillus pockets and inflammation of intestinal epithelium. Besides, upregulation of p53 and its target genes, and widespread apoptosis in intestinal epithelium of *Mdm2*^{-/-intestines} mice were detected. Unexpectedly, these intestinal abnormalities disappeared with increased age. Intestines can recover completely from the *Mdm2*-deletion mediated cellular loss through a series of compensation mechanisms, including selection against *Mdm2*-null cells, overgrowth of *Mdm2*-retaining cells due to loss of Cre recombinase and accelerated proliferative capacity of intestinal epithelial cells. Eventually, the organism survived and bypassed the *Mdm2* deletion in intestinal epithelium [169].

Contrary to their findings, renal tubular epithelial cell cannot completely compensate for *Mdm2*-deletion mediated cell death, as we demonstrated in our experiments. It is noteworthy that intestinal epithelial cells have an extremely rapid cellular turn-over and only take 24 and 60 hours to renew the entire epithelial layer [106, 180]. On the other hand, renal tubular cells are mainly quiescent and have a low turn-over under physiological conditions [43, 44], but turn to be highly proliferative after injury [181].

Our observation of renal fibrosis is in accordance with Zhang's study, in which also interrupted induction regime on conditional knockout mice was applied [120]. Similarly, kidneys of experimental mice upon discontinuous and global *Mdm2* deletion exhibit a fibrosis phenotype. Zhang attributed this phenomenon to remodeling process of epithelial-mesenchymal-transition (EMT) [120]. However, a growing number of recent studies have doubted the role of EMT, or even its existence in renal fibrosis [182, 183]. Herein, we presume that the observed renal fibrosis in *Mdm2*^{-/-tubulus} mice, which is a common feature of chronic kidney disease, is driven by maladaptive repair in response to acute kidney injury.

Recently, there is an emerging concept that acute kidney injury and chronic kidney disease are not distinct pathological processes, but represent a continuum and are interconnected with each other [2, 170, 184, 185]. Acute kidney injury (AKI) is an independent risk factor for development of chronic kidney disease (CKD), and in turn, patients with CKD are more susceptible to AKI ("acute-on-chronic renal failure") [184, 186-188]. Patients with AKI in the history have a 9-fold higher risk to develop CKD, and a 3-fold higher risk for progression into ESRD than have matched patients without AKI [189].

How does AKI accelerate the progression of CKD? An increasingly accepted theory is that maladaptive repair following AKI drives persistent organ dysfunction and thus predisposes to CKD [184] (Figure 30). Maladaptive repair is more likely to happen, especially when the kidney injury is severe and persistent and/or the patient is elderly. During maladaptive repair in response to AKI, complex changes in heterogeneous cell population within the kidney environment occur. These include vascular dropout, recruitment of profibrotic and pro-inflammatory macrophages and premature cell-cycle arrest of injured tubular cells [2, 184]. Notably, tubular cells that arrested at G2/M checkpoint for a prolonged period release increased amount of profibrotic factors such as transforming growth factor beta (Tgf-beta), which contributes to overproduction of extracellular matrix and progressive fibrosis [44, 190]. The underlying pathophysiological mechanism for the AKI to CKD transition is not well understood yet and remains under controversy and debate [2].

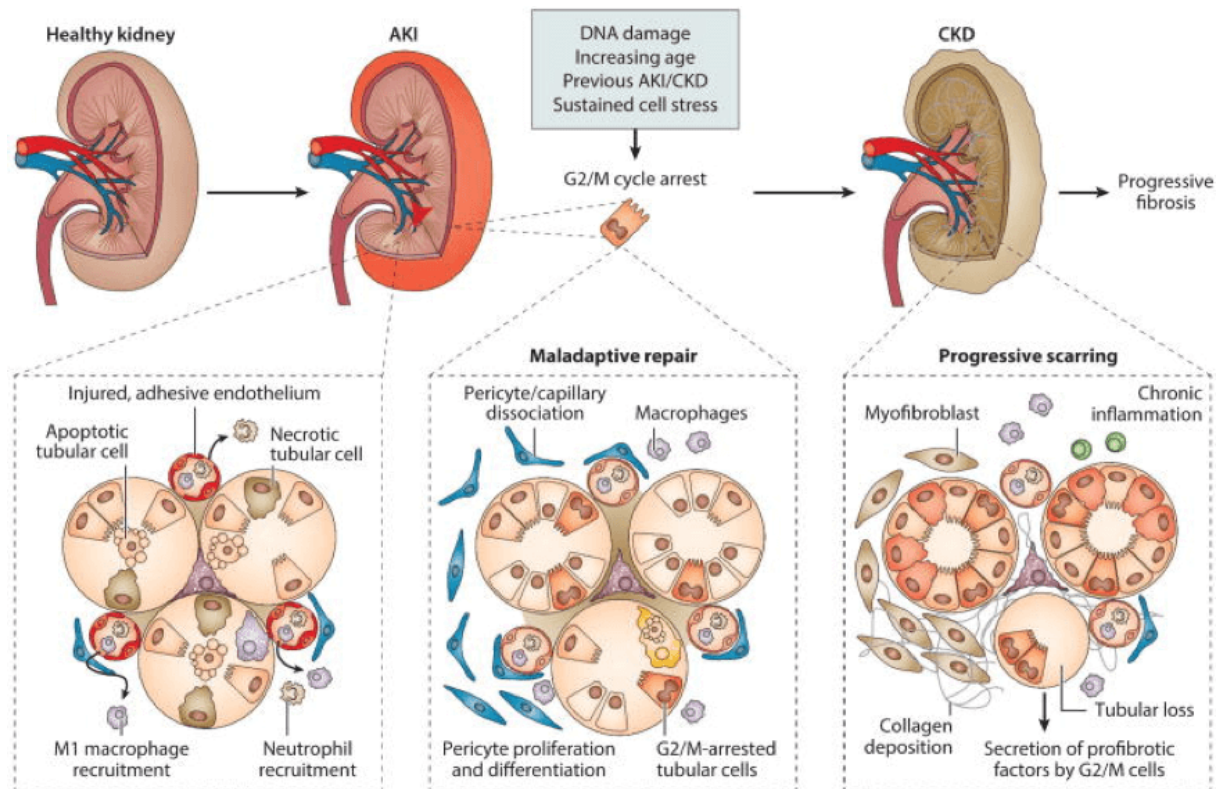


Figure 30: Maladaptive repair after acute kidney injury leads to chronic kidney disease

Acute kidney injury is potentially reversible and resolves after adaptive repair. However, if the injury is severe or persistent, maladaptive repair is more likely to occur. Recruited macrophages, growth-arrested tubular cells and proliferating myofibroblasts mediate inflammation and fibrogenesis within the kidney. Moreover, dissociation of endothelium and pericytes results in endothelial dysfunction and vascular dropout, which exacerbates tissue hypoxia. Finally, accumulation of extracellular matrix, chronic inflammation and sustained cellular malfunction lead to renal parenchymal scarring, decline of kidney function and chronic kidney disease. Picture taken from Zuk *et al.* [2] with permission (order license Id: 433590886439, confirmation number: 11713651).

5.3 MDM2 inhibitors might have detrimental effects on patients

Over the last decade, MDM2 inhibitors have been rigorously researched in treating cancer with wild type p53, which constitutes approximately half of all tumors. As MDM2 is the chief negative regulator of tumor suppressor protein p53, antagonizing MDM2 protein results in restoration of p53 activity. Consequently, p53-mediated pathways of apoptosis and cell cycle arrest are activated, which suppresses tumor development and progression. Among various approaches of antagonizing MDM2, blockade of protein-protein interaction is the most developed strategy. For example, the sensationally discovered small molecule nutlin occupies the p53-binding pocket of MDM2 and abrogates their interaction. As a result, p53 molecule accumulates and its tumor suppressor network is fostered [191]. Interestingly, nutlins were found to have additional anti-angiogenic effects, thereby reducing blood supply for tumor and starving cancer cells [191, 192]. The successful anti-cancer efficacy of nutlins and nutlin-derivatives were authenticated by proof-of-concept studies [144, 146, 148]; some of such compounds are being probed in clinical trials [145].

Despite the promising clinical prospects of MDM2 inhibitors as anti-cancer therapeutics, their potential adverse effects can be dose-limiting and should be kept in mind (Table 8).

First, MDM2 inhibitors may have toxicities on normal tissues. Upon systemic MDM2 administration, not only tumor cells are exposed to the drug effects, but also normal tissues such as bone marrow, gastrointestinal tract and kidney. For example, small molecule MDM2 antagonist RG7112 was evaluated in a clinical trial of patients with liposarcoma, which is characterized by a high frequency of *MDM2* gene amplification and wild-type p53 [145, 154]. All enrolled patients experienced at least one adverse event, most commonly nausea (82%), vomiting (65%), asthenia (53%) and diarrhea (53%). Moreover, serious hematologic adverse effects were observed in patients, such as neutropenia (35%) and thrombocytopenia (18%) [154]. In another clinical study of RG7112 in patients with hematologic malignances, severe adverse effects were reported in more than 10% patients, with most frequent being grade 4 febrile neutropenia (3%) and pneumonia (2%).

As for kidneys, our study demonstrates that renal epithelial tubular cells experience deleterious effects upon *Mdm2* deletion, regardless of treatment regime. Both acute kidney injury and chronic kidney disease can occur in the absence of *Mdm2* in tubu-

lar epithelium. Our finding is consistent with the previous study of podocyte-specific *Mdm2*-knockout mice, which developed focal segmental glomerular nephritis, accompanied with proteinuria, progressive loss of podocytes and reduced life span. This study suggests that podocytes lacking *Mdm2* undergo cell death and fail to maintain the glomerular filtration barrier. Taken together, special caution regarding kidney's homeostasis should be taken when treating cancer with MDM2 inhibitors, and a close monitoring of the patient's kidney function is necessary.

Second, MDM2 inhibitors can impair wound healing [123]. For example, nutlin inhibits tissue regeneration and repair process after acute kidney injury, as the proliferative effect of *Mdm2* is dampened [136, 193, 194]. Patients treated with nutlin can be therefore more susceptible to undergo maladaptive repair and incomplete healing following acute kidney injury. Third, there exists a concern that prolonged use of MDM2 inhibitors can induce mutations in wild type p53 gene, thereby favoring development of second tumor [195].

In summary, MDM2 inhibitors in cancer therapy are promising, but more studies are required for further evaluations.

Table 8: Effects of MDM2 inhibitors

Desired effects	Potential adverse effects
Suppression of tumor development via <ul style="list-style-type: none"> ➤ Upregulation of p53 activity ➤ Anti-angiogenic effects 	<ul style="list-style-type: none"> ➤ Toxicities on normal tissues ➤ Impairment of wound healing ➤ p53 mutation by prolonged use of MDM2 inhibitor ➤ Induction of second tumor development

5.4 How do tubular cells die in the absence of *Mdm2*?

We reported that *Mdm2*^{-/-tubulus} mice underwent acute kidney injury with upregulation of p53 and its target genes *p21* and *Puma* in the kidney. How do tubular cells die upon *Mdm2* deletion? We expected that activated p53 would induce apoptotic pathway. However, *Mdm2*^{-/-tubulus} mice kidneys exhibit only modest apoptotic activity on cleaved caspase 3 and TUNEL immunostaining, which did not correlate with the extent of cell loss and tubular injury in renal epithelium. Furthermore, light microscopy as well as electron microscopy did not detect characteristic morphological features of apoptosis in tubular cells, such as cellular shrinkage, membrane blebbing and chromatin condensation. Additionally, necrosis or autophagy were not detected by morphology neither. The exact cell death mode in tubular cells upon *Mdm2* deletion remains unknown and need to be further explored.

Previously, Thomasova *et al.* proposed a new cell death mode, namely podoptosis (p53-overactivation related cell death) observed in podocyte-specific *Mdm2* knockout mice and podocytes cell culture [138]. Based on biochemical signaling pathway, their *in vitro* data excluded apoptosis and other recognized regulated cell death pathways such as necroptosis, pyroptosis, pyronecrosis, ferroptosis and parthanatos etc. Thus, they defined this distinct, p53-overactivation-related form of cell death, referred as “podoptosis”. Whether podoptosis also occurs in renal tubular cells, remains unknown. Nowadays, cell death modalities are not defined by morphological but by biochemical criteria according to the Nomenclature Committee on Cell Death (NCCD) [196]. Thus, comprehensive *in vitro* experiments should be accomplished to define the molecular mechanism of cell death in renal tubular cells upon *Mdm2* depletion.

5.5 Limitations of study and future directions

We determined the effects of *Mdm2* deletion in renal tubular epithelial cells by generation of conditional gene knockout mice. However, our study has methodic limitations. First, the results rely on animal models with transgenic mice, which do not fully exemplify the complexity of human biology. A direct translation from laboratory into clinical situations is thus restricted. Second, the Cre/loxP system may not have 100% efficacy of Cre recombination, thus 100% *Mdm2* gene deletion may not have occurred. Such phenomenon is also reported in other mouse experiments using Cre/loxP system [120, 169]. Third, we isolated RNA from total kidneys, hence, the measured intrarenal mRNA expression is not specific for the tubules, but for the entire cell populations within the kidney.

Future studies include generation of p53 and MDM2 double knockout mice (*p53^{-/-}tubulus*; *Mdm2^{-/-}tubulus*) to examine if the deleterious phenotype of *Mdm2^{-/-}tubulus* mice is p53-dependent. Also, *in vitro* experiments with primary cells isolated from mice and/or human kidneys should be performed, to define the precise molecular mechanism of cell death upon *Mdm2*-deletion in tubular epithelium, as described in 5.4. Moreover, our hypothesis can be tested in other animal models, such as in established zebrafish model with *Mdm2* knockdown through injection of specific morpholinos into fertilized eggs [139]. Finally, in clinical studies of treating cancers with MDM2 inhibitors, follow-up of patients' kidney function and biopsies can reveal short-term as well as long-term effects of low MDM2 levels on human kidneys.

6 Abbreviations

Listed alphabetically

AKI	Acute kidney injury
ABC	Avidin-biotin-complex
a-Sma	Alpha smooth muscle actin
BUN	Blood urea nitrogen
cDNA	Complementary DNA
CKD	Chronic kidney disease
Cdk	Cycline-dependent kinase
Cre	Cause recombination
DAMP	Damage-associated molecular pattern
DAPI	4',6-diamidino-2-phenylindole
DNA	Deoxyribonucleic acid
EMT	Epithelial-mesenchymal-transition
ESRD	End stage renal disease
FSGN	Focal segmental glomerulonephritis
GFR	Glomerular filtration rate
IGFBP7	Insulin-like growth factor-binding protein-7
IL	Interleukin
kDa	Kilo Dalton
Kim-1	Kidney Injury Molecule-1
L-FABP	Liver-type fatty acid-binding protein
LoxP	Locus of crossing over of <i>P1</i> phage
mRNA	Messenger RNA
Mdm2	Murine double minute 2

MOMP	Mitochondrial outer membrane permeabilization
NF- κ B	Nuclear factor-kappa-light-enhancer of activated B-Cells
Ngal	Neutrophil gelatinase-associated lipocalin
NPC	Nephron genitor cells
PAS	Periodic acid-Schiff
PCR	Polymerase chain reaction
Podoptosis	p53-overactivation related cell death
PRR	Pathogen recognition receptors
Puma	p53-upregulated mediator of apoptosis
RNA	Ribonucleic acid
RT	Reverse transcriptase
RT-PCR	Real-time polymerase chain reaction
SEM	Standard error of the mean
SLE	Systemic lupus erythematoses
Tgf- β	Transforming growth factor β
THP	Tamm-Horsfall protein
Timp-2	Tissue inhibitor of metalloproteinases 2
TLRs	Toll-like receptors
TNF	Tumor necrosis factor
TUNEL	Terminal Deoxytransferase Uridine Triphosphate Nick End Labeling
UB	Ureteric bud

7 List of Figures

Figure 1: Morphological hallmarks of tubular epithelial cells during ischemic injury.	10
Figure 2: Ischemic injury and adaptive repair in renal epithelium.	13
Figure 3: Potential use of new biomarkers for acute kidney injury.	15
Figure 4: Schematic structure of p53 protein and p53-induced pathways.	18
Figure 5: Intrinsic and extrinsic apoptotic pathways.	21
Figure 6: Distinct morphological features of apoptosis and necrosis.	22
Figure 7: Schematic structure of Mdm2 protein.	23
Figure 8: p53-Mdm2 autoregulatory feedback loop.	24
Figure 9: Mdm2 is strongly expressed in renal tubular cells.	29
Figure 10: Nutlin inhibits p53-MDM2 interaction.	31
Figure 11: Generation of tubular cell-specific <i>Mdm2</i> knockout mice.	41
Figure 12: Genotyping for wild-type and floxed <i>Mdm2</i> gene.	43
Figure 13: Principle of Nano drop.	45
Figure 14: RNA integrity check with gel electrophoresis.	46
Figure 15: Principle of real-time quantitative PCR.	48
Figure 16: Avidin-biotin-complex method for immunohistochemistry staining.	52
Figure 17: <i>Mdm2</i> expression was reduced in <i>Pax8rtTA-Cre; Mdm2^{flox/flox}</i> mice treated with doxycycline.	57
Figure 18: Kaplan-Meyer survival curve of <i>Mdm2^{-/-tubulus}</i> and control mice.	60
Figure 19: Serum creatinine and urea concentration.	61
Figure 20: Upregulation of <i>p53</i> , <i>p21</i> and <i>Puma</i> in renal tubules lacking <i>Mdm2</i>	62
Figure 21: Upregulation of tubulus damage markers in <i>Mdm2^{-/-tubulus}</i> mice kidneys. ..	63
Figure 22: Acute tubular injury in <i>Mdm2^{-/-tubulus}</i> mice kidneys.	65
Figure 23: Cellular loss in renal tubules of <i>Mdm2^{-/-tubulus}</i> mice.	67
Figure 24: Ultrastructural pathology in tubular cells of <i>Mdm2^{-/-tubulus}</i> mice.	69

Figure 25: Caspase-3, Ki-67 and p53 immunostaining in kidney sections. 71

Figure 26: p53/Ki-67 and TUNEL immunofluorescence in kidney sections. 72

Figure 27: *Pax8rtTA-Cre;Mdm2^{flox/flox}* mice subjected to intermittent doxycycline treatment showed impaired kidney function und upregulated tubulus damage markers. 74

Figure 28: Intermittent *Mdm2* depletion in tubular cells results in kidney fibrosis. 76

Figure 29: Upregulation of fibrosis markers in kidney lysates of *Pax8rtTA-Cre;Mdm2^{flox/flox}* mice subjected to intermittent doxycycline treatment. 77

Figure 30: Maladaptive repair after acute kidney injury leads to chronic kidney disease 87

8 Liste of Tables

Table 1: Pooled incidence rate of acute kidney injury in hospitalized patients.....	6
Table 2: Staging of acute kidney injury (table from KDIGO 2012 [9])	8
Table 3: Novel biomarkers for acute kidney injury (modified from [57, 62])	14
Table 4: Comparison of apoptosis, necrosis and autophagy	22
Table 5: Primers used for PCR	36
Table 6: Comparison of different gene alterations in transgenic animals.....	40
Table 7: Phenotypes of mice with tissue-specific Mdm2-knockout	82
Table 8: Effects of MDM2 inhibitors	89

9 Bibliography

1. Hoste, E.A. and M. Schurgers, *Epidemiology of acute kidney injury: how big is the problem?* Crit Care Med, 2008. **36**(4 Suppl): p. S146-51.
2. Zuk, A. and J.V. Bonventre, *Acute Kidney Injury*. Annu Rev Med, 2016. **67**: p. 293-307.
3. Siew, E.D. and A. Davenport, *The growth of acute kidney injury: a rising tide or just closer attention to detail?* Kidney Int, 2015. **87**(1): p. 46-61.
4. Lameire, N., J. Vanmassenhove, and A. Lewington, *Did KDIGO guidelines on acute kidney injury improve patient outcome?* Intensive Care Med, 2017. **43**(6): p. 921-923.
5. Mehta, R.L., et al., *International Society of Nephrology's Oby25 initiative for acute kidney injury (zero preventable deaths by 2025): a human rights case for nephrology*. The Lancet, 2015. **385**(9987): p. 2616-2643.
6. Lameire, N.H., et al., *Acute kidney injury: an increasing global concern*. The Lancet, 2013. **382**(9887): p. 170-179.
7. Chertow, G.M., et al., *Acute kidney injury, mortality, length of stay, and costs in hospitalized patients*. J Am Soc Nephrol, 2005. **16**(11): p. 3365-70.
8. Fischer, M.J., et al., *Uncomplicated acute renal failure and hospital resource utilization: a retrospective multicenter analysis*. Am J Kidney Dis, 2005. **46**(6): p. 1049-57.
9. Kidney Disease: Improving Global Outcomes (KDIGO) Acute Kidney Injury Work Group. *KDIGO Clinical Practice Guideline for Acute Kidney Injury*. Kidney International supplements 2012 [cited 2 1]; Available from: http://kdigo.org/clinical_practice_guidelines/pdf/KDIGO_AKI_Guideline.pdf.
10. Susantitaphong, P., et al., *World incidence of AKI: a meta-analysis*. Clin J Am Soc Nephrol, 2013. **8**(9): p. 1482-93.
11. Kaddourah, A., et al., *Epidemiology of Acute Kidney Injury in Critically Ill Children and Young Adults*. N Engl J Med, 2017. **376**(1): p. 11-20.
12. Bellomo, R., et al., *Acute kidney injury in the ICU: from injury to recovery: reports from the 5th Paris International Conference*. Ann Intensive Care, 2017. **7**(1): p. 49.
13. Hilton, R., *Acute renal failure*. BMJ, 2006. **333**(7572): p. 786-90.
14. Rahman, M., F. Shad, and M.C. Smith, *Acute kidney injury: a guide to diagnosis and management*. Am Fam Physician, 2012. **86**(7): p. 631-9.
15. Kaufman, J., et al., *Community-acquired acute renal failure*. Am J Kidney Dis, 1991. **17**(2): p. 191-8.
16. Kelly, K.J., *Distant effects of experimental renal ischemia/reperfusion injury*. J Am Soc Nephrol, 2003. **14**(6): p. 1549-58.
17. Kramer, A.A., et al., *Renal ischemia/reperfusion leads to macrophage-mediated increase in pulmonary vascular permeability*. Kidney Int, 1999. **55**(6): p. 2362-7.
18. Liu, M., et al., *Acute kidney injury leads to inflammation and functional changes in the brain*. J Am Soc Nephrol, 2008. **19**(7): p. 1360-70.
19. Rabb, H., et al., *Acute renal failure leads to dysregulation of lung salt and water channels*. Kidney Int, 2003. **63**(2): p. 600-6.
20. Grams, M.E. and H. Rabb, *The distant organ effects of acute kidney injury*. Kidney Int, 2012. **81**(10): p. 942-8.

21. Molitoris, B.A., *Therapeutic translation in acute kidney injury: the epithelial/endothelial axis*. J Clin Invest, 2014. **124**(6): p. 2355-63.
22. Sharfuddin, A.A. and B.A. Molitoris, *Pathophysiology of ischemic acute kidney injury*. Nat Rev Nephrol, 2011. **7**(4): p. 189-200.
23. Bonventre, J.V. and L. Yang, *Cellular pathophysiology of ischemic acute kidney injury*. J Clin Invest, 2011. **121**(11): p. 4210-21.
24. Molitoris, B.A. and T.A. Sutton, *Endothelial injury and dysfunction: role in the extension phase of acute renal failure*. Kidney Int, 2004. **66**(2): p. 496-9.
25. Solez, K., L. Morel-Maroger, and J.D. Sraer, *The morphology of "acute tubular necrosis" in man: analysis of 57 renal biopsies and a comparison with the glycerol model*. Medicine (Baltimore), 1979. **58**(5): p. 362-76.
26. Molitoris, B.A., et al., *siRNA targeted to p53 attenuates ischemic and cisplatin-induced acute kidney injury*. (1533-3450 (Electronic)).
27. Dagher, P.C., *Apoptosis in ischemic renal injury: roles of GTP depletion and p53*. (0085-2538 (Print)).
28. Imamura, R., et al., *Intravital two-photon microscopy assessment of renal protection efficacy of siRNA for p53 in experimental rat kidney transplantation models*. (1555-3892 (Electronic)).
29. Bonventre, J.V. and A. Zuk, *Ischemic acute renal failure: an inflammatory disease?* Kidney Int, 2004. **66**(2): p. 480-5.
30. Linkermann, A., et al., *Regulated cell death in AKI*. J Am Soc Nephrol, 2014. **25**(12): p. 2689-701.
31. Ratliff, B.B., et al., *Messengers without borders: mediators of systemic inflammatory response in AKI*. J Am Soc Nephrol, 2013. **24**(4): p. 529-36.
32. Conger, J.D. and R.W. Schrier, *Renal hemodynamics in acute renal failure*. Annu Rev Physiol, 1980. **42**: p. 603-14.
33. Conger, J.D., J.B. Robinette, and W.S. Hammond, *Differences in vascular reactivity in models of ischemic acute renal failure*. Kidney Int, 1991. **39**(6): p. 1087-97.
34. Kelly, K.J., et al., *Intercellular adhesion molecule-1-deficient mice are protected against ischemic renal injury*. J Clin Invest, 1996. **97**(4): p. 1056-63.
35. Chen, G.Y. and G. Nunez, *Sterile inflammation: sensing and reacting to damage*. Nat Rev Immunol, 2010. **10**(12): p. 826-37.
36. Janeway, C., K.M. Murphy, and C. Weaver, *Janeway's immunobiology*. 9th edition ed. 2017, New York ; London: Garland Science Taylor & Francis Group.
37. Anders, H.J., *Toll-like receptors and danger signaling in kidney injury*. J Am Soc Nephrol, 2010. **21**(8): p. 1270-4.
38. Barton, G.M., et al., *A cell biological view of Toll-like receptor function: regulation through compartmentalization*. (1474-1741 (Electronic)).
39. Rusai, K., et al., *Toll-like receptors 2 and 4 in renal ischemia/reperfusion injury*. (1432-198X (Electronic)).
40. Jang, H.R., et al., *The interaction between ischemia-reperfusion and immune responses in the kidney*. J Mol Med (Berl), 2009. **87**(9): p. 859-64.
41. Wu, H., et al., *TLR4 activation mediates kidney ischemia/reperfusion injury*. (0021-9738 (Print)).
42. Leemans, J.C., et al., *Renal-associated TLR2 mediates ischemia/reperfusion injury in the kidney*. (0021-9738 (Print)).
43. Nadasdy, T., et al., *Proliferative activity of intrinsic cell populations in the normal human kidney*. J Am Soc Nephrol, 1994. **4**(12): p. 2032-9.

44. Thomasova, D. and H.J. Anders, *Cell cycle control in the kidney*. Nephrol Dial Transplant, 2014. **0**: p. 1-9.
45. Price, P.M., R.L. Safirstein, and J. Megyesi, *The cell cycle and acute kidney injury*. Kidney Int, 2009. **76**(6): p. 604-13.
46. Witzgall, R., et al., *Localization of proliferating cell nuclear antigen, vimentin, c-Fos, and clusterin in the postischemic kidney. Evidence for a heterogenous genetic response among nephron segments, and a large pool of mitotically active and dedifferentiated cells*. J Clin Invest, 1994. **93**(5): p. 2175-88.
47. Bonventre, J.V., et al., *Dedifferentiation and proliferation of surviving epithelial cells in acute renal failure*. 2003(1046-6673 (Print)).
48. Kramann, R., T. Kusaba, and B.D. Humphreys, *Who regenerates the kidney tubule?* Nephrol Dial Transplant, 2015. **30**(6): p. 903-10.
49. Spiegel, D.M., P.D. Wilson, and B.A. Molitoris, *Epithelial polarity following ischemia: a requirement for normal cell function*. Am J Physiol, 1989. **256**(3 Pt 2): p. F430-6.
50. Basile, D.P., *The endothelial cell in ischemic acute kidney injury: implications for acute and chronic function*. Kidney Int, 2007. **72**(2): p. 151-6.
51. Horbelt, M., et al., *Acute and chronic microvascular alterations in a mouse model of ischemic acute kidney injury*. Am J Physiol Renal Physiol, 2007. **293**(3): p. F688-95.
52. Strimbu, K. and J.A. Tavel, *What are biomarkers?* Curr Opin HIV AIDS, 2010. **5**(6): p. 463-6.
53. Biomarkers Definitions Working Group, *Biomarkers and surrogate endpoints: preferred definitions and conceptual framework*. Clin Pharmacol Ther, 2001. **69**(3): p. 89-95.
54. Lameire, N., et al., *The cell cycle biomarkers: promising research, but do not oversell them*. Clin Kidney J, 2016. **9**(3): p. 353-8.
55. Murray, P.T., et al., *Potential use of biomarkers in acute kidney injury: report and summary of recommendations from the 10th Acute Dialysis Quality Initiative consensus conference*. Kidney Int, 2014. **85**(3): p. 513-21.
56. Siew, E.D., L.B. Ware, and T.A. Ikizler, *Biological markers of acute kidney injury*. J Am Soc Nephrol, 2011. **22**(5): p. 810-20.
57. Malhotra, R. and E.D. Siew, *Biomarkers for the Early Detection and Prognosis of Acute Kidney Injury*. Clin J Am Soc Nephrol, 2017. **12**(1): p. 149-173.
58. Mishra, J., et al., *Neutrophil gelatinase-associated lipocalin (NGAL) as a biomarker for acute renal injury after cardiac surgery*. Lancet, 2005. **365**(9466): p. 1231-8.
59. Melnikov, V.Y., et al., *Impaired IL-18 processing protects caspase-1-deficient mice from ischemic acute renal failure*. J Clin Invest, 2001. **107**(9): p. 1145-52.
60. Haase, M., et al., *The outcome of neutrophil gelatinase-associated lipocalin-positive subclinical acute kidney injury: a multicenter pooled analysis of prospective studies*. J Am Coll Cardiol, 2011. **57**(17): p. 1752-61.
61. Han, W.K., et al., *Kidney Injury Molecule-1 (KIM-1): a novel biomarker for human renal proximal tubule injury*. Kidney Int, 2002. **62**(1): p. 237-44.
62. Ostermann, M., B.J. Philips, and L.G. Forni, *Clinical review: Biomarkers of acute kidney injury: where are we now?* Crit Care, 2012. **16**(5): p. 233.
63. Kashani, K., et al., *Discovery and validation of cell cycle arrest biomarkers in human acute kidney injury*. Crit Care, 2013. **17**(1): p. R25.
64. Seo, D.W., et al., *Shp-1 mediates the antiproliferative activity of tissue inhibitor of metalloproteinase-2 in human microvascular endothelial cells*. J Biol Chem, 2006. **281**(6): p. 3711-21.

65. Zuo, S., et al., *IGFBP-rP1 induces p21 expression through a p53-independent pathway, leading to cellular senescence of MCF-7 breast cancer cells*. J Cancer Res Clin Oncol, 2012. **138**(6): p. 1045-55.
66. Devarajan, P., *Update on mechanisms of ischemic acute kidney injury*. J Am Soc Nephrol, 2006. **17**(6): p. 1503-20.
67. Lameire, N., W.V. Biesen, and R. Vanholder, *Acute kidney injury*. Lancet, 2008. **372**(9653): p. 1863-1865.
68. Nickolas, T.L., et al., *Diagnostic and prognostic stratification in the emergency department using urinary biomarkers of nephron damage: a multicenter prospective cohort study*. J Am Coll Cardiol, 2012. **59**(3): p. 246-55.
69. Endre, Z.H., et al., *Improved performance of urinary biomarkers of acute kidney injury in the critically ill by stratification for injury duration and baseline renal function*. Kidney Int, 2011. **79**(10): p. 1119-30.
70. Lane, D.P., *Cancer. p53, guardian of the genome*. Nature, 1992. **358**(6381): p. 15-6.
71. Linzer, D.I. and A.J. Levine, *Characterization of a 54K dalton cellular SV40 tumor antigen present in SV40-transformed cells and uninfected embryonal carcinoma cells*. Cell, 1979. **17**(1): p. 43-52.
72. Lane, D.P. and L.V. Crawford, *T antigen is bound to a host protein in SV40-transformed cells*. Nature, 1979. **278**(5701): p. 261-3.
73. Matlashewski, G., et al., *Isolation and characterization of a human p53 cDNA clone: expression of the human p53 gene*. EMBO J, 1984. **3**(13): p. 3257-62.
74. Levine, A.J., *p53, the cellular gatekeeper for growth and division*. Cell, 1997. **88**(3): p. 323-31.
75. Vousden, K.H. and X. Lu, *Live or let die: the cell's response to p53*. Nature Reviews Cancer, 2002. **2**(8): p. 594-604.
76. Alberts, *Molecular biology of the cell*. 6. ed. ed. 2015, New York, NY [u.a.]: Garland Science.
77. Zhang, X.P., F. Liu, and W. Wang, *Two-phase dynamics of p53 in the DNA damage response*. Proc Natl Acad Sci U S A, 2011. **108**(22): p. 8990-5.
78. Reisman, D., et al., *Transcriptional Regulation of the p53 Tumor Suppressor Gene in S-Phase of the Cell-Cycle and the Cellular Response to DNA Damage*. Biochem Res Int, 2012. **2012**: p. 808934.
79. Fischer, M., et al., *The p53-p21-DREAM-CDE/CHR pathway regulates G2/M cell cycle genes*. Nucleic Acids Res, 2016. **44**(1): p. 164-74.
80. Nigro, J.M., et al., *Mutations in the p53 gene occur in diverse human tumour types*. Nature, 1989. **342**(6250): p. 705-8.
81. Vousden, K.H. and D.P. Lane, *p53 in health and disease*. Nat Rev Mol Cell Biol, 2007. **8**(4): p. 275-83.
82. Grier, J.D., et al., *Tissue-specific differences of p53 inhibition by Mdm2 and Mdm4*. Mol Cell Biol, 2006. **26**(1): p. 192-8.
83. Vousden, K.H. and C. Prives, *P53 and prognosis: new insights and further complexity*. Cell, 2005. **120**(1): p. 7-10.
84. Baker, S.J., et al., *Chromosome 17 deletions and p53 gene mutations in colorectal carcinomas*. Science, 1989. **244**(4901): p. 217-21.
85. Hollstein, M., et al., *Database of p53 gene somatic mutations in human tumors and cell lines*. Nucleic Acids Res, 1994. **22**(17): p. 3551-5.
86. Hollstein, M., et al., *p53 mutations in human cancers*. Science, 1991. **253**(5015): p. 49-53.

87. Levine, A.J., et al., *The 1993 Walter Hubert Lecture: the role of the p53 tumour-suppressor gene in tumorigenesis*. Br J Cancer, 1994. **69**(3): p. 409-16.
88. Donehower, L.A., et al., *Mice deficient for p53 are developmentally normal but susceptible to spontaneous tumours*. Nature, 1992. **356**(6366): p. 215-21.
89. Srivastava, S., et al., *Germ-line transmission of a mutated p53 gene in a cancer-prone family with Li-Fraumeni syndrome*. Nature, 1990. **348**(6303): p. 747-9.
90. Malkin, D., et al., *Germ line p53 mutations in a familial syndrome of breast cancer, sarcomas, and other neoplasms*. Science, 1990. **250**(4985): p. 1233-8.
91. Varley, J.M., *Germline TP53 mutations and Li-Fraumeni syndrome*. Hum Mutat, 2003. **21**(3): p. 313-20.
92. Koshland, D.E., Jr., *Molecule of the year*. Science, 1993. **262**(5142): p. 1953.
93. Vousden, K.H., *p53: death star*. Cell, 2000. **103**(5): p. 691-4.
94. Ringshausen, I., et al., *Mdm2 is critically and continuously required to suppress lethal p53 activity in vivo*. Cancer Cell, 2006. **10**(6): p. 501-14.
95. Kerr, J.F., A.H. Wyllie, and A.R. Currie, *Apoptosis: a basic biological phenomenon with wide-ranging implications in tissue kinetics*. Br J Cancer, 1972. **26**(4): p. 239-57.
96. Galluzzi, L., *Guidelines for the use and interpretation of assays for monitoring cell death in higher eukaryotes*. 2009.
97. Danial, N.N. and S.J. Korsmeyer, *Cell death: critical control points*. Cell, 2004. **116**(2): p. 205-19.
98. Bennett, M., et al., *Cell surface trafficking of Fas: a rapid mechanism of p53-mediated apoptosis*. Science, 1998. **282**(5387): p. 290-3.
99. Kroemer, G., et al., *Classification of cell death: recommendations of the Nomenclature Committee on Cell Death 2009*. Cell Death Differ, 2009. **16**(1): p. 3-11.
100. Kruiswijk, F., C.F. Labuschagne, and K.H. Vousden, *p53 in survival, death and metabolic health: a lifeguard with a licence to kill*. Nat Rev Mol Cell Biol, 2015. **16**(7): p. 393-405.
101. Cahilly-Snyder, L., et al., *Molecular analysis and chromosomal mapping of amplified genes isolated from a transformed mouse 3T3 cell line*. Somat Cell Mol Genet, 1987. **13**(3): p. 235-44.
102. Fakharzadeh, S.S., S.P. Trusko, and D.L. George, *Tumorigenic potential associated with enhanced expression of a gene that is amplified in a mouse tumor cell line*. EMBO J, 1991. **10**(6): p. 1565-9.
103. Oliner, J.D., et al., *Amplification of a gene encoding a p53-associated protein in human sarcomas*. Nature, 1992. **358**(6381): p. 80-3.
104. Iwakuma, T. and G. Lozano, *MDM2, an introduction*. Mol Cancer Res, 2003. **1**(14): p. 993-1000.
105. Boddy, M.N., P.S. Freemont, and K.L. Borden, *The p53-associated protein MDM2 contains a newly characterized zinc-binding domain called the RING finger*. Trends Biochem Sci, 1994. **19**(5): p. 198-9.
106. Moyer, S.M., C.A. Larsson, and G. Lozano, *Mdm proteins: critical regulators of embryogenesis and homeostasis*. J Mol Cell Biol, 2017.
107. Momand, J., et al., *The mdm-2 oncogene product forms a complex with the p53 protein and inhibits p53-mediated transactivation*. Cell, 1992. **69**(7): p. 1237-45.

108. Gareth L. Bond, W.H.a.A.J.L., *MDM2 is a central node in the p53 pathway: 12 years and counting*. *Current Cancer Drug Targets*, 2005. **5**: p. 3-8.
109. Stommel, J.M. and G.M. Wahl, *Accelerated MDM2 auto-degradation induced by DNA-damage kinases is required for p53 activation*. *EMBO J*, 2004. **23**(7): p. 1547-56.
110. Jones, S.N., et al., *Overexpression of Mdm2 in mice reveals a p53-independent role for Mdm2 in tumorigenesis*. *Proc Natl Acad Sci U S A*, 1998. **95**(26): p. 15608-12.
111. Lundgren, K., et al., *Targeted expression of MDM2 uncouples S phase from mitosis and inhibits mammary gland development independent of p53*. *Genes Dev*, 1997. **11**(6): p. 714-25.
112. Ganguli, G., J. Abecassis, and B. Wasylyk, *MDM2 induces hyperplasia and premalignant lesions when expressed in the basal layer of the epidermis*. *EMBO J*, 2000. **19**(19): p. 5135-47.
113. Watanabe, T., et al., *Overexpression of the MDM2 oncogene in leukemia and lymphoma*. *Leuk Lymphoma*, 1996. **21**(5-6): p. 391-7, color plates XVI following 5.
114. Momand, J., et al., *The MDM2 gene amplification database*. *Nucleic Acids Res*, 1998. **26**(15): p. 3453-9.
115. Thomasova, D., et al., *p53-independent roles of MDM2 in NF-kappaB signaling: implications for cancer therapy, wound healing, and autoimmune diseases*. *Neoplasia*, 2012. **14**(12): p. 1097-101.
116. Kastan, M.B., *Wild-type p53: tumors can't stand it*. *Cell*, 2007. **128**(5): p. 837-40.
117. El-Dahr, S., S. Hilliard, and Z. Saifudeen, *Regulation of kidney development by the Mdm2/Mdm4-p53 axis*. *J Mol Cell Biol*, 2017. **9**(1): p. 26-33.
118. Jones, S.N., et al., *Rescue of embryonic lethality in Mdm2-deficient mice by absence of p53*. *Nature*, 1995. **378**(6553): p. 206-8.
119. Montes de Oca Luna, R., D.S. Wagner, and G. Lozano, *Rescue of early embryonic lethality in mdm2-deficient mice by deletion of p53*. *Nature*, 1995. **378**(6553): p. 203-6.
120. Zhang, Y., et al., *Tissue-specific and age-dependent effects of global Mdm2 loss*. *J Pathol*, 2014. **233**(4): p. 380-91.
121. Mendrysa, S.M., et al., *mdm2 is critical for inhibition of p53 during lymphopoiesis and the response to ionizing irradiation*. *Mol Cell Biol*, 2003. **23**(2): p. 462-72.
122. Terzian, T., et al., *Haploinsufficiency of Mdm2 and Mdm4 in tumorigenesis and development*. *Mol Cell Biol*, 2007. **27**(15): p. 5479-85.
123. Ebrahim, M., et al., *MDM2 beyond cancer: podoptosis, development, inflammation, and tissue regeneration*. *Histol Histopathol*, 2015. **30**(11): p. 1271-82.
124. Gu, L., H.W. Findley, and M. Zhou, *MDM2 induces NF-kappaB/p65 expression transcriptionally through Sp1-binding sites: a novel, p53-independent role of MDM2 in doxorubicin resistance in acute lymphoblastic leukemia*. *Blood*, 2002. **99**(9): p. 3367-75.
125. Ponnuswamy, A., T. Hupp, and R. Fahraeus, *Concepts in MDM2 Signaling: Allosteric Regulation and Feedback Loops*. *Genes Cancer*, 2012. **3**(3-4): p. 291-7.
126. Allam, R., et al., *Mdm2 promotes systemic lupus erythematosus and lupus nephritis*. *J Am Soc Nephrol*, 2011. **22**(11): p. 2016-27.

127. Liu, G., et al., *p53 Attenuates lipopolysaccharide-induced NF-kappaB activation and acute lung injury*. J Immunol, 2009. **182**(8): p. 5063-71.
128. Ihling, C., et al., *Co-expression of p53 and MDM2 in human atherosclerosis: implications for the regulation of cellularity of atherosclerotic lesions*. J Pathol, 1998. **185**(3): p. 303-12.
129. Hashimoto, T., et al., *Inhibition of MDM2 attenuates neointimal hyperplasia via suppression of vascular proliferation and inflammation*. Cardiovasc Res, 2011. **91**(4): p. 711-9.
130. Gurtner, G.C., et al., *Wound repair and regeneration*. Nature, 2008. **453**(7193): p. 314-21.
131. Martin, P., *Wound healing--aiming for perfect skin regeneration*. Science, 1997. **276**(5309): p. 75-81.
132. Gannon, H.S., et al., *Mdm2-p53 signaling regulates epidermal stem cell senescence and premature aging phenotypes in mouse skin*. Dev Biol, 2011. **353**(1): p. 1-9.
133. Hilliard, S., et al., *Tight regulation of p53 activity by Mdm2 is required for ureteric bud growth and branching*. Dev Biol, 2011. **353**(2): p. 354-66.
134. El-Dahr, S., et al., *The MDM2-p53 pathway: multiple roles in kidney development*. Pediatr Nephrol, 2014. **29**(4): p. 621-7.
135. Hilliard, S.A., X. Yao, and S.S. El-Dahr, *Mdm2 is required for maintenance of the nephrogenic niche*. Dev Biol, 2014. **387**(1): p. 1-14.
136. Mulay, S.R., et al., *MDM2 (murine double minute-2) links inflammation and tubular cell healing during acute kidney injury in mice*. Kidney Int, 2012. **81**(12): p. 1199-1211.
137. Mulay, S.R., et al., *Podocyte loss involves MDM2-driven mitotic catastrophe*. J Pathol, 2013. **230**(3): p. 322-35.
138. Thomasova, D., et al., *Murine double minute-2 prevents p53-overactivation-related cell death (podoptosis) of podocytes*. J Am Soc Nephrol, 2014.
139. Thomasova, D., et al., *MDM2 prevents spontaneous tubular epithelial cell death and acute kidney injury*. Cell Death Dis, 2016. **7**(11): p. e2482.
140. Mulay, S.R., et al., *Murine Double Minute-2 Inhibition Ameliorates Established Crescentic Glomerulonephritis*. Am J Pathol, 2016. **186**(6): p. 1442-53.
141. McNicholas, B.A. and M.D. Griffin, *Double-edged sword: a p53 regulator mediates both harmful and beneficial effects in experimental acute kidney injury*. Kidney Int, 2012. **81**(12): p. 1161-4.
142. Humphreys, B.D., et al., *Intrinsic epithelial cells repair the kidney after injury*. Cell Stem Cell, 2008. **2**(3): p. 284-91.
143. Shangary, S. and S. Wang, *Small-molecule inhibitors of the MDM2-p53 protein-protein interaction to reactivate p53 function: a novel approach for cancer therapy*. Annu Rev Pharmacol Toxicol, 2009. **49**: p. 223-41.
144. Vassilev, L.T., *MDM2 inhibitors for cancer therapy*. Trends Mol Med, 2007. **13**(1): p. 23-31.
145. Burgess, A., et al., *Clinical Overview of MDM2/X-Targeted Therapies*. Front Oncol, 2016. **6**: p. 7.
146. Vassilev, L.T., et al., *In vivo activation of the p53 pathway by small-molecule antagonists of MDM2*. Science, 2004. **303**(5659): p. 844-8.
147. Secchiero, P., et al., *Recent advances in the therapeutic perspectives of Nutlin-3*. Curr Pharm Des, 2011. **17**(6): p. 569-77.
148. Tovar, C., et al., *Small-molecule MDM2 antagonists reveal aberrant p53 signaling in cancer: Implications for therapy*. Proceedings of the National

- Academy of Sciences of the United States of America, 2006. **103**(6): p. 1888-1893.
149. Kim, E.S. and J.M. Shohet, *Reactivation of p53 via MDM2 inhibition*. Cell Death Dis, 2015. **6**: p. e1936.
150. Dickens, M.P., R. Fitzgerald, and P.M. Fischer, *Small-molecule inhibitors of MDM2 as new anticancer therapeutics*. Semin Cancer Biol, 2010. **20**(1): p. 10-8.
151. Vu, B., et al., *Discovery of RG7112: A Small-Molecule MDM2 Inhibitor in Clinical Development*. ACS Med Chem Lett, 2013. **4**(5): p. 466-9.
152. Zhao, Y., et al., *Small-molecule inhibitors of the MDM2-p53 protein-protein interaction (MDM2 Inhibitors) in clinical trials for cancer treatment*. J Med Chem, 2015. **58**(3): p. 1038-52.
153. ClinicalTrials.gov, i.f.R.; Available from: <https://www.clinicaltrials.gov/ct2/results?cond=&term=rg7112&cntry1=&state1=&recrs=>.
154. Ray-Coquard, I., et al., *Effect of the MDM2 antagonist RG7112 on the P53 pathway in patients with MDM2-amplified, well-differentiated or dedifferentiated liposarcoma: an exploratory proof-of-mechanism study*. Lancet Oncol, 2012. **13**(11): p. 1133-40.
155. Andreeff, M., et al., *Results of the Phase I Trial of RG7112, a Small-Molecule MDM2 Antagonist in Leukemia*. Clin Cancer Res, 2016. **22**(4): p. 868-76.
156. Lewandoski, M., *Conditional control of gene expression in the mouse*. Nature, 2001. **2**: p. 743-755.
157. Schmidt, O., *Genetik und Molekularbiologie*. 2017, Berlin ; Heidelberg: Springer Spektrum. 1 Online-Ressource (XVI, 320 Seiten 145 Abb., 132 Abb. in Farbe).
158. Kos, C.H., *Cre/loxP system for generating tissue-specific knockout mouse models*. Nutr Rev, 2004. **62**(6 Pt 1): p. 243-6.
159. Poleev, A., et al., *PAX8, a human paired box gene: isolation and expression in developing thyroid, kidney and Wilms' tumors*. Development, 1992. **116**(3): p. 611-23.
160. Plachov, D., et al., *Pax8, a murine paired box gene expressed in the developing excretory system and thyroid gland*. Development, 1990. **110**(2): p. 643-51.
161. Traykova-Brauch, M., et al., *An efficient and versatile system for acute and chronic modulation of renal tubular function in transgenic mice*. Nat Med, 2008. **14**(9): p. 979-84.
162. Grier, J.D., W. Yan, and G. Lozano, *Conditional allele of mdm2 which encodes a p53 inhibitor*. Genesis, 2002. **32**(2): p. 145-7.
163. Joppien, S., S.L. Maier, and D.S. Wendling, *BASICS Experimentelle Doktorarbeit*. 1. Aufl. ed. Basics. 2011, München: Elsevier, Urban & Fischer.
164. Xiong, Y., H. Zhang, and D. Beach, *D type cyclins associate with multiple protein kinases and the DNA replication and repair factor PCNA*. Cell, 1992. **71**(3): p. 505-14.
165. Yu, J. and L. Zhang, *No PUMA, no death: implications for p53-dependent apoptosis*. Cancer Cell, 2003. **4**(4): p. 248-9.
166. Jeffers, J.R., et al., *Puma is an essential mediator of p53-dependent and -independent apoptotic pathways*. Cancer Cell, 2003. **4**(4): p. 321-8.
167. Villunger, A., et al., *p53- and drug-induced apoptotic responses mediated by BH3-only proteins puma and noxa*. Science, 2003. **302**(5647): p. 1036-8.

168. X. Ding, C.R., ed. *Acute kidney injury : from diagnosis to care*. Contributions to nephrology. 2016, Karger: Basel ; Freiburg. VII, 147 Seiten.
169. Valentin-Vega, Y.A., H. Okano, and G. Lozano, *The intestinal epithelium compensates for p53-mediated cell death and guarantees organismal survival*. *Cell Death Differ*, 2008. **15**(11): p. 1772-81.
170. Francoz, C., M.K. Nadim, and F. Durand, *Kidney biomarkers in cirrhosis*. *J Hepatol*, 2016. **65**(4): p. 809-24.
171. Chavez-Reyes, A., et al., *Switching mechanisms of cell death in mdm2- and mdm4-null mice by deletion of p53 downstream targets*. *Cancer Res*, 2003. **63**(24): p. 8664-9.
172. Lengner, C.J., et al., *Osteoblast differentiation and skeletal development are regulated by Mdm2-p53 signaling*. *J Cell Biol*, 2006. **172**(6): p. 909-21.
173. Maetens, M., et al., *Distinct roles of Mdm2 and Mdm4 in red cell production*. *Blood*, 2007. **109**(6): p. 2630-3.
174. de Vries, W.N., et al., *Expression of Cre recombinase in mouse oocytes: a means to study maternal effect genes*. *Genesis*, 2000. **26**(2): p. 110-2.
175. Livera, G., et al., *Loss of oocytes due to conditional ablation of Murine double minute 2 (Mdm2) gene is p53-dependent and results in female sterility*. *FEBS Lett*, 2016. **590**(16): p. 2566-74.
176. Xiong, S., et al., *Synergistic roles of Mdm2 and Mdm4 for p53 inhibition in central nervous system development*. *Proc Natl Acad Sci U S A*, 2006. **103**(9): p. 3226-31.
177. Francoz, S., et al., *Mdm4 and Mdm2 cooperate to inhibit p53 activity in proliferating and quiescent cells in vivo*. *Proc Natl Acad Sci U S A*, 2006. **103**(9): p. 3232-7.
178. Zhang, Y., X. Zhang, and H. Lu, *Aberrant activation of p53 due to loss of MDM2 or MDMX causes early lens dysmorphogenesis*. *Dev Biol*, 2014. **396**(1): p. 19-30.
179. Boesten, L.S., et al., *Mdm2, but not Mdm4, protects terminally differentiated smooth muscle cells from p53-mediated caspase-3-independent cell death*. *Cell Death Differ*, 2006. **13**(12): p. 2089-98.
180. Creamer, B., R.G. Shorter, and J. Bamforth, *The turnover and shedding of epithelial cells. I. The turnover in the gastro-intestinal tract*. *Gut*, 1961. **2**: p. 110-8.
181. Borges, F.T. and N. Schor, *Regenerative medicine in kidney disease: where we stand and where to go*. *Pediatr Nephrol*, 2017.
182. Barnes, J.L. and W.F. Glass, 2nd, *Renal interstitial fibrosis: a critical evaluation of the origin of myofibroblasts*. *Contrib Nephrol*, 2011. **169**: p. 73-93.
183. Kriz, W., B. Kaissling, and M. Le Hir, *Epithelial-mesenchymal transition (EMT) in kidney fibrosis: fact or fantasy?* *J Clin Invest*, 2011. **121**(2): p. 468-74.
184. Chawla, L.S., et al., *Acute kidney injury and chronic kidney disease as interconnected syndromes*. *N Engl J Med*, 2014. **371**(1): p. 58-66.
185. Ferenbach, D.A. and J.V. Bonventre, *Acute kidney injury and chronic kidney disease: From the laboratory to the clinic*. *Nephrol Ther*, 2016. **12 Suppl 1**: p. S41-8.
186. Okusa, M.D., G.M. Chertow, and D. Portilla, *The nexus of acute kidney injury, chronic kidney disease, and World Kidney Day 2009*. *Clin J Am Soc Nephrol*, 2009. **4**(3): p. 520-2.
187. Hsu, R.K. and C.Y. Hsu, *The Role of Acute Kidney Injury in Chronic Kidney Disease*. *Semin Nephrol*, 2016. **36**(4): p. 283-92.

188. Ishani, A., et al., *Acute kidney injury increases risk of ESRD among elderly*. J Am Soc Nephrol, 2009. **20**(1): p. 223-8.
189. Coca, S.G., S. Singanamala, and C.R. Parikh, *Chronic kidney disease after acute kidney injury: a systematic review and meta-analysis*. Kidney Int, 2012. **81**(5): p. 442-8.
190. Yang, L., et al., *Epithelial cell cycle arrest in G2/M mediates kidney fibrosis after injury*. Nat Med, 2010. **16**(5): p. 535-43, 1p following 143.
191. Binder, B.R., *A novel application for murine double minute 2 antagonists: the p53 tumor suppressor network also controls angiogenesis*. Circ Res, 2007. **100**(1): p. 13-4.
192. Secchiero, P., et al., *Antiangiogenic activity of the MDM2 antagonist nutlin-3*. Circ Res, 2007. **100**(1): p. 61-9.
193. Hagemann, J.H., et al., *Nrf2 signalling promotes ex vivo tubular epithelial cell survival and regeneration via murine double minute (MDM)-2*. Nephrol Dial Transplant, 2013. **28**(8): p. 2028-37.
194. Fledderus, J.O. and R. Goldschmeding, *Nrf2 implicated as a novel therapeutic target for renal regeneration after acute kidney injury*. Nephrol Dial Transplant, 2013. **28**(8): p. 1969-71.
195. Aziz, M.H., H. Shen, and C.G. Maki, *Acquisition of p53 mutations in response to the non-genotoxic p53 activator Nutlin-3*. Oncogene, 2011. **30**(46): p. 4678-86.
196. Galluzzi, L., et al., *Molecular definitions of cell death subroutines: recommendations of the Nomenclature Committee on Cell Death 2012*. Cell Death Differ, 2012. **19**(1): p. 107-20.

10 Acknowledgment

There are many people who have helped and inspired me through my doctoral study. Hereby I would like to express my sincere appreciation to all of them.

First and foremost, I would like to thank my supervisor Professor Hans-Joachim Anders and co-supervisor Privatdozent Dana Thomasova. They provided me a great opportunity to conduct my doctoral study in this prestigious international research center. Thank you for guiding my way with a lot of patience, sharing your knowledge and advising me with constructive suggestions. Thank you for the kind mentoring within and outside the lab, such as in the Medical School. You are my role models as a scientist as well as a person. My great gratitude also for Privatdozent Bruno Luckow. His dedication in science and meticulous work style has influenced me a lot.

I thank my dear lab friends--Martrez, Nina, Santhosh, Simone, Mohsen, Julian, Steffi, Jyaysi, Shrikant, Satish, Lukas, Maia, Johnny, Johannes, Anja and Xie. You taught me not only lab methods but also critical thinking, trouble shooting and team spirit. I remember the lab lunch and intercultural exchange we had together. I remember the warm words and encouragement you gave me. After work we went to Oktoberfest, celebrated birthdays and festivals and shared delicious food. You wonderful people made my time in Anders and Vielhauer's laboratory full of unforgettable memories.

I am indebted to the excellent technicians Jana and Dan, who performed histology and genotyping procedures. My gratefulness also for Professor Helen Liapis from Washington University for her cooperation in this research work and sharing her expertise about electron microscopy. I thank Munich-International Nephrology and Internal Medicine (MINI) Research School for seminars of molecular biology and financial support for my academic work.

I owe my deepest gratitude to my family. My parents and my husband always stand by my side and have accompanied me through good and bad times, along with their love and selfless support. Without them, this thesis would not have been possible.

Finally, I would like to express my immense gratitude to the animals that have been sacrificed for scientific research of human beings.